# SOUTHEASTERN GEOLOGY

PUBLISHED AT DUKE UNIVERSITY DURHAM, NORTH CAROLINA

VOL.22. NO.2 MAY, 1981

SOUTHEASTERN GEOLOGY

PUBLISHED QUARTERLY

AT

DUKE UNIVERSITY



This journal welcomes original papers on all phases of geology, geophysics, and geochemistry as related to the Southeast. Transmit manuscripts to S. DUNCAN HERON, JR., BOX 6665, COLLEGE STATION, DURHAM, NORTH CAROLINA 27708. Observe the following:

1) Type the manuscript with double space lines and submit in duplicate.
2) Cite references and prepare bibliographic lists in accordance with the method found within the pages of this journal.
3) Submit line drawings and complex tables as finished copy.
4) Make certain that all photographs are sharp, clear, and of good contrast.
5) Stratigraphic terminology should abide by the code of Stratigraphic Nomenclature (AAPG, v. 45, 1961).

Proofs will be sent authors.

Reprints must be ordered prior to publication; prices available upon request. Subscriptions to Southeastern Geology are $8.00 per volume (US and Canada) $10.00 per volume (foreign). Inquiries should be sent to: SOUTHEASTERN GEOLOGY, BOX 6665, COLLEGE STATION, DURHAM, NORTH CAROLINA 27708. Make checks payable to: Southeastern Geology.

SOUTHEASTERN GEOLOGY

Table of Contents

Vol. 22, No. 2

May, 1981

# MINERALOGY AND PETROLOGY OF THE DAY BOOK DUNITE AND ASSOCIATED ROCKS, WESTERN NORTH CAROLINA

By

Samuel E. Swanson

Geophysical Institute
University of Alaska
Fairbanks, Alaska 99701

## ABSTRACT

Results of mapping and petrographic and electron microprobe analyses show the Day Book dunite to be a typical body of alpine ultramafic rock surrounded by regionally metamorphosed rocks of the Blue Ridge thrust sheet. The dunite is predominately olivine with minor amounts of chromian spinel and orthopyroxene. A variety of metamorphic minerals are found in the dunite including talc, tremolite, anthophyllite, chlorite, serpentine and magnesite. The country rocks consist of amphibolite (hornblende + plagioclase + quartz + sphene + garnet; or hornblende + plagioclase + quartz + clinopyroxene + sphene) and interlayered mica gneiss (quartz + plagioclase + biotite + white mica $\pm$ garnet $\pm$ staurolite $\pm$ kyanite $\pm$ chlorite). Intrusive into the dunite and the country rocks are white mica and garnet-bearing granodiorite pegmatites. Pegmatite contacts crosscut the regional foliation. Contacts between the dunite and country rocks and pegmatite are characterized by a metasomatic reaction zone consisting of essentially monomineralic bands of anthophyllite (if the rock is pegmatite or mica gneiss) talc and vermiculite or chlorite (if the country rock is amphibolite).

Electron microprobe analyses of olivine, chromian spinel and chlorite do not reveal any compositional zoning. Olivine compositions range from $Fo_{92-95}$. Chromian spinels have compositional trends similar to those found in other alpine ultramafic rocks. Temperatures, calculated from co-existing olivine and chromian spinel, range from 1070° to 1184°C and average 1141°C--results similar to those from other alpine ultramafics. However, much of the chromian spinel is associated with a chromian-bearing chlorite (kämmererite) that is apparently an alteration product of the spinel. Therefore, the significance of the calculated temperatures is thus open to some question.

Metamorphism of the dunite is indicated by the abundance of metamorphic minerals both in veins and within the dunite. The dunite is cut by a series of veins that are apparently related to the pegmatites. Many of the same texturally stable mineral assemblages are found in both the veins and the dunite and include; tremolite + talc + forsterite, talc + anthophyllite + forsterite, tremolite + talc +anthophyllite, tremolite + anthophyllite + forsterite, and talc + forsterite + magnesite. The assemblage talc + anthophyllite + magnesite was only found within the veins, whereas the assemblages involving orthopyroxene (talc + forsterite + orthopyroxene and tremolite + forsterite + orthophyroxene) are confined to the dunite. Many of the amphiboles show partial to complete replacement by talc. Mineral assemblages in the dunite and in the veins are consistent with the middle amphibolite grade of regional metamorphism (550-650°C, 5-6 kb) observed in the country rock. Analysis of the mineral assemblage in light of experimental work in the system $MgO$-$SiO_2$-$H_2O$-$CO_2$ shows that the fluid phase which accompanied the metamorphism became more enriched in $H_2O$ with time. This is consistent with the change in fluid composition during the crystallization of a granitic magma. Metamorphism of the country rocks and the dunite was apparently contemporaneous with pegmatite intrusion. Serpentine, found as both fracture fillings and coronas surrounding other silicates, is a late-stage alteration product that is unrelated to any metamorphic event observed in the country rocks.

Evidence of recrystallization in the dunite is found in the olivine fabric. A

porphyroclastic texture with large, irregular, deformed olivine grains surrounded by fine-grained, undeformed, polygonal matrix characterizes the dunite. The polygonal texture has grain boundaries that meet at 120° triple junctions and is clearly the result of annealing after formation of the large deformed olivines.

At least three different episodes of crystallization have left their imprint on the Day Book dunite. An initial phase involved the formation of the large olivine porphyroblasts. A second period coincided with the peak of regional metamorphism and pegmatite intrusion and formed the polygonal olivine texture. The third phase of recrystallization is related to the serpentinization of the ultramafic. If anything is to be learned about the intrusion of the dunite into the crust or its subsequent emplacement into the Blue Ridge, the polygonal olivine fabric is <u>not</u> the place to look for clues.

## INTRODUCTION

Alpine ultramafic rocks are dunites and peridotites (or their serpentinized equivalents) that occur as linear belts within or parallel to the axial region of mountain belts (Hess, 1955; Mores & MacGregor, 1972). Contacts between the ultramafic rocks and country rocks usually do not show any effects of contact metamorphism and are generally concordant with regional structures. Mineralogically, alpine ultramafic rocks are composed of magnesium-rich olivine, pyroxene, and subordinate amounts of chromian spinel. Textures of the ultramafic rocks suggest recrystallization, especially of olivine (Raleigh, 1965).

Alpine ultramafic rocks found in regionally metamorphosed terranes such as the Appalachians, are generally conformable to the regional foliation. Mineral assemblages in these ultramafic rocks indicate a P-T of equilibration similar to the surrounding metamorphic rocks (Moores and MacGregor, 1972). Aditionally, many of these bodies show textural evidence for recrystallization. Interpretation of the history of alpine ultramafic rocks is difficult due to the masking effect of the regional metamorphism. Moores and MacGregor (1972) have suggested that these ultramafic rocks may represent melanges or overthrust sheets that have been metamorphosed subsequent to emplacement.

### Ultramafics of the Southern Appalachians

Within the Appalachian Mountains, hundreds of small bodies of ultramafic rock define two narrow belts that parallel the structural trends from Newfoundland to Alabama (Larabee, 1966). In North Carolina, one group of ultramafic rocks occurs in the allochthonous Blue Ridge thrust sheet and a second group is located in the Piedmont Province (Fig. 1). On a smaller scale, individual bodies are conformable to the foliation of the country rock. Petrology of the ultramafics varies from relatively unaltered dunite and peridotite to completely altered serpentinites. Misra and Keller (1978) have summarized much of the data on ultramafic rocks from the Southern Appalachian Mountains.

Ultramafic rocks in North Carolina are the source of a number of mineral resources including olivine, chromite, vermiculite, and asbestos (commonly anthophyllite) (Hunter, 1941; Hunter, et al., 1942; Murdock and Hunter, 1946; Conrad et al., 1963). Pegmatitic granitic rocks, often found intruding the ultramafic rocks, have reacted with the dunites and peridotites to produce some of the vermiculite and asbestos (Kulp and Brobst, 1954) and corundum (Pratt and Lewis, 1905).

Several studies of ultramafic rock bodies in the North Carolina portion of the Blue Ridge Province have been concerned mainly with petrofabric analysis of olivines or the mineralogy of a particular phase. Astwood (et al., 1972) studied the optical orientation of polygonal olivine in two ultramafic bodies in southwestern North Carolina and did not find any preferred orientation. Other ultramafic bodies in the North Carolina Blue Ridge do show preferred orientation of olivine microfabrics and these structures suggest syntectonic recrystallization (Greengerg, 1976; Bluhm and Zimmerman, 1977; Dribus et al., 1977). Some of the North Carolina ultramafics show

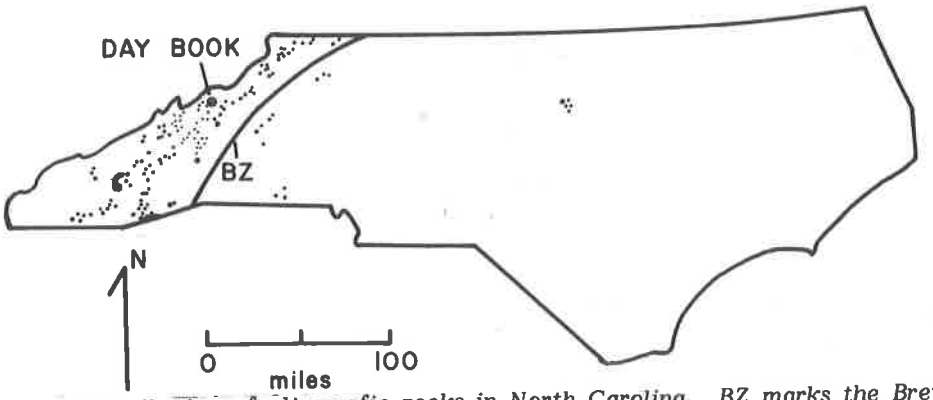


*Figure 1. Distribution of ultramafic rocks in North Carolina. BZ marks the Brevard Zone and divides Ultramafics in the Blue Ridge (to the west) from ultramafics in the Piedmont.*

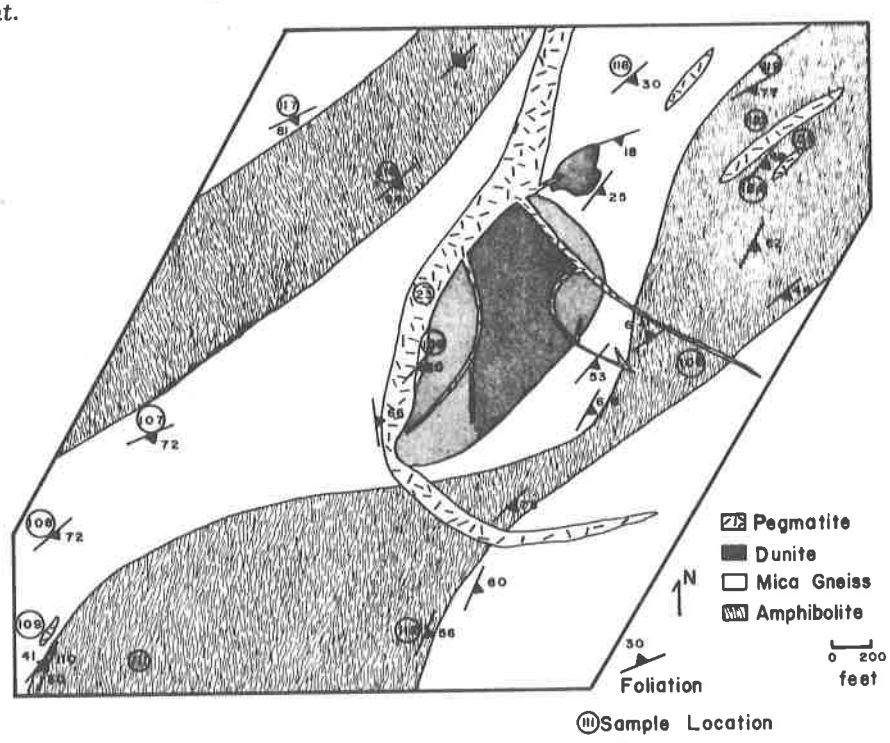


*Figure 2. Geologic map of the Day Book dunite. Numbers in circles are samples locations referred to in Tables 1 and 2.*

significant serpentinization that apparently took place *in situ* (Neuhauser and Carpenter, 1971) as a constant or variable (Madison and Condie, 1969) volume process. Olivine from the ultramafics has a near constant composition of $Fo_{92.5}$ (Carpenter and Phyfer, 1975). Chromite compositions follow the same trend shown by other alpine ultramafics (Fletcher and Carpenter, 1972; Swanson and Whittkopp, 1976), but some of the massive varieties show affinities for chromian-spinels from layered intrusions (Carpenter and Fletcher, 1979).

As much of the work done in ultramafics in the Southern Appalachians has been topical in nature, i.e., individual studies have concentrated on topics such as petrofabric analysis or petrology, it is difficult to develop a complete geologic history for individual bodies or the ultramafic belt as whole from the scattered, limited data available. The purpose of this paper is to present as complete a description of a representative ultramafic body as is possible with presently available data. In so doing

I have included some previously published data in an attempt to present a comprehensive analysis. Some information important to a complete description of an ultramafic body including a petrofabric analysis and mineral and bulk rock chemical analyses are not complete or have not been undertaken, for the body selected. It is hoped that the remaining studies will be completed in the future.

### Previous Work

The Day Book dunite (Figs. 1 and 2) was selected for study because of the excellent exposures afforded by an active olivine mining operation and because this body is familiar to many geologists. This dunite is typical of many of ultramafics in the Blue Ridge belt and various aspects have been studied by several different workers at different times.

Several papers that discuss the economic minerals associated with the ultramafic rocks in North Carolina mention the Day Book deposit. Hunter (1941) described the olivine and presented a map of the Day Book deposit. Analyses of chromian spinel from Day Book are given by Hunter (et al., 1942), Bentzen (1970) and Carpenter and Fletcher (1979). Murdock and Hunter (1946) mention the vermiculite at Day Book and Kulp and Brobst (1954) ascribed the development of vermiculite to metasomatic alteration between the dunite and intruding granitic pegmatites. Kulp and Brobst also presented bulk rock analyses of the dunite, weathered pegmatite, and metasomatic products, along with a much improved geologic map of the ultramafic body. Lack of a contact aureole and the distribution of transition metals in bulk rock samples led Phyfer and Carpenter (1969) to conclude that the Day Book dunite was emplaced as a crystal mush or as a serpentinite that dehydrated during subsequent thermal metamorphism. Election microprobe analyses of olivine from Day Book show a compositional range of $Fo_{92.0-92.6}$ (Carpenter and Phyfer, 1975). McCormick (1975) studied the chlorite associated with the olivine and chromian spinel in the Day Book dunite and concluded it was kämmererite. Swanson and Raymond (1976) studied veins in the Day Book dunite and concluded the veins were formed from $H_2O$-$CO_2$ fluids formed during the intrusion of pegmatites into the dunite. Swanson and Whittkopp (1976) feel that, based on setting and mineralogy, the Day Book dunite represents an alpine ultramafic that was dehydrated and recrystallized following the model originally proposed by Phyfer and Carpenter (1969). Tien (1977) reported on the occurrence of aragonite, dolomite, magnesite and huntite as fracture fillings in the dunite formed during weathering.

## COUNTRY ROCKS

### Metamorphic Rocks

The Day Book dunite is surrounded on three sides by gneisses and amphibolites of the Blue Ridge thrust sheet (Fig. 2). A detailed discussion of the structural complexities is beyond the scope of this report, but minor structural features observed in the area are consistent with the multi-deformational history of the Blue Ridge outlined by Butler (1973).

The predominate metamorphic rock is a biotite gneiss. Within the biotite gneiss more aluminous layers and lenses have been metamorphosed to kyanite gneiss. Layers of kyanite gneiss range in thickness from a few millimeters to tens of meters and are discontinuous along the strike of the regional foliation. Amphibolites occur as layers and as occasional blocks surrounded by biotite gneiss. The thickness of individual amphibolite layers also varies along strike.

Mineral assemblages in the metamorphic rocks are given in Table 1. Diagnostic mineral assemblages in the pelitic bulk compositions include quartz + plagioclase + white mica + biotite + garnet + staurolite + kyanite + chlorite, whereas the assemblage hornblende + plagioclase + quartz $\pm$ garnet + sphene and hornblende + clinopyroxene + plagioclase + quartz + sphene characterize the amphibolites. These assemblages are indicative of a medium grade (Winkler, 1976) or the middle amphibolite facies (Turner, 1968) of regional metamorphism. Differences in mineral assemblages in the micaceous

*Table 1. Mineralogy of the Country Rocks.*

| Sample Number[1] | % Flds[2] | % Qtz | % Amph | % Epid | % Gar | % Sph | % Cpx | % Opa | % Ky | % Sta | % Wm | % Biot |
|---|---|---|---|---|---|---|---|---|---|---|---|---|
| Mica Gneiss | | | | | | | | | | | | |
| 103 | 29.5 | 20.5 | --- | --- | 1.7 | --- | --- | 2.1 | --- | 2.1 | 17.9 | 26.2 |
| 106 | 38.0 | 14.0 | --- | --- | 3.9 | --- | --- | 0.5 | 12.9 | --- | 4.5 | 26.2 |
| 108 | 51.7 | 16.2 | --- | 1.2 | tr | --- | --- | --- | --- | --- | tr | 30.9 |
| 110 | 61.9 | 8.5 | --- | --- | 1.0 | --- | --- | 0.7 | 5.6 | --- | 5.6 | 16.7 |
| 118 | 41.4 | 28.5 | --- | --- | --- | --- | --- | --- | --- | --- | 0.2 | 29.9 |
| Amphibolite | | | | | | | | | | | | |
| 100 | 3.2 | 4.1 | 54.9 | 34.6 | tr | 3.2 | --- | --- | --- | --- | --- | --- |
| 102 | 14.9 | 8.2 | 72.5 | --- | --- | 4.4 | --- | --- | --- | --- | --- | --- |
| 110 | 13.0 | 8.1 | 76.6 | 1.0 | --- | 1.3 | --- | --- | --- | --- | --- | --- |
| 111 | 15.1 | 10.3 | 67.2 | 5.9 | --- | 1.5 | --- | --- | --- | --- | --- | --- |
| 112 | 20.2 | 4.0 | 50.9 | 23.2 | --- | 0.9 | 0.8 | --- | --- | --- | --- | --- |
| 116 | 26.3 | 6.3 | 63.8 | 0.9 | tr | 1.7 | --- | 1.0 | --- | --- | --- | tr |
| 119 | 27.4 | 9.7 | 58.9 | 2.7 | --- | 1.1 | --- | 0.2 | --- | --- | --- | --- |
| 121 | 12.9 | 10.9 | 51.4 | 17.7 | --- | 2.8 | 3.3 | --- | --- | --- | --- | --- |
| 122 | 18.0 | 7.9 | 53.9 | 17.2 | --- | 3.0 | --- | --- | --- | --- | --- | --- |

Flds-feldspar, Qtz-quartz, Amph-hornblende, Epid-epidote, Gar-garnet, Sph-sphene, Cpx-clinopyroxene, Opa-opaque, Ky-kyanite, Sta-staurolite, Wm-white mica, Biot-biotite, tr-trace amount.

[1]Location given on Figure 2.
[2]For amphibolites, all of the feldspar is plagioclase.

rocks or the amphibolites are due to differences in bulk compositions rather than local gradients in pressure-temperature. Contacts between the country rocks and the dunite are characterized by a metasomatic reaction zone where magnesium from the dunite has combined with silica, aluminum, potassium and water from the country rocks to produce a series of essentially monomineralic bands. Immediately adjacent to the dunite is a zone of anthophyllite with long, fibrous crystals oriented perpendicular to the contact with the country rock. Much of the anthophyllite has been replaced by talc that still retains the fibrous habit of the anthophyllite. The next zone located successively outward from the dunite consists of talc. Finally, immediately adjacent to the country rock, there is a zone of either vermiculite (if the country rock is mica gneiss) or chlorite (if the country rock is amphibolite).

Country rocks around the dunite have been assigned to the Ashe Formation by Butler (1973). Elsewhere in the Blue Ridge, Rankin (1973) equates the amphibolite and mica gneiss of the Ashe Formation to metamorphosed basalt and graywacke, respectively. Blocks of amphibolite up to 5 m in length are found within the mica gneiss. Mapping on a larger scale may show that the amphibolites of Fig. 2 are also blocks surrounded by gneiss as suggested by Swanson and Whittkopp (1976).

## Igneous Rocks

Intrusive into the metamorphic rocks and the dunite are quartz monzonite-granodiorite pegmatites (Fig. 2). Pegmatitic rocks found within the ultramafic bodies are weathered to kaolinite plus quartz, but the pegmatitic texture is still preserved. The large pegmatite along the western margin of the ultramafic and the dikes within the country rock are fresher and consist of perthitic alkali feldspar, quartz, plagioclase, muscovite, and garnet. Modal analyses of the pegmatites are given in Table 2 along with a chemical analysis of a weathered pegmatite from Kulp and Brobst (1954).

Pegmatites show two different relations with the country rocks. Most of the dikes are conformable to the regional foliation, whereas a few dikes associated with the ultramafic body cross-cut the metamorphic foliation (Fig. 2). Within the ultramafic body, pegmatites follow joints (Figs. 3 and 4), the trend of which cross-cuts the regional foliation.

Some of the pegmatites within the country rocks are crudely zoned. The margins are medium-grained (1-5 mm) quartz monzonite. Quartz with large crystals of muscovite (to 25 cm) is found in the core of the pegmatite bodies. Some of the pegmatite bodies were mined for muscovite during World War II.

Along the contact between the pegmatitic rocks and the dunite bodies is an extensive metasomatic reaction zone. Width of the reaction zone is directly proportional to the width of the pegmatite mass. The reaction zone represents a movement of silica, aluminum, potassium, and $H_2O$ from the granitic magma toward

*Table 2. Modal[1] and Chemical Composition of Day Book Pegmatites.*

| | 100* | 23* |
|---|---|---|
| Quartz | 32.6 | 31.7 |
| Plagioclase | 49.2 | 31.2 |
| K-Feldspar | 15.8 | 35.1 |
| Other+ | 2.4 | 2.0 |

+Includes garnet and white mica.

*Sample locations given on Figure 2.

| Kulp and Brobst (1954) | |
|---|---|
| $SiO_2$ | 55.66 |
| $Al_2O_3$ | 25.05 |
| $Fe_2O_3$ | 1.62 |
| FeO | 0.45 |
| MgO | 2.00 |
| CaO | 4.89 |
| $Na_2O$ | 4.51 |
| $K_2O$ | 0.61 |
| $H_2O$ | 1.09 |
| $H_2O^+$ | 3.09 |

[1]Based on point counting (5.0 mm. between points) stained slabs (Laniz et.al., 1964) of pegmatite. Total area analyzed was in excess of 600 sq. cm.

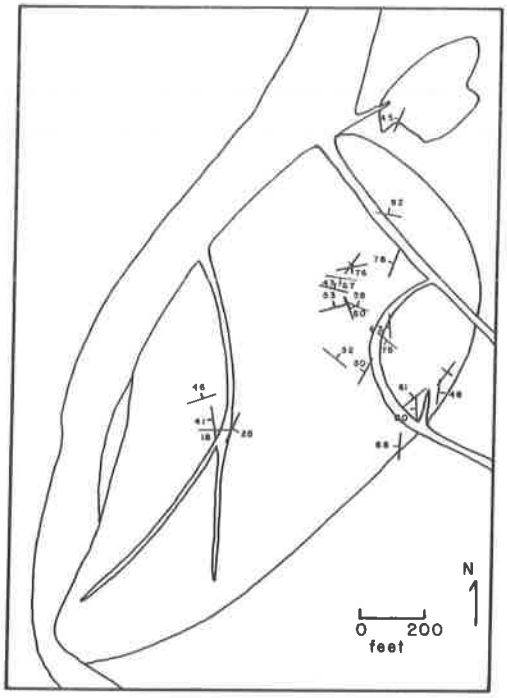


*Figure 3. Attitudes of serpentine-filled fractures in the dunite.*

the dunite body and movement of magnesium from the ultramafic body toward the pegmatitic body. Mineralogically, this chemical zonation is reflected by vermiculite adjacent to the pegmatite, followed by talc and anthophyllite (Fig. 5). Vermiculite apparently represents weathered phlogopite (Kulp and Brobst, 1954). As mentioned previously, pegmatites in the dunite are deeply weathered. Compositional data on the pegmatites supports the model of desilicification (Kulp and Brobst, 1954). Work is currently in progress to develop a diffusion model for the pegmatite-dunite contacts.

## MINERALOGY AND PETROLOGY OF THE DUNITE

The Day Book dunite (Fig. 2) consists of two bodies separated by a small septa of mica gneiss. All of the dunite is lithologically similar, consisting of the primary minerals olivine, orthopyroxene and accessory chromian spinel. Color of the dunite ranges from pale green in less a altered rock to olive black with increasing serpentinization. Within the dunite the degree of serpentinization generally increases toward the contact with the country rock and the pegmatite. The dunite is fine-

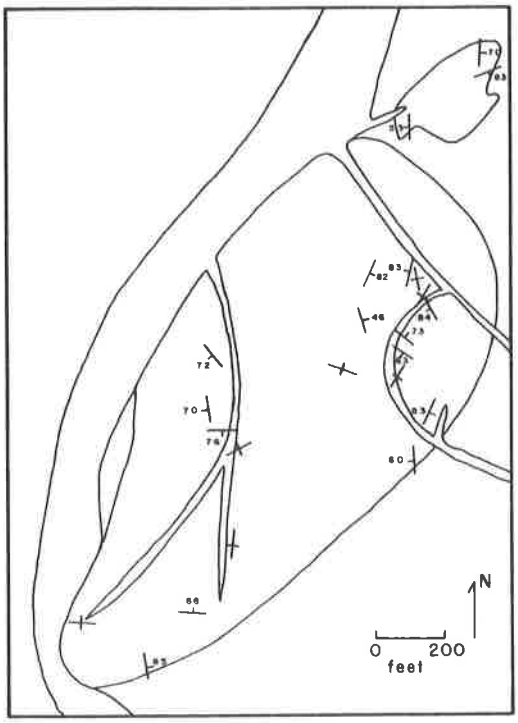


*Figure 4. Attitudes of veins in the dunite.*

grained with an average olivine grain size of 0.2 mm. A metasomatic reaction zone characterizes the contact between the dunite and the country rock and is a common feature in the ultramafic rocks of the region (Conrad et al., 1963).

A planar orientation of chromian spinel layers and pods is the only definite foliation observable in the dunite in the field (Fig. 6). Layers vary from irregular concentrations of a few chromite grains less than 1 cm in thickness to layers 30 cm wide composed almost entirely of chromian spinel. The thickest layer was mined during World War I (Hunter et al., 1942). Observations of chromian spinel foliations are generally restricted to the excellent exposures along the quarry walls. Pods of chromite also weakley define a foliation. The pods observed *in situ* during this study are less than 20 cm in greatest dimension, but blocks in the quarry rubble suggest that pods up to 3 m across occur in the dunite. Attitudes of chromian spinel layering define two trends within the dunite (Fig. 6). One set of attitudes is approximately parallel to the margin of the ultramafic while a second set is at right angle to the first set. In places the chromian spinel layering is folded into isoclinal folds with an amplitudes of 5-20 cm.

Two different types of shear fractures filled with serpentinization products cut the dunite bodies (Fig. 3 and 4). Shear zones vary in thickness from 0.2-2 m. Mineral assemblages of the shear zones are different in each of the bodies. In the smaller mass of dunite, a shear zone is filled with long-fiber chrysotile (?). The larger dunite body has a shear zone 1-2 m wide filled with brecciated, partially serpentinized fragments of dunite. In addition to serpentine this zone contains chalcedony, nickel silicates, and a variety of carbonate minerals formed as weathering products (Tien, 1977). It has not been possible to trace shear zones from the dunite into the country rock, but crosscutting relations suggest the shear zones were formed after the last metamorphic event.

Joints are common in both of the dunite bodies (Figs. 3 and 4). Dunite adjacent to the joints is serpentinized and the joint surfaces are covered with serpentine and magnetite. Attitudes of joints show the same pattern as the chromian spinel layering. One set follows the trend of the dunite bodies and the regional foliation, whereas a second set is perpendicular to this trend (Figs. 3 and 4). In some instances, pegmatite

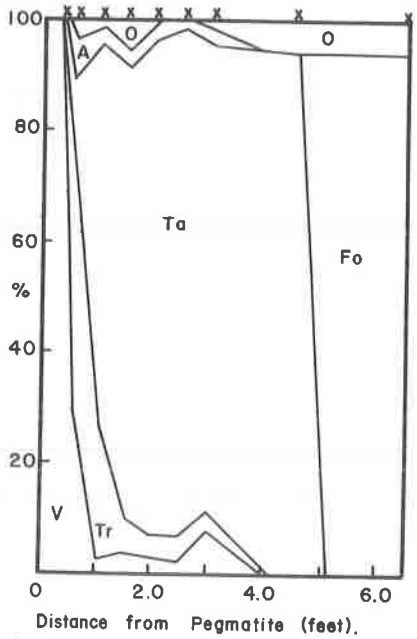


*Figure 5. Mineralogy of the contact zone between pegmatite and dunite at point 93 (Fig. 7) as determined by model analyses of thin sections from localities shown by crosses on the top of the diagram. V is vermiculite, Tr is tremolite, Ta is talc, Fo is olivine, A is anthophyllite and O represents the sum of chlorite + serpentine + opaques.*

*Table 3. Mineralogy of Veins in the Day Book Dunite.*

| | Minerals Present | | | | | | | | Texturally Stable Mineral Assemblages | | | | | |
|---|---|---|---|---|---|---|---|---|---|---|---|---|---|---|
| Sample Number | Ta | Fo | Ch | M | Tr | S | Antho | Opaque | Tr+Ta +Fo | Ta+Fo +Antho | Tr+Ta +Antho | Ta+M +Antho | Ta+Fp +M | Tr+Fo +Antho |
| 4 | M | tr | m | | | tr | tr | | X | X | X | | | |
| 10 | M | tr | m | | M | m | m | | X | X | X | | | X |
| 21A* | M | m | M | | tr | m | | | | X | | | | |
| 21B* | M | m | m | | m | tr | | | X | | | | | |
| 38 | M | M | M | | | m | | | | | | | | |
| 58 | M | tr | m | | | tr | M | | | X | X | | | |
| 63-A* | M | m | m | | m | tr | tr | | X | | X | | | |
| 63-B* | M | m | tr | | | m | | tr | | | | | | |
| 65 | M | m | tr | | M | tr | m | | X | X | X | | | |
| 69 | M | m | m | tr | m | tr | | | | | | | X | |
| 71B* | tr | m | tr | tr | M | tr | m | | | X | | X | | |
| 84A* | M | M | m | | tr | M | tr | | | | | | | |
| 84B* | M | M | m | | m | m | M | | | | | | | |
| 84C* | m | M | m | | m | tr | m | | | | | | | |
| 90A* | tr | m | M | | m | tr | | | X | | | | | |
| 90B* | m | m | M | | m | tr | | | X | | | | | |
| 90C* | M | m | m | | m | tr | tr | | | X | X | | | |
| 92 | M | m | m | | tr | tr | tr | | | X | X | | | |
| 93 | M | | M | | | tr | | | | | | | | |
| 94A* | tr | m | M | | tr | tr | tr | | X | X | | | | |
| 94B* | M | tr | m | | | tr | | | | | | | | |
| 94C* | M | tr | m | | | m | | | | | | | | |
| 94D* | M | | tr | | | m | | | | | | | | |
| 94E* | tr | tr | M | m | M | | tr | | | | | X | X | |
| 94F* | m | m | m | | M | tr | | | | | | | | |
| 94G* | M | M | m | | m | tr | tr | | | X | | | | |
| 94H* | M | tr | M | m | | tr | | | | X | | | X | |
| 94I* | M | tr | tr | M | tr | m | | tr | | | | | | |
| 94J* | M | m | tr | | m | m | tr | | | X | | | | |

M = major constituent, m = minor constituent, tr = trace amount
*Letters after sample number indicates multiple samples from the same outcrop
Ta = talc, Fo = olivine, Ch = chlorite, M = magnesite, Tr - tremolite, S = serpentine, Antho = anthophyllite,
Opaque includes chromian spinel and magnetite.

bodies and associated veins have intruded the dunite along joints.

The mineral assemblages of the veins are similar to metasomatic zones betwen pegmatite and dunite, but additionally the veins contain local segregations of

*Table 4. Composition of the Day Book Dunite.*

| | A | B | C | D |
|---|---|---|---|---|
| $SiO_2$ | 40.67 | 40.93 | 40.86 | 42.40 |
| $Al_2O_3$ | 0.75 | 1.52 | | |
| $Cr_2O_3$ | 0.32 | -- | 2.18 | 1.06 |
| $TiO_2$ | 0.01 | -- | | |
| $Fe_2O_3$ | 1.15 | 7.60 | 7.66 | 8.62 |
| FeO | 6.56 | | | |
| MgO | 48.77 | 48.77 | 49.31 | 45.92 |
| CaO | 0.00 | 0.19 | 0.00 | 0.00 |
| $Na_2O$ | 0.00 | 0.13 | -- | -- |
| $K_2O$ | 0.03 | | | |
| $H_2O$ | 0.08 | | | |
| $H_2O'$ | 1.38 | 1.09 | 0.63 | 1.23 |
| $CO_2$ | 0.12 | | | |
| NiO | 0.31 | -- | -- | -- |
| MnO | 0.12 | -- | -- | -- |
| Total | 100.27 | 100.13 | 100.64 | 99.23 |

A - dunite (Kulp and Brobst, 1954)
B - average of five commercial olivine shipments (Hunter, 1941)
C - dunite; 95% olivine, 2% chromian spinel, 2% talc, 1% chlorite (Hunter, 1941)
D - saxonite; 83% olivine, 10% tremolite, 5% chlorite, 2% chromian spinel plus traces of orthopyroxene, talc and antigorite (Hunter, 1941)

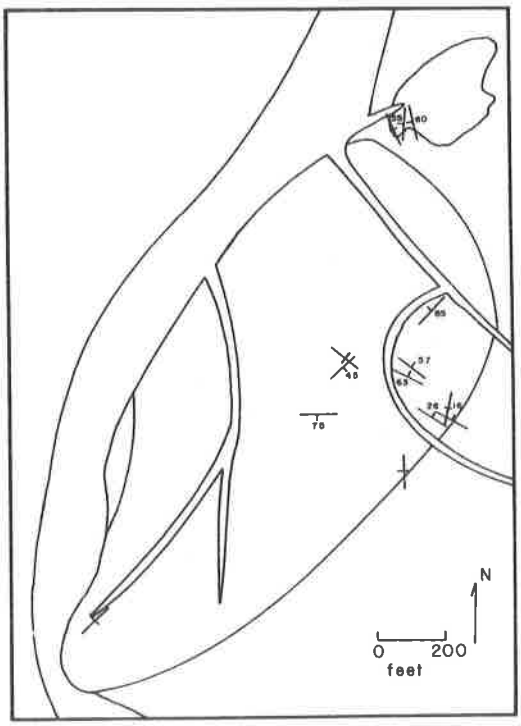


*Figure 6. Attitudes of chromian spinel layers in the dunite.*

magnesite. Much of the magnesite is coarse-grained with individual crystals up to 20 cm. Texturally stable mineral assemblages are found in different locations. Table 3 gives the plotted mineral assemblages found in the veins and the sample locations are in Figure 7.

## Bulk Composition

The chemical compositions of the Day Book dunite, given in Table 4 are those reported by Hunter (1941) and Kulp and Brobst (1954). Note that one analysis represents an average of five commercial olivine shipments from the quarry and this

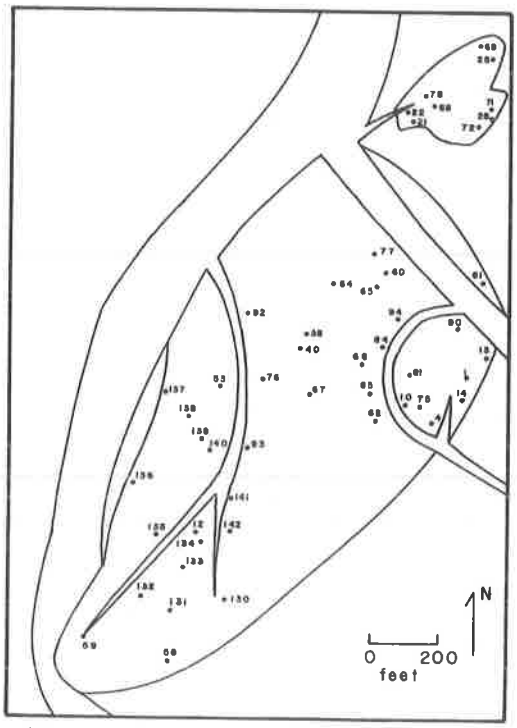


*Figure 7. Sample localities in the dunite.*

average is probably the best value for the fresh dunite at Day Book.

All of the analyzed samples contain small amounts of serpentine, chlorite,and chromian spinel. Water in the analyses is found in the serpentine or in other hydrous phases such as talc, chlorite, or tremolite. Chromian spinel and chlorite are the only abundant phases that contain significant amounts of aluminum and chromium. Tremolite is the only calcium-bearing phase in the analyzed samples. The abundances of other components (such as magnesium or nickel) can be explained by the abundance of olivine.

## Methods of Analysis

Mineral compositions were determined with an Applied Research Laboratories EMX-SM electron beam microprobe. Analyses were made on at least five different parts of several different grains per sample with an excitation potential of 15 kv. Compositional zoning was not found in any of the minerals. Raw data were corrected following the method Bence and Albee (1968). For the spinels, an estimate of ferrous-ferric content was made using a technique modified from Carmichael (1967). This technique, when applied to standards determined by wet chemistry, gives ferrous-ferric contents similar to those measured by wet chemistry. Mineral identification was checked by X-ray diffraction.

Modal analyses were done on standard thin sections for dunite and on slabs of pegmatite that were stained to distinguish plagioclase and alkali feldspar. Point spacing in the dunite analyses was 1 mm and 500 to 600 points were counter per sample. The extreme variability of the modal mineralogy of the dunite on even the handspecimen scale made determination of more points impractical.

## Anhydrous Minerals

Olivine: By far the most abundant mineral in the ultramafic rock is olivine which ranges from approximately 80 to 99 modal per cent and averages about 95 percent.

*Table 5. Composition of Olivine.*

| | A | B | C | D | E | F | G | H | I | J |
|---|---|---|---|---|---|---|---|---|---|---|
| $SiO_2$ | 42.34 | 42.05 | 41.99 | 41.79 | 41.59 | 41.26 | 40.94 | 40.43 | 40.74 | 40.88 |
| MgO | 53.73 | 53.42 | 53.45 | 52.41 | 52.34 | 51.91 | 49.70 | 50.17 | 50.19 | 49.96 |
| FeO | 4.37 | 4.48 | 4.58 | 6.42 | 6.41 | 6.31 | 7.78 | 7.27 | 7.12 | 7.15 |
| NiO | 0.53 | 0.53 | 0.53 | 0.40 | 0.42 | 0.41 | 0.44 | 0.43 | 0.40 | 0.43 |
| MnO | 0.06 | 0.06 | 0.06 | 0.09 | 0.09 | 0.09 | 0.11 | 0.10 | 0.10 | 0.10 |
| Total | 101.03 | 100.54 | 100.61 | 101.11 | 100.85 | 99.98 | 98.97 | 98.40 | 98.55 | 98.52 |
| ions in Structural formula | | | | | | | | | | |
| Si | 1.00 | 1.00 | 1.00 | 1.00 | 1.00 | 1.00 | 1.00 | 1.00 | 1.00 | 1.00 |
| Mg | 1.90 | 1.90 | 1.90 | 1.87 | 1.87 | 1.86 | 1.82 | 1.84 | 1.84 | 1.83 |
| Fe | 0.09 | 0.09 | 0.09 | 0.13 | 0.13 | 0.13 | 0.01 | 0.01 | 0.01 | 0.01 |
| Ni | 0.01 | 0.01 | 0.01 | <0.01 | <0.01 | 0.01 | 0.00 | 0.00 | 0.00 | 0.00 |
| Mn | 0.00 | 0.00 | 0.00 | <0.01 | <0.01 | <0.01 | | | | |
| %Fo | 95 | 95 | 95 | 94 | 94 | 93 | 92 | 93 | 93 | 93 |

A-C olivine associated with chromian spinel E-G of Table 6.
D-F olivine 6 associated with chromian spinel A-D of Table 6.
G-J from Carpenter and Phyfer (1975)

Most of the olivine forms a mosaic of equant polygonal grains that meet at approximately 120° triple junctions. These olivine crystals do not show kink bands or undulatory extinction and the grain size ranges from 0.05 to 2 mm and averages 0.2 mm. Within this fine grained matrix of olivine there are larger olivine grains that range up to 29 cm in length. The larger olivine grains show kink bands, undulatory extinction, and have irregular boundaries where they contact the mosaic of smaller crystals. Such a texture, larger deformed grains surrounded by a polygonal matrix, is termed porphyroclastic and is thought to represent a metamorphic texture (Pike and Schwarzman, 1977). Chemical compositions and structural formula of olivine from the Day Book dunite are given in Table 5. Olivine from the Day Book dunite does not show any compositional zoning. Individual olivine grains are homogeneous. Additionally, no significant variation in olivine composition exists within the dunite body (Carpenter and Phyfer, 1975). Compositional differences shown in Table 5 are apparently the result of different analytical facilities and data reduction procedures.

Day Book olivine compositions are typical of the high-magnesium olivines from alpine ultramafic rocks (Moores and MacGregor, 1972). The high-magnesium content and restricted range of compositions of olivine in alpine ultramafic rocks contrast with the wider compositonal range (including more iron-rich varieties) of olivines from stratiform ultramafic rocks. Similar magnesium-rich olivine compsitions are found in the alpine ultramafic rocks of active tectonic belts (Challis, 1965; Loney et al., 1971) and older mountain systems, such as the Appalachians.

Chromian Spinel: Chromian spinel, which occurs as an accessory phase in the Day Book dunite, generally makes up less than one percent of the rock. Local layers and pods are dominately chromian spinel. Subhedral to euhedal octahedra characterize the chromian spinel in the dunite. Often the chromian spinel is surrounded by kämmererite, a chromian chlorite.

The chemical compositions of chromian spinels from the Day Book dunite are given in Table 6. Iron in the electron microprobe analyses was determined as total iron and the amount of FeO and $Fe_2O_3$ was calculated based on a method modified from Carmichael (1967).

Chromian spinels from the Day Book dunite show a relatively large range of compositions in comparison to olivine. The range in composition is due largely to differences in cation ratios of $Cr/(Cr+Al+Fe^{+3})$ and to a lesser extent $Mg/(Mg+Fe^{+2})$. This compositional difference is shown on Figure 8 along with data for the chromian spinels from the Burro Mountain peridotite, a typical alpine-type ultramafic from the Coast Ranges of California (Loney et. al., 1971). Chromian spinels from the Day Book dunite show the same compoitional trend as typical alpine-type ultramafics. One chromian spinel does not fall on the typical alpine-ultramafic trend. This is a chip sample across a chromian spinel layer that was analyzed by wet chemistry (Hunter, et al., 1942). The different composition may reflect a difference in the analytical method. Alternatively, this abhorrent chromian spinel may be part of a different compositional trend.

Fletcher and Carpenter (1972) suggest that chromian spinels from the Day Book

*Table 6. Composition of Chromian Spinel.*

| | A | B | C | D | E | F | G | H | I | J |
|---|---|---|---|---|---|---|---|---|---|---|
| $Cr_2O_3$ | 62.43 | 62.82 | 62.34 | 62.03 | 58.88 | 58.86 | 58.78 | 44.20 | 55.5 | 57.2 |
| $Al_2O_3$ | 5.98 | 6.80 | 5.98 | 5.24 | 12.72 | 11.80 | 12.68 | 21.30 | -- | -- |
| $Fe_2O_3$* | 4.57 | 3.43 | 4.24 | 5.04 | 2.32 | 2.66 | 2.46 | | | |
| FeO | 19.30 | 18.97 | 20.32 | 19.50 | 14.31 | 14.51 | 14.21 | 20.05 | 19.6 | 20.0 |
| MgO | 9.13 | 9.43 | 8.15 | 8.75 | 13.07 | 12.69 | 13.21 | 14.48 | -- | -- |
| MnO | 0.16 | 0.56 | 0.60 | 0.62 | 0.45 | 0.46 | 0.46 | -- | -- | -- |
| Total | 101.57 | 102.01 | 102.14 | 101.18 | 101.75 | 100.98 | 101.80 | 100.03 | 75.10 | 77.20 |
| ions in formula + | | | | | | | | | | |
| Cr | 13.16 | 13.16 | 13.21 | 13.18 | 11.75 | 11.90 | 11.73 | -- | -- | -- |
| Al | 1.88 | 2.12 | 1.89 | 1.69 | 3.79 | 3.56 | 3.77 | -- | -- | -- |
| $Fe^{+3}$ | 0.92 | 0.68 | 0.86 | 1.04 | 0.44 | 0.51 | 0.47 | -- | -- | -- |
| $Fe^{+2}$ | 4.30 | 4.20 | 4.67 | 4.45 | 3.02 | 3.10 | 3.00 | -- | -- | -- |
| Mg | 3.63 | 3.73 | 3.26 | 3.56 | 4.92 | 4.84 | 4.94 | -- | -- | -- |
| Mn | 0.14 | 0.13 | 0.14 | 0.14 | 0.10 | 0.10 | 0.10 | -- | -- | -- |
| $\epsilon R^{+3}$ | 15.96 | 15.96 | 15.96 | 15.91 | 15.98 | 15.97 | 15.97 | -- | -- | -- |
| $(Cr/Cr+Al+Fe^{+3})$ | 0.82 | 0.82 | 0.83 | 0.83 | 0.74 | 0.75 | 0.73 | -- | -- | -- |
| $(Al/Cr+Al+Fe^{+3})$ | 0.12 | 0.13 | 0.12 | 0.11 | 0.24 | 0.22 | 0.24 | -- | -- | -- |
| $(Fe^{+3}/Cr+Al+Fe^{+3})$ | 0.06 | 0.04 | 0.05 | 0.07 | 0.03 | 0.03 | 0.03 | -- | -- | -- |
| $\epsilon R^{+2}$ | 8.07 | 8.06 | 8.10 | 8.15 | 8.04 | 8.04 | 8.04 | -- | -- | -- |
| $(Mg/Mg+Fe^{+2})$ | 0.46 | 0.47 | 0.41 | 0.44 | 0.62 | 0.61 | 0.62 | -- | -- | -- |
| $(Fe^{+2}/Fe^{+2}+Fe^{+3})$ | 0.82 | 0.86 | 0.84 | 0.81 | 0.87 | 0.86 | 0.86 | -- | -- | -- |
| | K | L | M | N | O | P | Q | R | S | T |
| $Cr_2O_3$ | 60.55 | 61.84 | 57.20 | 58.49 | 66.55 | 60.23 | 61.00 | 59.07 | 61.62 | 60.86 |
| $Al_2O_3$ | 5.24 | 7.63 | 4.56 | 10.00 | 5.29 | 3.11 | 7.51 | 10.54 | 7.63 | 9.68 |
| $Fe_2O_3$ | | | | | | | | | | |
| FeO | 26.39 | 21.87 | 29.18 | 20.86 | 19.69 | 28.45 | 20.52 | 18.32 | 19.56 | 16.68 |
| MgO | 6.87 | 8.51 | 7.81 | 10.13 | 9.24 | 8.17 | 10.77 | 11.43 | 11.93 | 12.38 |
| MnO | 0.38 | 0.44 | 0.43 | 0.43 | 00.35 | 0.50 | 0.30 | 0.35 | 0.30 | 0.37 |
| Total | 99.52 | 100.35 | 99.40 | 100.10 | 101.18 | 100.59 | 100.23 | 99.80 | 101.17 | 100.07 |
| ions in formula+ | | | | | | | | | | |
| Cr | 13.25 | 13.14 | 12.45 | 12.18 | 14.12 | 13.02 | 12.77 | 12.21 | 12.69 | 12.54 |
| Al | 1.71 | 2.42 | 1.48 | 3.13 | 1.67 | 1.00 | 2.34 | 3.25 | 2.34 | 2.98 |
| $Fe^{+3}$ | 1.01 | 0.41 | 1.98 | 0.64 | 0.18 | 1.93 | 0.84 | 0.51 | 0.92 | 0.45 |
| $Fe^{+2}$ | 5.09 | 4.50 | 4.70 | 3.93 | 4.22 | 4.55 | 3.68 | 3.47 | 3.31 | 3.18 |
| Mg | 2.83 | 3.41 | 3.20 | 3.98 | 3.70 | 3.33 | 4.25 | 4.46 | 4.61 | 4.74 |
| Mn | 0.09 | 0.10 | 0.10 | 0.10 | 0.08 | 0.12 | 0.07 | 0.08 | 0.07 | 0.08 |
| $R^{+3}$ | 15.97 | 15.97 | 15.91 | 15.95 | 15.97 | 15.95 | 15.95 | 15.97 | 15.95 | 15.97 |
| $(Cr/Cr+Al+Fe^{+3})$ | 0.83 | 0.82 | 0.79 | 0.76 | 0.89 | 0.82 | 0.80 | 0.77 | 0.79 | 0.78 |
| $(Al/Cr+Al+Fe^{+3})$ | 0.11 | 0.15 | 0.09 | 0.20 | 0.10 | 0.06 | 0.15 | 0.20 | 0.15 | 0.19 |
| $(Fe^{+3}/Cr+Al+Fe^{+3})$ | 0.06 | 0.03 | 0.12 | 0.04 | 0.01 | 0.12 | 0.05 | 0.03 | 0.06 | 0.03 |
| $R^{+2}$ | 8.01 | 8.01 | 8.00 | 8.01 | 8.00 | 8.00 | 8.00 | 8.01 | 7.99 | 8.00 |
| $(Mg/Mg+Fe^{+2})$ | 0.36 | 0.43 | 0.41 | 0.50 | 0.47 | 0.42 | 0.54 | 0.56 | 0.58 | 0.60 |
| $(Fe^{+2}/Fe^{+2}+Fe^{+3})$ | 0.83 | 0.92 | 0.70 | 0.86 | 0.96 | 0.70 | 0.81 | 0.87 | 0.78 | 0.88 |

K-T From Carpenter and Fletcher,(1979)

| | U | V | W | X | Y | Z | AA | BB | CC | DD |
|---|---|---|---|---|---|---|---|---|---|---|
| $Cr_2O_3$ | 61.07 | 60.23 | 61.12 | 61.43 | 60.78 | 60.18 | 59.97 | 60.54 | 60.54 | 60.64 |
| $Al_2O_3$ | 10.20 | 10.75 | 10.20 | 9.99 | 9.68 | 9.35 | 10.30 | 10.93 | 10.15 | 10.45 |
| $Fe_2O_3$ | | | | | | | | | | |
| FeO | 15.47 | 16.03 | 16.05 | 16.21 | 17.66 | 17.30 | 16.65 | 15.70 | 17.72 | 16.52 |
| MgO | 12.97 | 13.29 | 12.95 | 12.50 | 12.39 | 12.28 | 12.76 | 13.20 | 11.53 | 12.64 |
| MnO | 0.26 | 0.36 | 0.34 | 0.32 | 0.32 | 0.31 | 0.28 | 0.30 | 0.38 | 0.33 |
| Total | 100.08 | 100.79 | 100.71 | 100.50 | 100.89 | 99.48 | 100.07 | 100.75 | 100.40 | 100.68 |
| ions in formula+ | | | | | | | | | | |
| Cr | 12.48 | 12.17 | 12.42 | 12.50 | 12.40 | 12.46 | 12.26 | 12.24 | 12.46 | 12.34 |
| Al | 3.10 | 3.24 | 3.09 | 3.03 | 2.94 | 2.88 | 3.14 | 3.30 | 3.11 | 3.17 |
| $Fe^{+3}$ | 0.37 | 0.54 | 0.47 | 0.45 | 0.62 | 0.66 | 0.56 | 0.43 | 0.40 | 0.46 |
| $Fe^{+2}$ | 2.95 | 2.86 | 2.98 | 3.03 | 3.17 | 3.12 | 3.02 | 2.91 | 3.44 | 3.07 |
| Mg | 4.99 | 5.06 | 4.96 | 4.80 | 4.77 | 4.79 | 4.92 | 5.03 | 4.47 | 4.85 |
| Mn | 0.06 | 0.08 | 0.07 | 0.07 | 0.07 | 0.07 | 0.06 | 0.06 | 0.08 | 0.07 |
| $R^{+3}$ | 15.95 | 15.95 | 15.98 | 15.98 | 15.96 | 16.00 | 15.96 | 15.97 | 15.97 | 15.97 |
| $(Cr/Cr+Al+Fe^{+3})$ | 0.79 | 0.77 | 0.78 | 0.78 | 0.78 | 0.78 | 0.76 | 0.76 | 0.78 | 0.77 |
| $(Al/Cr+Al+Fe^{+3})$ | 0.19 | 0.20 | 0.19 | 0.19 | 0.18 | 0.18 | 0.20 | 0.21 | 0.19 | 0.20 |
| $(Fe^{+3}/Cr+Al+Fe^{+3})$ | 0.02 | 0.03 | 0.03 | 0.03 | 0.04 | 0.04 | 0.04 | 0.03 | 0.03 | 0.03 |
| $R^{+2}$ | 8.00 | 8.00 | 8.01 | 7.90 | 8.01 | 7.98 | 8.00 | 8.00 | 7.98 | 7.99 |
| $(Mg/Mg+Fe^{+2})$ | 0.63 | 0.64 | 0.62 | 0.61 | 0.60 | 0.61 | 0.62 | 0.63 | 0.57 | 0.61 |
| $(Fe^{+2}/Fe^{+2}+Fe^{+3})$ | 0.89 | 0.84 | 0.86 | 0.87 | 0.84 | 0.83 | 0.84 | 0.87 | 0.90 | 0.87 |

U-DD From Carpenter and Fletcher (1979)

A-D Sample 22, dessemínated chromian spinel, associated with olivine A-C of Table 5.
E-G Podiform chromian spinel from quarry rubble, associated with olivine D-F of Table 5.
H- From Hunter, Murdoc, and MacCarthy (1942)
I&J - From Bentzen (1970)
*Calculated from $Fe_{total}$ = FeO based on the method of Carmichael (1967)
+Based on 32 oxygen atoms

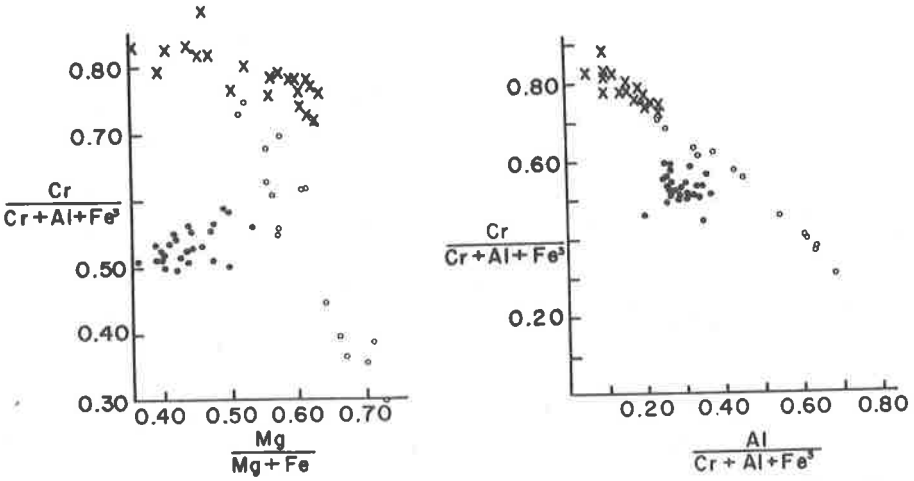


*Figure 8. Comparison of chromian spinel compositions from Day Book (X's), Burro Mt. peridotite (open circles; Loney, et al., 1971) and Stillwater complex (closed circles; Jackson, 1969).*

*Table 7. Composition of Chlorite.*

| | A | B | C | D | E |
|---|---|---|---|---|---|
| $SiO_2$ | 31.47 | 32.59 | 32.79 | 32.87 | 34.29 |
| $Al_2O_3$ | 15.64 | 13.03 | 13.11 | 13.43 | 12.22 |
| $Cr_2O_3$ | 2.82 | 3.78 | 4.07 | 3.80 | 6.39 |
| FeO | 1.72 | 1.41 | 1.40 | 1.43 | 1.33 |
| MgO | 31.95 | 32.85 | 32.54 | 32.76 | 33.82 |
| MnO | 0.01 | 0.01 | 0.01 | 0.01 | 0.01 |
| CaO | -- | -- | -- | -- | 0.02 |
| NiO | 0.27 | 0.22 | 0.21 | 0.22 | 0.43 |
| $Na_2O$ | -- | -- | -- | -- | 0.08 |
| $K_2O$ | -- | -- | -- | -- | 0.01 |
| $H_2O$ | -- | -- | -- | -- | 12.56 |
| Total | 83.88 | 83.89 | 84.13 | 84.52 | 101.16 |

A-D associated with podiform chromian spinel (E-G, Table 6) and olivine (D-F, Table 5).
E - from McCormick (1975)

dunite show two compositional trends. One trend of disseminated grains parallels the Burro Mountain trend on a MgO/RO vs. $Cr_2O_3/R_2O_3$ plot while massive chromian spinels from the pods define a trend described as a constant $Cr_2O_3/R_2O_3$ ratio with a variable MgO/RO ratio similar to chromian spinels from stratiform ultramafic complexes, such as the Stillwater Complex. Fletcher and Carpenter (1972) believe that this difference in chromian spinel compositions is due to partial recrystallization, wherein disseminated chromian spinels recrystallized during regional metamorphism while the massive pods of chromian spinel escaped the metamorphism. A difference in composition between chromian spinels with different textures was not confirmed in the present study (Figure 8, Table 6).

Analyses of disseminated and massive chromian spinel from several ultramafic bodies in western North Carolina do not show any significant difference between the different textural varieties (Carpenter and Fletcher, 1979). Trends described by Fletcher and Carpenter (1972) for the chromian spinels from the Day Book dunite are not apparent from the data of Carpenter and Fletcher (1979) as shown in Figure 8. Disseminated and massive chromian spinels compositions from the Day Book dunite follow the trend defined by chromian spinels of the alpine-type ultramafic bodies.

Associated with the chromian spinel is a chromian chlorite, kämmererite. This chlorite is found along the margins of both disseminated and massive (podiform) chromian spinel grains. Textural relations (Fig. 9) suggest that the kämmererite formed from the chromian spinel during metamorphism.

Compositions of the kämmererite from the Day Book dunite are given in Table 7. The chlorites are enriched in aluminum and magnesium relative to the associated chromian spinel. Presumably disseminated chromian spinels would be more susceptible

to recrystallization than the massive chromian spinels. Indeed, many of the disseminated chromian spinels are mantled by epitaxial kämmererite suggesting recrystallization of these spinels accompanied by a loss of magnesium and aluminum. However, kämmererite is also associated with the more massive chromian spinels (McCormick, 1975) and this together with the single compositional trend defined by the Day Book samples (Fig. 8) suggests both disseminated and massive chromian spinels reequilibrated with the kämmererite.

Cation Distribution Between Olivine and Chromian Spinel. The distribution of Mg and $Fe^{+2}$ between coexisting olivine and chromian spinel may be used as geothermometer (Irvine, 1965; Jackson, 1969). The exchange reactions for the chromian spinel end members can be combined to give

$$Fe^{+2}Si_{0.5}O_4 + Mg(Cr_\alpha Al_\beta Fe_\delta^{+3})_2O_4 = MgSi_{0.5}O_4 + Fe^{+2}(Cr_\alpha Al_\beta Fe_\delta^{+3})_2O_4 \quad (1)$$

where $\alpha + \beta + \delta = 1$ and represent the mole fractions of the trivalent cations in the spinel. Following Irvine (1965) and Jackson (1969), the equilibrium distribution coefficient for the exchange reaction between olivine and chromian spinel is

$$Kd = \frac{X_{Mg}^{ol} \quad X_{Fe^{+2}}^{chr}}{X_{Fe^{+2}}^{ol} \quad X_{Mg}^{chr}} \quad (2)$$

where $X_{Mg}^{ol}$ and $X_{Fe^{+2}}^{ol}$ are the mole fractions of the olivine end members $FeSi_{0.5}O_2$ and $MgSi_{0.5}O_2$, $X_{Mg}^{chr}$ and $X_{Fe^{+2}}^{chr}$ are the mole fractions of $Mg(Cr_\alpha Al_\beta Fe_\delta)_2O_4$ and $Fe(Cr_\alpha Al_\beta Fe_\delta)_2O_4$ in chromian spinel. Jackson (1969) has compiled the standard Gibbs free energy data for the end members of the olivine-chromian spinel series and derived a geothermometer based on coexisting olivine and chromian spinel as given by

$$T^o = \frac{5580\alpha + 1018\beta - 1720\delta + 2400}{0.90\alpha + 2.56\beta - 3.08\delta - 1.47 + 1.987 \ \ln Kd} \quad (3)$$

with T in degrees Kelvin $\alpha$, $\beta$ and $\delta$ defined by equation (1) and Kd defined in equation (2). Substitution of this value along with the composition of trivalent cations in the olivine and chromian spinel into equation (3) yields an estimate of the temperature of equilibration of the olivine and spinel. Temperature of crystallization obtained from this equation for coexisting olivine and chromian spinel from the Day Book dunite range from 1070 to 1184°C with an average of 1141°C. Jackson (1969) tabulates the uncertainties in the standard free energy measurements in the olivine and chromian spinel series and estimates a uncertainty in temperatures measured with equation (6) of $\pm$ 300°C. Clearly the variation of temperatures calculated for the Day Book dunite is not significant.

An alternative approach to Mg-$Fe^{+2}$ distribution between olivine and coexisting chromian spinel is given by Irvine (1965). The technique used thermodynamic data to calculate "equipotential surfaces" which represent theoretical equilibrium compositions for coexisting olivine and chromian spinel. Comparison of natural samples to the theoretical results gives an indication of attinment of equilibrium between olivine and chromian spinel (Loney et al., 1971).

Distribution of the analyzed olivine-chromian spinels from the Day Book dunite show a fairly close agreement to the calculated equipotential lines (Fig. 10). However, all of the values fall below the equipotential line that corresponds to the olivine in the samples. In other words, the chromian spinels from the Day Book dunite coexist with more Mg-rich olivine than predicted from the thermodynamic calculations of Irvine (1965). A certain amount of scatter is common the equipotential plots (Loney et al., 1971), but the scatter is random and not the systematic pattern shown on Figure 10. Several possibilities may explain the compositional pattern shown on Figure 10, for example, the olivine may have been enriched in Mg, the chromian spinel may have been depleted in Cr or Mg. However, the association of kämmererite with the chromian spinel (Fig. 9) discussed previously suggests the formation of this Mg-rich chlorite (Table 7) depleted the spinel in Mg thus explaining the pattern observed on Figure 10. Formation of kämmererite also requires other components from the spinel (such as Al and Cr, Table 7), but the high Mg-content of the chlorite relative to these other components shows the greatest effect on chromian spinel compositions accompanying chlorite formation will be a decrease in the Mg-content. The pattern on Figure 10

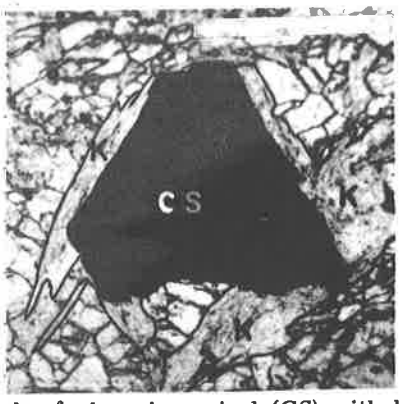


*Figure 9. Photomicrograph of chromian spinel (CS) with kämmerite overgrowth (K). White bar is 1.0 mm.*

*Table 8. Mineralogy of the Day Book Dunite.*

| Sample Number | %Fo | %Opx | % Opaque | %S | %Ta | %Ch | %Tr | % Antho | Tr+Ta +Fo | Ta+Fo +Antho | Tr+Ta +Antho | Tr+Fo+ Antho | Ta+Fo +Opx | Tr+Fo +Opx | Fo+Ta+ M | Tr+Ta +Opx |
|---|---|---|---|---|---|---|---|---|---|---|---|---|---|---|---|---|
| 1 | 83 | 1 | 1 | 1 | 11 | 3 | 2 | 1 | X | | | | | | | |
| 13 | 95 | | 1 | 3 | | 1 | | | | | | | | | | |
| 25 | 91 | 1 | tr | 1 | 1 | 3 | 2 | 1 | | | | | X | X | | X |
| 38 | 80 | tr | tr | 14 | 5 | 1 | | | | | | | X | | | |
| 53 | 64 | tr | 1 | 29 | 5 | 1 | | 1 | | | | | X | | X | |
| 58 | 92 | | 1 | 1 | 5 | 1 | 1 | | X | X | X | | | | | |
| 59A* | 98 | | 1 | tr | 2 | 1 | | | | | | | | | | |
| 59B* | 95 | | 1 | 1 | 1 | 1 | 1 | | | | | | | | | |
| 60A* | 84 | tr | 1 | 2 | 10 | 3 | tr | 1 | X | | | | X | | | |
| 60B* | 81 | | 1 | 4 | 7 | 6 | 1 | 1 | X | | | | | | | |
| 61 | 67 | tr | 1 | 26 | 4 | 2 | tr | tr | | | | | X | | | |
| 62 | 87 | tr | 2 | 11 | tr | 1 | | | | | | | | | | |
| 63 | 86 | | 1 | 5 | 4 | 1 | 2 | 2 | X | | | X | | | | |
| 64 | 89 | | tr | 8 | 1 | 1 | 1 | | X | | | | | | | |
| 66 | 85 | tr | tr | 4 | 4 | 4 | 1 | 2 | X | | | | X | | | X |
| 67 | 82 | | tr | 1 | 10 | 2 | 2 | 1 | X | | | | | | | |
| 68 | 78 | | 1 | 3 | 12 | 3 | tr | 3 | | X | | | | | | |
| 69 | 73 | | tr | 6 | 10 | 6 | 2 | 2 | | | X | | | | X | |
| 71 | 82 | 3 | tr | 1 | | 12 | 1 | | | | | | X | | | |
| 72 | 75 | | 1 | 23 | 1 | 1 | | | | | | | | | | |
| 76 | 91 | tr | tr | 2 | 18 | 5 | 3 | 2 | | | | | | | | |
| 77 | 89 | 4 | tr | 2 | 1 | 2 | 3 | 1 | | | | | | X | | |
| 78 | 97 | | 1 | 2 | 1 | 1 | 1 | | | | | | | | | |
| 81 | 90 | tr | 1 | 4 | 2 | 2 | 2 | 4 | X | X | | | | | | |
| 90 | 70 | 1 | tr | 2 | 18 | 5 | 3 | 2 | X | X | | | | | | |
| 92 | 89 | tr | 2 | tr | 5 | 2 | 1 | tr | | X | | | X | | | |
| 130 | 80 | 1 | tr | 10 | 9 | 1 | 1 | | | | | | | | | |
| 131 | 90 | | 1 | 1 | 7 | 1 | 1 | | X | | | | | | | |
| 132 | 99 | | 1 | 1 | | 1 | | | | | | | | | | |
| 133 | 84 | | 1 | 1 | 12 | 2 | 1 | tr | X | X | X | | | | | |
| 134 | 92 | | 2 | 5 | | 1 | tr | | | | | | | | | |
| 135 | 85 | | 1 | 1 | 11 | 2 | 1 | | X | | | | | | | |
| 136 | 62 | | 1 | 30 | 6 | 1 | 1 | | X | | | | | | | |
| 137 | 65 | 13 | 1 | 8 | 4 | 6 | 4 | | X | | | X | | | | |
| 138 | 83 | | tr | 3 | 10 | 3 | 1 | tr | X | | X | | | | | |
| 139 | 91 | | 1 | 1 | 4 | 4 | 1 | | X | | | | | | | |
| 140 | 95 | | 1 | 1 | 2 | 1 | | | | | | | | | | |
| 141 | 86 | | 1 | 2 | 9 | 1 | 2 | 1 | X | | X | | | | | |
| 142 | 72 | | 1 | 2 | 22 | 4 | 4 | | | | | | | | | |

suggests disequilibrium between the chromian spinel and olivine from the Day Book dunite, probably related to the formation of chlorite from the spinel. In light of this, the significance of the temperatures calculated from equation (3) based on an equilibrium coexistence of olivine and chromian spinel is open to discussion.

Orthopyroxene: Distribution of small amounts of fine-grained (generally less than 1 mm), subhedral enstatite (Table 8) does not form any apparent pattern in the dunite. Much of the orthopyroxene is included within the porphyroclastic olivine texture. However, in some samples, orthopyroxenes form grains up to 5 mm in maximum dimension with irregular grain boundaries similar to the olivine porphyroblasts. The orthopyroxene has a low birefrigence, parallel extinction and is not pleochroic. Enstatite is texturally stable with several of the metamorphic minerals including talc, tremolite and chlorite.

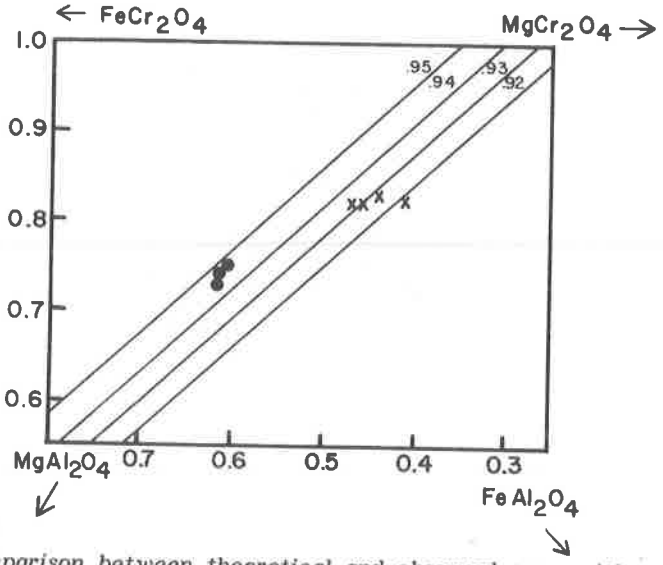


*Figure 10. Comparison between theoretical and observed compositions of olivine and chromian spinel in the Day Book dunite. Lines are intersections of theoretical Mg-$Fe^{+2}$ equipotential surfaces for olivine with cation fractions of Mg of 0.95, 0.94, 0.93 and 0.92 at 1200°C. Crosses represent olivine with an average cation fraction of Mg of 0.935 (D-F, Table 5) and dots represent olivine with an average cation fraction of Mg of 0.955 (A-C, Table 5), different data points represent different chromian spinel grains within the samples.*

## Volatile-Bearing Minerals

Talc, chlorite serpentine, tremolite, anthophyllite, and magnesite are all found as metamorphic products withjn the dunite. Modal amounts of these minerals vary greatly over relatively small areas and values listed in Table 8 should only be regarded as an estimate of a variable population. All of these minerals contain a volatile component (either $H_2O$ or $CO_2$) and the variability of the modal mineralogy is probably related to the fluid distribution during the metamorphism. The abundance of volatilte-bearing phases increases greatly near the veins and pegmatites that transect the dunite bodies.

Dunite: At least three varieties of phyllosilicates are associated with the dunite. Talc forms anhedral grains that reach several centimeters in their largest dimension and occurs in the dunite and as an important constituent of talc schist associated with the pegmatites. Talc is found in textural equilibrium with olivine and orthopyroxene plus many of the other metamorphic minerals in the dunite (Table 8). In many cases, talc is found replacing anthophyllite along cleavage planes, resulting in talc with a fibrous habit. Chlorite found in the dunite is light brown in color and does not show pleochroism. The chlorite forms subhedral to anhedral grains up to a centimeter across in the dunite and epitaxial overgrowths occur on chromian spinel. Analyses of the chlorite (Table 7) show the material to be kämmererite. Serpentine forms coronas around olivine grains in the dunite. As the amount of serpentine increases, the color of the dunite changes from light green to black. The serpentine is younger than other metamorphic minerals such as talc or tremolite, as indicated by cross-cutting relations and local replacement of these minerals by serpentine.

Tremolite and anthophyllite are found in the Day Book dunite as euhedral to subhedral crystals up to four centimeters long (Table 8). Tremolite forms blade-like crystals with an inclined extinction. Anthophyllite occurs in acicular masses with parallel extinction. Some tremolite crystals show an overgrowth of anthophyllite. These overgrowths on tremolite may be magnesiocummingtonite rather than antho-phyllite (Evans, 1977; Whitney, personal communication, 1977). Both of these amphiboles are also found in the contact zone between the pegmatitic rocks and the dunite (Fig. 5).

*Table 9. Composition of Magnetite.*

| | |
|---|---|
| $TiO_2$ | 0.04 |
| $Al_2O_3$ | 0.01 |
| $Cr_2O_3$ | 0.00 |
| $Fe_2O_3$* | 64.58 |
| FeO | 34.45 |
| MnO | 0.04 |
| MgO | 0.22 |
| NiO | 0.00 |
| Total | 99.34 |

Sample from a serpentine-filled fracture at location 63 on Figure 2.
*Calculated from $Fe_{total}$ = FeO based on the method of Carmichael (1967).

Other metamorphic minerals found in the dunite are confined to zones of extensive alteration and include magnetite and magnesite. In dunite that shows extensive serpentinization, octahedra of magnetite to 0.5 mm are found with the serpentine. Magnesite is found in some dunite samples and is associated with extensive development of talc and amphiboles. The carbonate forms anhedral grains up to 4 cm across which shows good rhombohedral cleavage and a very high relief.

Veins: The mineralogy of the veins is very similar to that of the dunite, but the modes vary considerably between dunite and veins. The modes of the veins are dominated by talc, but also include subordinate amounts of tremolite, anthophyllite, olivine, magnesite, serpentine and chlorite. The veins show crude zonation from a olivine-amphibole margins to talc $\pm$ magnesite interiors. Many of the veins do not contain magnesite, but when magnesite is present, it is found in the central portion of the veins.

The veins and dunite also differ in grain size. Minerals in the veins are coarser-grained than their counterparts in the dunite. For example, magnesite in the veins forms crystals up to 20 cm across whereas the largest magnesite crystal found in the dunite is 4 cm in maximum dimension. The dominance of fluid-bearing phases and the coarser grain size in the veins suggests formation in more fluid-rich evironment than the bulk of the dunite.

Joint and Shear-Zone Fillings: A third group of metamorphic minerals is found as joint coatings and fracture fillings that cross-cut the dunite and its associated veins. The most common minerals in these fractures are serpentines. Long fiber, white asbestiform serpentine fills a shear zone in the smaller of the two dunite bodies (Fig. 3). Another shear zone in the larger dunite mass contains serpentine, magnetite, and chalcedony. Joint surfaces in the dunite are also coated with serpentine, chalcedony, aragonite and magnetite (Table 9). Tien (1977) described fracture fllings of aragonite, dolomite, magnesite and huntite from the Day Book dunite formed during weathering. With the exception of aragonite, which forms radiating clusters with crystals up to 2 cm long, the carbonates are all fine-grained and in this respect differ from the coarse-grained magnesite found in the veins.

## PETROGENESIS OF THE DUNITE

### Primary Features

Few of the structural, mineralogic or petrologic features of the Day Book dunite can be uniquely related to either the initial intrusion, tectonic emplacement or subsequent deformation of the ultramafic body. Concentration of chromian spinel into layers and pods most likely represents a primary magmatic feature. Carpnter and Fletcher (1979) argue that the chromian spinels from pods in Southern Appalachian ultramafics yield compositional trends consistent with magmatic crystallization, while disseminated chromian spinel appears to have suffered subsolidus recrystallization. Results of the present study suggest that both disseminated and massive chromian spinel from the Day Book dunite define a single compositional trend related to recrystallization. Thus, the structure of the layered chromian spinel at Day Book appears to be a primary feature of magmatic crystallization, but the compositon has

been modified by post-magmatic recrystallization perhaps associated with the folding of the chromian spinel layers.

Dominance of olivine, chromian spinel, and enstatite in the dunite (Table 8) might be used as an argument for a primary magmatic origin of the ultramafic rock. However, other clearly metamorphic minerals such as talc, tremolite and chlorite are also common in the dunite and the significance of modal mineralogy is thus open to question. Tremolite is a very common, Ca-bearing phase in the dunite, suggesting that a Ca-bearing magmatic mineral may have been originaly present in the dunite. Considering the abundance of olivine and the calcium content of the dunite (as evidenced by the presence of tremolite and the dunite bulk compositon, Table 4), original magmatic mineralogy of the dunite is best approximated by olivine + orthopyroxene + clinopyroxene + chromian spinel.

Textural relations of olivine in ultramafic rocks from the Southern Appalachians have been attributed, at least in part, to crystallization and recrystallization in the mantle (Sailor and Kuntz, 1972; Bluhm and Zimmerman, 1977; Hahn and Hemlich, 1977). Olivine in many of the ultramafics occurs as coarse to very coarse-grained porphyroblasts with kink bands and irregular grain boundaries surrounded by a fine-grained granoblastic polygonal fabric of undeformed olivine. The olivine porphyroblasts are thought to represent a relic texture, whereas the finer-grained polygonal grains are clearly a recrystallization texture (Spry, 1969). To the authors' knowledge all of the petrofabric studies on olivine from the Southern Appalachians have utilized these polygonal recrystallization textures and have not distinguished between different types of textures in petrofabric analyses. Thus, the significance of such studies is questionable. Clearly the fabric measured is a recrystallization texture, but where did this recrystallization take place? Did it occur deep in the mantle, near the magmatic source, in the mantle during diapiric rise, in the crust during emplacement or is the texture the result of some subsequent metamorphic epsiode that took place after the emplacement of the ultramafic body in the crust? The complex textures found in the ultramafics seems to argue for recrystallization during more than one deformation (Bluhm and Zimmerman, 1977). However, until petrofabric analyses of texturally different coexisting olivines are combined with detailed structural studies of the surrounding country rocks, it will be very difficult to distinguish between mantle emplacement or post emplacement recrystallization textures in the ultramafic rocks.

The presence of large olivine porphyroblasts does indicate a relict texture, but a relic of what? The general argument is that these large deformed grains represent mantle-derived material, deformed during emplacement, which escaped recrystallization (Misra and Keller, 1978). However, work with metamorphic olivine has shown that large porphyroblasts of olivine can be developed during the prograde metamorphism of low grade ultramafic rocks (Evans and Trommsdorff, 1974; Vance and Dungan, 1977). It thus appears possible that these porphyroblasts may represent olivine formed during prograde metamorphism and that the granoblastic-polygonal olivine could represent recrystallization during cooling or during a subsequent metamorphic event. In contrast to this interpretation, Lappin (1967) found that olivine porphyroblasts and granoblastic-polygonal olivine in ultramafic rocks from Norway had significantly different fabrics and he argued against a prograde-retrograde metamorphic origin for the two olivine textures. Clearly, more work is needed on olivine petrofabrics from the Southern Appalachians, before a primary or secondary origin can be ascribed to these textures.

## Metamorphism of the Day Book Dunite

Ultramafic rocks at Day Book have been metamorphosed as indicated by the abundance of metamorphic minerals in the dunite (Table 8), textural equilibrium between the metamorphic minerals, and the granoblastic-polygonal olivine fabric developed by recrystallization. The homogeneity of the dunite texture and minerals (no zoning was detected either optically or in the microprobe analyses), together with the repeated occurrence of rather simple mineral assemblages (forsterite + talc + tremolite, Table 8 for example) strongly argues for attainment of equilibrium during metamorphism of the Day book dunite (Evans and Trommsdorf, 1970). The

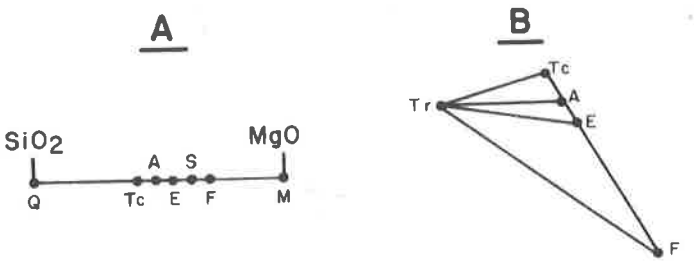


*Figure 11. Compositional relations in the volatile-free portion of the system MgO-$SiO_2$-$H_2O$-$CO_2$ (A) and a portion of the system CaO-MgO-$SiO_2$ (B). Phases shown include quartz (Q), talc (Tc), anthophyllite (A), orthopyroxene (E), serpentine (S), olivine (F), magnesite (M), and tremolite (Tr).*

metamorphism appears to have been, with the exception of the volatile components $H_2O$, $CO_2$, and $O_2$, isochemical as evidenced by the dominance of $SiO_2$-poor (i.e., forsterite-bearing) assemblages in the dunite. An obvious exception to this argument for isochemical metamorphism is the monomineralic metasomatic contact zones associated with the country rock and pegmatite contacts.

The bulk composition of the dunite, plus the relatively simple mineral compositions, permits a close comparison to the synthetic system MgO-$SiO_2$-$H_2O$-$CO_2$ or, for the tremolite-bearing assemblages, with the system CaO-MgO-$SiO_2$-$H_2O$ (Evans and Trommsdorf, 1974; and Evans, 1977). Most reactions involving Mg-rich silicates in these ultramafic systems are changed little in P-T-$X_{fluid}$ space by the presence of small amounts of FeO (Evans and Trommsdorff, 1970; Winkler, 1976). Thus the small amounts of iron in the Day Book dunite (Table 4) should have little effect on conclusions based on the Fe-free system. The presence of $Al_2O_3$ in ultramafic systems will result in the formation of an Mg-rich chlorite in all but the highest grades of metamorphism (Winkler, 1976). Evans (1977) has treated the Al-bearing phase separately from the phases in the system CaO-MgO-$SiO_2$, thus taking advantage of simple triangular geometry in the volatile-free system. Considering the ubiquitous occurrence of chlorite in both the veins (Table 3) and the dunite (Table 8) at Day Book, a similar approach will be used in this paper. The resulting geometrical representations for phases observed in the Day Book dunite in the systems MgO-$SiO_2$ and CaO-MgO-$SiO_2$ are shown in Figure 11.

Evans and Trommsdorff (1974) have developed a model based on petrographic and experimental studies for the metamorphism of ultramafic rocks in the system MgO-$SiO_2$-$H_2O$-$CO_2$ and a portion of their model is reproduced here at Figure 12. The two isobaric T-$X_{fluid}$ sections ($P_3$ and $P_4$) best represent the P-T conditions during the metamorphism of the Day Book dunite because a number of the three-phase univariant assemblages represented on these isobaric sections are also found in the dunite and in the veins. The critical assemblages (Table 10) are located around the MFAT invariant point at $P_4$ and around the FEAT and MFET invariant points at $P_3$. Actually only the assemblage TEF is unique to $P_3$ suggesting that pressure during metamorphism of the Day Book dunite was closer to $P_4$ than to $P_3$. The passage of the reaction EAT through the invariant point MFET generates a new invariant point MFAT as the pressure decreases from $P_3$ to $P_4$. The association of three of the critical assemblages (Table 10) with the new invariant point together with one assemblage (TEF) unique to the old invariant point, suggests the metamorphism occurred at pressures near the crossing of MFET by EAT. At such a pressure all of the observed critical assemblages in the system MgO-$SiO_2$-$H_2O$-$CO_2$ (Table 10) would be stable or slightly metastable. Occurrence of metastable assemblages may then be explained as retrograde assemblages, by slight variations in fluid composition or by the influence of FeO on the system.

Discussion of the stability relations of tremolite-bearing assemblages must be treated in terms of the system CaO-MgO-$SiO_2$-$H_2O$. Evans (1977) has developed an excellent model for the metamorphism of ultramafic rocks in this system and the following discussion will be largely based on his work. Critical tremolite-bearing mineral assemblages are given in Table 11 and Figure 13. As in the case of the MgO-

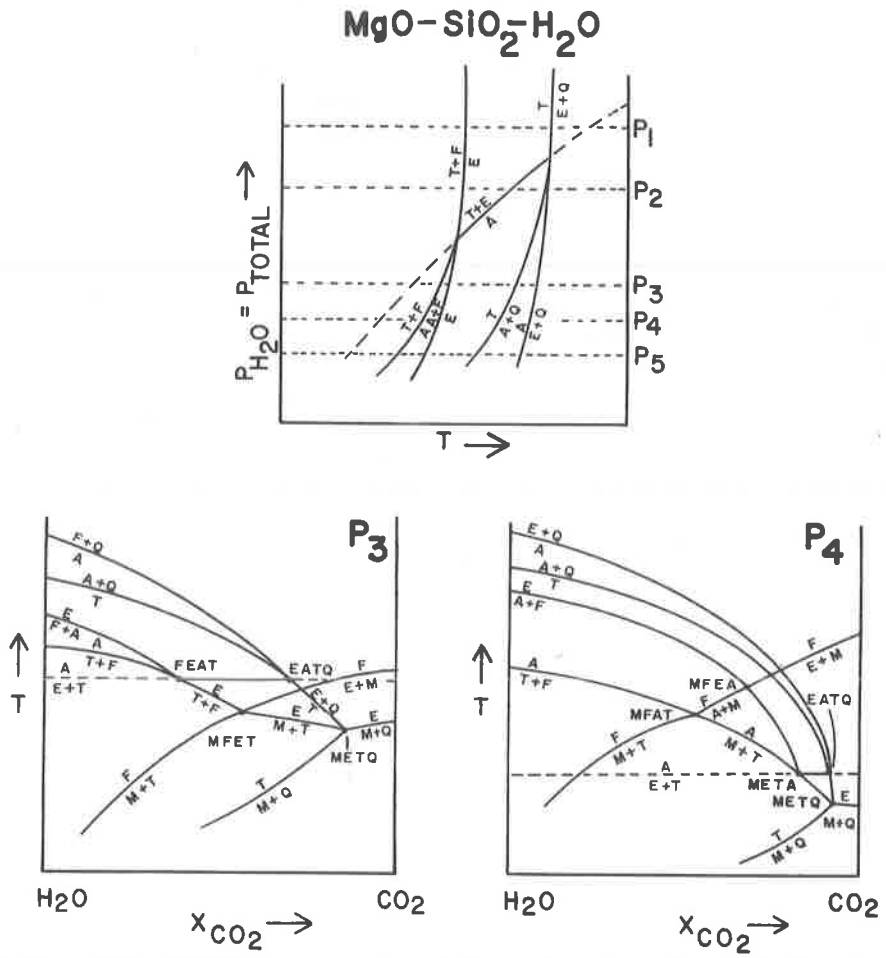


*Figure 12. Phase relations in a portion of the system MgO-$SiO_2$-$H_2O$-$CO_2$ (Evans and Trommsdorff, 1974b).*

*Table 10. Occurrence of Key Mineral Assemblages in the System MgO-$SiO_2$-$H_2O$-$CO_2$.*

| | Ta+Fo +M | Ta+Fo +Opx | Ta+Fo+ Antho | Ta+M+ Antho |
|---|---|---|---|---|
| Veins | 3 | 0 | 12 | 2 |
| Dunite | 2 | 9 | 6 | 0 |

$SiO_2$-$H_2O$-$CO_2$ system, similar mineral assemblages are found in both the dunite and the veins, the major difference being in the relative amounts of the phases present (Tables 3 and 8). The assemblage tremolite + anthophyllite + enstatite was not noted in any of the samples, but this may be due to a sampling problem related to the overall scarcity of enstatite rather than a gap in the bulk compositions of the ultramafic rock.

Metamorphic assemblages (Tables 3 and 8) and critical mineral assemblages used to define metamorphic reactions (Tables 9 and 10) in the dunite and the veins found in the dunite are very similar. Assemblages that contain enstatite are unique to the dunite, as this phase is not found in the veins. The similarity of mineral assemblages in the dunite and the veins suggests the metamorphism of the dunite and the formation of the veins was the result of contemporaneous recrystallization at the same temperature, pressure, and fluid composition. Veins probably served as channels for the fluid that accompanied recrystallization of the dunite. In some cases, veins can be traced from the metasomatic reaction zone surrounding pegmatites, directly into the dunite. The veins contain a higher modal proportion of volatile-bearing phases than the

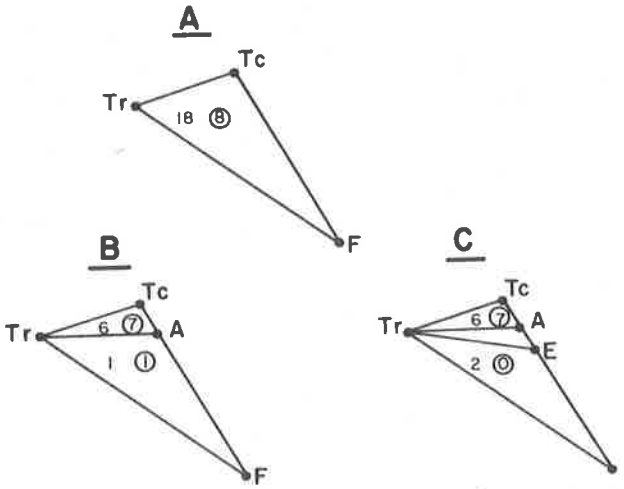


*Figure 13. Occurrences of mineral assemblages in a portion of the triangle CaO-MgO-$SiO_2$ in the dunite and associated veins (circled). All assemblages include chlorite.*

*Table 11. Occurrence of Key Mineral Assemblages in the System CaO-MgO-$SiO_2$-$H_2O$.*

| | Tr+Ta +Fo | Tr+Ta+ Antho | Tr+Fo+ Antho | Tr+Fo +Opx | Tr+Ta +Opx |
|---|---|---|---|---|---|
| Veins | 8 | 7 | 1 | 0 | 0 |
| Dunite | 18 | 6 | 1 | 2 | 2 |

dunite (Tables 3 and 8) because of a higher original fluid content.

Variation of mineral assemblages within the veins and dunite is most likely due to local variations in bulk composition (particularly in the fluid phase) rather than gradients in pressure and/or temperature within the dunite. Figure 12 illustrates how small changes in the mole percent of $CO_2$ in the fluid phase ($X_{CO_2}$) can change mineral assemblages. For example, at pressures corresponding to $P_4$ and temperatures slightly less than the MFAT invariant point, a variation of 10-20 mole percent $CO_2$ can result in the following stable mineral assemblages: anthophyllite + magnesite, anthophyllite + talc, talc + quartz, anthophyllite + magnesite + talc, talc + magnesite, magnesite + talc + forsterite, magnesite + forsterite and talc + forsterite. Another effect of changing fluid composition is the steatization of tremolite and anthophyllite. Individual amphibole crystals commonly show partial to total replacement by talc. Within the contact zone between the pegmatites and the dunite, much of the talc has a fibrous structure that is thought to result from replacement of anthophyllite by talc. Reduction of $CO_2$ activity in the vapor can result in the isothermal breakdown of anthophyllite as shown on Figure 12 at $P_4$ (reactions T+F=A and M+T=A). The common steatization of anthophyllite in the Day Book dunite suggests that the composition of the vapor phase in the ultramafic rock became more enriched in $H_2O$ during the course of the metamorphism. The effect of variation in volatile-free bulk composition is shown in Figure 11. Occurrence of the assemblages tremolite + talc + anthophyllite or tremolite + forsterite + anthophyllite is controlled by the bulk composition and not by any variation in temperature or pressure.

Mineral assemblages in the Day Book dunite and surrounding country rocks indicate recrystallization under conditions corresponding to medium grade (Winkler, 1976) or the middle amphibolite facies of regional metamorphism (Turner, 1968; Evans, 1977). Estimates of pressure and temperature based on mineral assemblages in pelitic rocks yield 550-650°C and 5 to 6 Kb (Winkler, 1976).

Serpentine is found throughout the dunite and associated veins (Tables 3 and 8) as both fracture fillings (Fig. 3) and coronas surrounding Mg-silicates. Textural and structural relations clearly indicate the serpentinization is younger than the major metamorphism that recrystallized the dunite. Fluids that accompany serpentinization are $H_2O$-rich and serpentine is unstable even in the presence of small amounts of $CO_2$ (Johannes, 1969). Thus, the early period of talc-tremolite-anthophyllite- magnesite-

chlorite metamorphism with its relatively $CO_2$-rich fluid is different from the serpentinization event, not only in terms of timing, but also in terms of fluid composition. Serpentinization is a low grade metamorphic process. Indeed, some workers believe serpentinization occurs in the weathering environment (Barnes, et al., 1969). Some of the shear zones in the Day Book dunite contain springs with associated thin coatings of chalcedony and serpentine--suggesting active serpentinization. The country rocks surrounding the Day Book dunite do not show any evidence of the retrograde metamorphism that might be related to serpentinization, thus supporting the argument for very low grade local development of serpentine.

## CONCLUSIONS

Mineral assemblages, textures and field relations indicate the Day Book dunite is an alpine ultramafic that was emplaced in graywackes and basalts prior to amphibolite grade regional metamorphism. Chromian spinel and olivine compositions from the Day Book body are similar to values from other alpine ultramafics. The absence of a contact aureole or other associated igneous rock also demonstrates the alpine nature of the ultramafic body. Country rock distributions shown in Figure 2 suggest a protolith with alternating, irregular layers of basaltic and clastic sedimentary rocks. Banding of thin layered amphibolites has been ascribed to metamorphic differentiation (Orville, 1969), but the scale involved at Day Book is too large to be explained by ion migration. On an outcrop scale, blocks of amphibolite from 3 cm to 5 m are found to be surrounded by more pelitic material. These structural relations may have resulted from polyphase folding accompanied by shearing or they may represent a metamorphic terrain in which protoliths of clastic sediment surrounded blocks of basalt--a rock distribution suggestive of a melange terrain (Raymond, 1977).

Regional metamorphism of the ultramafic and surrounding rocks has produced mineral assemblages corresponding to the middle amphibolite facies, 550-650°C and 5-6 kb. Such temperatures, in this pressure range closely approximate the solidus temperature for the Spruce Pine pegmatites (P.M. Fenn, personal communication, 1978). It is possible that the metamorphism of the dunite and country rock was also accompanied by pegmatite intrusion. Minerals found in the contact zone between the pegmatite and the dunite are the same (with the exception of vermiculite) as the minerals found in the dunite and the veins. Orientation of the veins (Fig. 4) suggests a genetic relation between the $H_2O$-$CO_2$ fluid that invaded the ultramafic and the pegmatites and, locally, veins can be traced from the pegmatites into the dunite.

Granitic magmas that contain an $H_2O$-$CO_2$ fluid phase initially evolve a vapor phase with a relatively high $CO_2$ content, but as crystallization of the magma proceeds the vapor becomes more enriched in $H_2O$ (Holloway, 1975; Swanson, 1979). In granitic melts, $H_2O$ is more soluble than $CO_2$, thus $H_2O$ is fractioned into the granitic liquid, while $CO_2$ will be concentrated in the vapor phase. As the melt crystallized, $H_2O$ is gradually expelled from the melt and added to the vapor phase, thus enriching the vapor in $H_2O$.

At Day Book, pegmatite intrusion was apparently accompanied by a relatively $CO_2$-rich vapor that moved into the dunite along fractures and produced the anthophyllite and magnesite-bearing assemblages. As the granitic magma crystallized, the fluid became more $H_2O$-rich, resulting in the replacement of anthophyllite and tremolite by talc. Textural relations suggest that magnesite and anthophyllite crystallized early in the ultramafic rocks, whereas talc formed later, thus supporting the argument for $H_2O$-enrichment in the vapor phase as a function of time.

Serpentinization of the Day Book dunite is a comparatively recent event, unrelated to the amphibolite grade regional metamorphism. Serpentine minerals are confined to fracture fillings or grain boundaries and do not show stable textural relations with any other Mg-silicates. Stability relations of the serpentine minerals suggest formation in an $H_2O$-rich environment at low temperatures, perhaps seven in the zone of weathering. Textures and phase equilibria results show the serpentinization post dates the major metamorphism of the Day Book dunite and surrounding country rocks.

Alpine ultramafic rocks found as conformable bodies in regionally metamorphosed

terrains, such as the Day Book dunite in the Blue Ridge of western North Caolina, have clearly suffered polyphase deformation and recrystallization. Textural and mineralogic data indicate the ultramafics have been recrystallized during regonal metamorphism and subsequently altered by serpentinization. Trying to unravel the emplacement history of such recrystallized rock is very difficult. The ultimate origin of these rocks is probably diapiric upwelling or intrusion from the mantle into the crust--few workers would argue this (Moores and MacGregor, 1972). However, the emplacement of these rocks into their present positions in the crust is a matter of some controversy (Misra and Keller, 1978). Whatever the emplacement mechanisms for the ultramafics, the data necessary to evaluate the models will not be found in the dominant polygonal olivine fabric that is clearly the result of recrystallization. Large, deformed olivine grains offer the best chance for olivine petrofabric data that bears on the question of emplacement mechanisms. However, without a detailed structural study of the surrounding country rocks, the significance of such data is still open to question. Study of the geologic history of these recrystallized ultramafics is a complex problem whose solution requires detailed petrologic and structural analysis of the ultramafics and enclosing country rocks.

## ACKNOWLEDGEMENTS

This project would not have been possible without the full and complete cooperation of the quarry operators at Day Book, Northwest Carolina Olivine and in particular Doug Wiseman, the plant manager. Electron microproble analyses were done by Raymond W. Whittkopp at the University of California at Davis. Cost of thin section preparation for this project was provided by research grants from the University of North Carolina at Charlotte (1975-75) and Appalachian State University (1976-1977; 1978-1979). The author wishes to thank his good friend Loren Raymond for support during the field work and for many stimulating discussions on Appalachian geology. Loren Raymond and John Carpenter reviewed an earlier version of the manuscript and made many useful suggestions.

## REFERENCES CITED

Astwood, P.M., Carpenter, J.R., and Sharp, W.E., 1972, A petrofabric study of the Dark Ridge and Balsam Gap dunites, Jackson County, North Carolina: Southeastern Geology, V. 14, p. 183-194.

Barnes, I., and O'Neil, J.R., 1969, The relationship between fluids in some fresh alpine-type ultramafics and possible modern serpentinization, western United States: Geol. Soc. America Bull., v. 80, p. 1947-1960.

Bence, A.E., and Albee, A.L., 1968, Empirical correction factors for the electron microanalysis of silicates and oxides: Jour. Geol., v. 76, p. 382-403.

Bentzen, E.H. III, 1970, Chemical composition of some North Carolina chromite: Econ. Geology, v. 65, p. 883-885.

Bluhm, C.T., and Zimmerman, J., 1977, Structure of the Frank ultramafic tectonite, Avery County, North Carolina (Abs.) Geol. Soc. America Abstracts with Programs, v. 9, p. 121.

Butler, J.R., 1973, Paleozoic deformation and metamorphism in part of the Blue Ridge thrust sheet, North Carolina: Am. Jour. Sci., v. 273-A, p. 72-88.

Carpenter, J.R., and Phyfer, D.W., 1969, Proposed origin of the "alpine-type" ultramafics of the Appalachians (discussion paper): Abstracts with Programs for 1969. Geol. Soc. America Ann. Mtg. part 7, p. 261-263.

Carpenter, J.R., and Phyfer, D.W., 1975, Olivine compositions from Southern Appalachian ultramafics: Southeastern Geology, v. 16, p. 169-172.

Carpenter, J.R., and Fletcher, J.S., 1979, Chromite paragenesis in alpine-type ultramafic rocks of the Southern Appalachians: Southeastern Geology, v. 20, p. 161-172.

Challis, G.A., 1965, The origin of New Zealand ultramafic intrusions. Jour. Pet., v. 6, p. 322-364.

Condie, K.C., and Madison, J.A., 1969, Compositional and volume changes accompanying progressive serpentinization of dunites from the Webster-Addie ultramafic body, North Carolinan: Am. Mineralogist, v. 54, p. 1173-1177.

Conrad, S.G., Wilson, W.F., Allen, E.P., and Wright, T.J., 1963, Anthophyllite asbestos in North Carolina: North Carolina Dept. Cons. Devel. Bull. 77, 61 p.

Dribus, J.R., Godson, W.L., Hahn, K.R., Krammer, T.W., Laston, D.L., Pesch, H.L., Schick, J.T., and Tata, S.S., 1976, Comparative petrography of some alpine ultramafic plutons in western North Carolina: Compass, v. 53, p. 33-45.

Dribus, J.R., Heimlich, R.A., nd Palmer, D.F., 1977, Petrology and petrofabric analysis of the Deposit No. 9 dunite, Macon County, North Carolina (Abs.): Geol. Soc. America Abstracts with Programs, v. 9, p. 135.

Evans, B.W., 1977, Metamorphism of alpine peridotite and serpentinite: Ann. Rev. Earth Planet, Sci., v. 5, p. 397-447.

Evans, B.W., and Trommsdorff, V., 1970, Regional metamorphism of ultramafic rocks in the Central Alps: Paragenesis in the system CaO-MgO-$SiO_2$-$H_2O$: Schweiz. Mineral. Petrog. Mitt., v. 50, p. 481-492.

Evans, B.W., and Trommsdorff, V., 1974a, On elogate olivine of metamorphic origin: Geology, v. 2, p. 131-132.

Evans, B.W., and Trommsdorff, V., 1974b, Stability of enstatite plus talc and metasomatism of metaperiodotite, Val d'Efra, Lepontine Alps: Am. Jour. Sci., v. 274-296.

Fletcher, J.S., and Carpenter, J.E., 1972, Chemical differences between massive and desseminated chromite from some ultramafics of the southern Appalachians and the petrogenetic implications (Abs.): Geol. Soc. America Abstracts with Programs, v. 4, p. 505-506.

Greenberg, J.K., 1976, The alpine ultramafic problem in the Southern Appalachians: the Webster-Addie dunite (Abs.): Geol. Soc. America Abstracts with Programs, v. 8, p. 185.

Hahn, K.R., and Heimlich, R.A., 1977, Petrology of the dunite exposed at the Mincey Mine, Macon County, North Carolina: Southeastern Geology, v. 19, p. 39-53.

Hess, H.H., 1955, Serpentines, orogeny, and epeirogeny: Geol. Soc. America Spec. Paper 62, p. 391-408.

Holloway, J.R., 1976, Fluids in the evolution of granitic magmas: consequences of finite $CO_2$ solubility: Geol. Soc. America Bull., v. 87, p. 1513-1518.

Hunter, C.E., 1941, Forsterite olivine deposits of North Carolina and Georgia: North Carolina Dept. Cons. Devel. Bull. 41, 117 p.

Hunter, C.E., Murdock, T.G., and McCarthy, G.R., 1942, Chromite deposits of North Carolina: North Carolina Geol. Econ. Survey, Bull. 42, 39 p.

Irvine, T.N., 1965, Chromian spinel as a petrogenetic indicator--Part 1, Theory. Can. Jour. Earth Sci., v. 2, p. 648-672.

Jackson, E.D., 1961, Primary textures and mineral associations in the ultramafic zone of the Stillwater Complex, Montana: U.S. Geol. Survey Prof. Paper 358, 106 p.

Jackson, E.D., 1969, Chemical variation in coexisting chromite and olivine in chromitite zones of the Stillwater Complex: Symposium on Magmatic Ore Deposits, Econ. Geol. Monograph 4, p. 41-71.

Johannes, W., 1969, An experimental investigation of the system MgO-$SiO_2$-$H_2O$-$CO_2$: Am. Jour. Sci., v. 267, p. 1083-1104.

Kulp, J.L., and Brobst, D.A., 1954, Notes on the dunite and the geochemistry of vermiculite at the Day Book dunite deposit, Yancey County, North Carolina: Econ. Geology, v. 49, p. 211-220.

Laniz, R.V., Stevens, R.E., and Norman, M.B., 1964, Staining of plagioclase and other minerals with F.D. and C. red No. 2: U.S. Geol. Survey Prof. Paper 501-B, p. B152-B153.

Lappin, M.A., 1967, Structural and petrofabric studies of the dunites of Almklovalen, Nordfiord, Norway in Wyllie, P.J., ed., Ultramafic and related rocks: John Wiley and Sons, N.Y., p. 183-190.

Larabee, D.M., 1966, Map showing distribution of ultramafic and intrusive mafic rocks from northern New Jersey to eastern Alabama: U.S. Geol. Survey Misc. Geologic Inv. Map I-476, 1:500,000.

Loney, R.A., Himmelberg, G.R., and Coleman, R.G., 1971, Structure and petrology of the Alpine-type peridotite at Burro Mountain, California, U.S.A.: Jour. Petrology, v. 12, p. 245-309.

McCormick, G.R., 1975, A chemical study of kämmererite, Day Book body, Yancey County, North Carolina: Am. Mineralogist, v. 60, p. 924-927.

Misra, K.C., and Keller, F.B., 1978, Ultramafic bodies in the Southern Appalachians: a review: Am. Jour. Sci., v. 278, p. 389-418.

Moores, E.M., and MacGregor, I.D., 1972, Types of alpine ultramafic rocks and their implications for fossil plate interactions: Geol. Soc. America Memoir 132, p. 209-223.

Murdock, T.G., and Hunter, C.E., 1946, The vermiculite deposits of North Carolina: North Carolina Geol. Econ. Survey Bull. 50, 44 p.

Neuhauser, K.R., and Carpenter, J.R., 1971, A structural and petrographic analysis of the Bank's Creek (North Carolina) serpentinite: Southeastern Geology, v. 13, p. 151-165.

Orville, P.M., 1969, A model for metamorphic differentiation origin of thin-layered amphibolites: Am. Jour. Sci., v. 267, p. 64-86.

Phyfer, D.W., and Carpenter, J.R., 1969, Geochemistry and petrology of the Day Book (NC) dunite (Abs.): Geol. Soc. America Abstracts with Programs v. 1, p. 62-63.

Pike, J.E.N., and Schwarzman, E.C., 1977, Classification of textures in ultramafic xenoliths: Jour. Geol., v. 85, p. 49-61.

Pratt, J.H., and Lewis, J.V., 1905, Corundum and the peridotites of western North Carolina: North Carolina Geol. Survey Bull. 1, 440 p.

Raleigh, C.B., 1965, Structure and petrology of an alpine peridotite on Cypress Island, Washington, U.S.A.: Beitr. Miner. Petrogr., v. 11, p. 719-741.

Rankin, D.W., Espenshade, G.H., and Shaw, K.W., 1973, Stratigraphy and structure of the metamorphic belt in northwestern North Carolina and southwestern Virginia: A study from the Blue Ridge across the Brevard fault zone to the Sauratown Mountains Anticlinorium: Am. Jour. Sci., v. 273-A, p. 1-40.

Raymond, L.R., 1977, Structural control of manganese deposits in subduction complexes: California Coast Range and Southern Appalachian examples (Abs.): Geol. Soc. America Abstracts with Programs, v. 9, p. 486-487.

Sailor, R.V., and Kuntz, M.A., 1973, Petrofabric and textural evidence for syntectonic recrystallization of the Buck Creek dunite, North Carolina (Abs.): Geol. Soc. America Abstracts with Programs, v. 3, p. 791-792.

Swanson, S.E., 1979, The effect of $CO_2$ on phase equilibria and crystal growth in the system $KAlSi_3O_8$-$NaAlSi_3O_8$-$CaAl_2Si_2O_8$-$SiO_2$-$H_2O$-$CO_2$: Am. Jour. Sci., v. 279, p. 703-720.

Swanson, S.E., and Raymond, L.A., 1976, Alteration of the Day Book dunite, Spruce Pine district, western North Carolina (Abs.): Geol. Soc. Am. Abstracts with Programs, v. 8, p. 282.

Swanson, S.E., and Whittkopp, R.W., 1976, Day Book dunite an alpine ultramafic in western North Carolina (Abs.): Trans. Am. Geophys. Union, v. 57,. p. 1025-1026.

Tien, P., 1977, Carbonate minerals from a dunite mine, Yancey County, North Carolina (Abs.): Geol. Soc. America Abstracts with Programs, v. 9, p. 190.

Turner, F.J., 1968, Metamorphic petrology: mineralogical and field aspects: McGraw-Hill, New York, 403 p.

Vance, J.A., and Dungan, M.A., 1977, Formation of peridotites by deserpentinization in the Darrington and Sultan areas, Cascade Mountains, Washington: Geol. Soc. America, v. 88, p. 1497-1508.

Winkler, H.G.F., 1976, Petrogenesis of metamorphic rocks, New York, Springer-Verlag, 334 p.

# AN IGNEOUS ORIGIN FOR THE HENDERSON AUGEN GNEISS, WESTERN NORTH CAROLINA: EVIDENCE FROM ZIRCON MORPHOLOGY

By

Robert E. Lemmon
Department of Geography and Earth Sciences
University of North Carolina at
Charlotte, NC 28223

## ABSTRACT

Zircon morphological studies were conducted on six samples collected from two belts of the Henderson augen gneiss cropping out in western North Carolina. Length/breadth ratios for suites from both belts were compared using the non-parametric Mann-Whitney U test. Based on the U test, zircon suites within each belt represent a single population (with one exception). U test comparison of zircon populations between the belts suggests that there are subtle but real differences. Mode maxima from length/breadth frequency plots, elongation ratios, and the reduced major axes plots indicate an igneous origin for both belts of augen gneiss. Volume frequency plots indicate, based on the lack of dispersion within each suite, an igneous origin for four zircon suites when compared with the Lilesville Pluton.

## INTRODUCTION

There has been considerable debate concerning the origin of the Henderson Gneiss. Keith (1903, 1905 and 1907) originally mapped the unit cropping out northwest and southeast of the Brevard Zone and defined it as the Henderson Granite. He interpreted the unit to be igneous in origin. Reed (1964) renamed the lithologies as the Henderson Gneiss and restricted its occurrence to outcrops southeast of the Brevard Zone, along the western edge of the Inner Piedmont throughout the southern Appalachians. Cazeau (1967) and Hatcher (1970) mapped portions of the Henderson Gneiss in South Carolina and interpreted it to be of metasedimentary origin. Odom and Fullagar (1973) inferred an igneous origin for the Henderson Gneiss based on correlative radiometric age determinations.

Zircon suites were studied from the Henderson Gneiss in conjunction with geologic mapping in western North Carolina. Samples were located from within the Bat Cave, Fruitland (Lemmon, 1973; Lemmon and Dunn, 1973a, 1973b) and the Hendersonville (Lemmon, unpublished data) 7-1/2 minute geologic quadrangles (Figure 1). In the map area the Henderson Gneiss was subdivided and mapped as an augen gneiss (Eag) and a biotite granitic gneiss (OSgg). Six zircon suites from the augen gneiss were analyzed and compared. Two suites from the Lilesville Pluton cropping out in Anson and Richmond Counties, and a sedimentary suite (TGS) from the Texasgulf, Inc. phosphate plant in Beaufort County, North Carolina are included for comparisons. Over 1700 data pair are involved in this study.

The purposes of the study are: 1) to determine the origin of the Henderson augen gneiss based on zircon morphology; 2) to compare zircon suites collected by random sampling from the augen gneiss; 3) to compare suites from the augen gneiss to zircon suites from the Lilesville Pluton and a sedimentary suite (TGS).

## PREVIOUS WORK

Articles dealing with zircon morphology and its application to petrogenetic problems are numerous (Poldervaart, 1955 and 1956; Alper and Poldervaart, 1957; Larson and Poldervaart, 1957; Eckelmann and Poldervaart, 1957; Ragland, 1969; Byerly

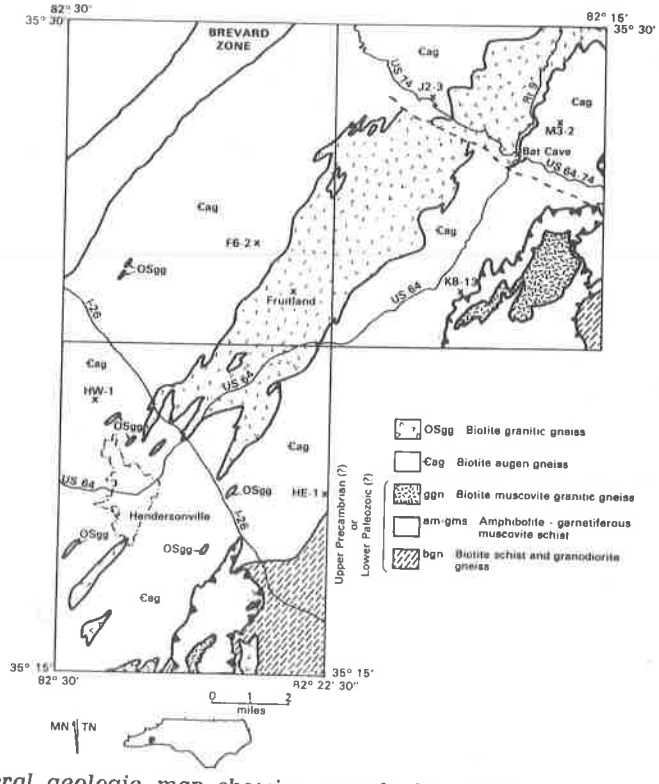


*Figure 1. General geologic map showing sample locations.*

and others, 1975). The effect of metamorphism on zircon morphology and evolution is a persistent problem (Schidlowski, 1963; Gastil and others, 1967; and Kalsbeck, 1967). Sinha and Glover (1978) working with four zircon suites (including one suite from the Henderson augen gneiss) have attempted to relate variations in U-Pb content to regional metamorphism. Their interpretation of age relations is based on the petrographic and structural framework developed by Roper and Dunn (1973) for rocks within the Brevard Zone.

Eckelmann and Kulp (1956) worked with zircon suites in an attempt to determine the origin and stratigraphic equivalence of the Henderson Granite and the Cranberry Gneiss. They sampled outcrops on both sides of the Brevard Zone in rocks mapped by Keith (1905) as Henderson Granite. As defined by Reed (1964), some of the samples they collected were from gneissic units other than the Henderson Gneiss.

## HENDERSON GNEISS (€ag)

The Henderson Gneiss is further restricted in the study area to an augen gneiss phase (€ag), cropping out in two wide belts (Figure 1). The augen gneiss ranges from quartz monzonite to granodiorite in composition and is characterized by abundant light gray to white perthitic microcline augen ranging up to 2.5 cm in diameter. The augen are ovoid in outline and often elongate in the plane of foliation forming a subhorizontal NE-SW lineation. Work done by Bond (1974) and Jagannadham (1972) indicates that the augen have a complex history. Some augen may result from an original rapakivi texture while others formed during one or more periods of porphyroblastic development. The augen are rimmed by a thin white finely granulated zone of quartz, plagioclase and potassic feldspar. The granulated zone, along with myrmekitic embayments into the microcline suggests that there has been crushing and subsequent minor recrystallization around the edge resulting in a porphyroclastic texture.

The augen gneiss is generally lepidoblastic to cataclastic in texture. The matrix

consists of an inequigranular mosaic of anhedral grains of oligoclase (An 12-19), quartz and microcline--all showing undulatory extinction. Biotite, occurring as anhedral to subhedral grains, defines the foliation within the gneiss. Accessory minerals include epidote, allanite, sphene, opaque minerals, ± garnet, zircon, apatite and chlorite.

The original chemical composition of the augen gneiss precludes using it as a metamorphic indicator. Therefore, the exact metamorphic subfacies is not well established. Hatcher (1969) suggests that these rocks were metamorphosed to the lower to middle amphibolite facies and subsequently retrogressed to the greenschist-amphibolite transitional facies. Justus (1971) classified these rocks in the greenschist-amphibolite transitional facies, based mainly on plagioclase composition. Griffin (1971) indicated that the metamorphic grade (of his non-migmatitic belt) drops from low almandine-amphibolite facies near the Walhalla Nappe to the greenschist facies northwestward near the Brevard Zone. Hadley and Nelson (1971) interpret the augen gneiss to be in the kyanite-staurolite subfacies of the almandine-amphibolite facies. Epidote is present as an accessory mineral; however, modal data (16 analyses) show no systematic decrease in the An content with an increase in modal percent epidote. For this reason I suggest that the amount of epidote in the rocks has had little effect on lowering the An content of the plagioclase. The oligoclase composition of the plagioclase seems to reflect the original chemical composition and/or range of chemical composition. I agree with Hadley and Nelson's (1971) interpretation that the augen gneiss is in the almandine-amphibolite facies. The subfacies classification could not be determined in the map area.

## BIOTITE GRANITIC GNEISS (OSgg)

The biotite granitic gneiss (OSgg) originally mapped as part of the Henderson Granite by Keith (1905 and 1907) is mapped as a distinct lithologic unit cropping out between two belts of augen gneiss (Figure 1). Contact relationships have been obscured by what is interpreted as a pronounced northwestward tectonic transport. Contacts are now parallel to the dominant southeastward dipping foliation. Xenoliths of the augen gneiss are infrequently found in the biotite granitic gneiss near the contact. Foliation within the xenoliths is parallel to regional foliation in both units. Elsewhere the contact varies from sharp to alternating zones of augen gneiss and biotite grantitic gneiss. Field evidence indicates that the biotite granitic gneiss is intrusive into the augen gneiss (possibly as a semi-concordant body).

The biotite granitic gneiss (OSgg) has been shown through radiometric ages (Odom and Russell, 1975) to be considerably younger than the augen gneiss. This study does not consider the biotite granitic gneiss to be a part of the Henderson Gneiss discussed by Reed (1964).

## LILESVILLE PLUTON

The Lilesville Pluton is one of a group of post-metamorphic plutons discussed by Butler and Ragland (1969). It is an epizonal intrusion, emplaced as a sheet or tongue-shaped partly concordant batholith (Waskom and Butler, 1971). It has a porphyritic rapakivi texture and ranges in composition from adamellite to granodiorite. The batholith was emplaced as a crystal mush and crystallized 326 ± 27 m.y. ago (Fullagar and Butler, 1979). Two zircon suites were collected from saprolite of the Lilesville Pluton for use in the comparative studies.

## SEDIMENTARY ZIRCON SUITE

A single zircon suite (TGS) was analyzed from the Texasgulf, Inc. phosphate plant near Aurora, North Carolina. The zircon concentrate was a product of mineral beneficiation at the plant and likely experienced abrasion during the beneficiation process. The sample is included to demonstrate the extremes that may be present in sedimentary zircon suites.

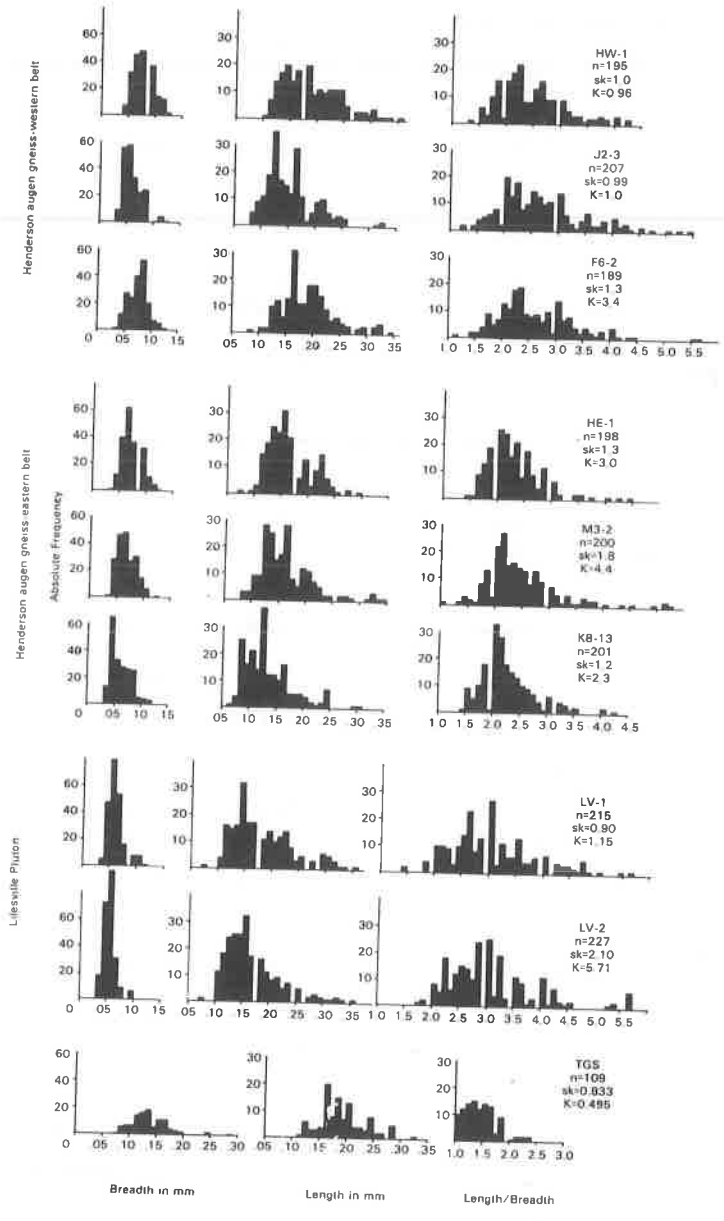


*Figure 2. Zircon size-frequency plots.*

## METHODS AND STATISTICAL TECHNIQUES

Saprolite samples weighing approximately fourty pounds were roll crushed to disaggregate and then passed through a 20 mesh sieve. Desliming involved gently agitating the material in a thirty gallon drum while allowing the clay and silt-sized fraction to decant off. The remaining material was dried and reduced to a few grams of zircon concentrate using separation techniques similar to Poldervaart (1955). Zircons were studied using a polarizing microscope with a mechanical stage under 100X magnification. Approximately 200 unbroken zircon grains were studied per slide, using a grid pattern such that the entire slide was covered. The length (l) and breadth (b)

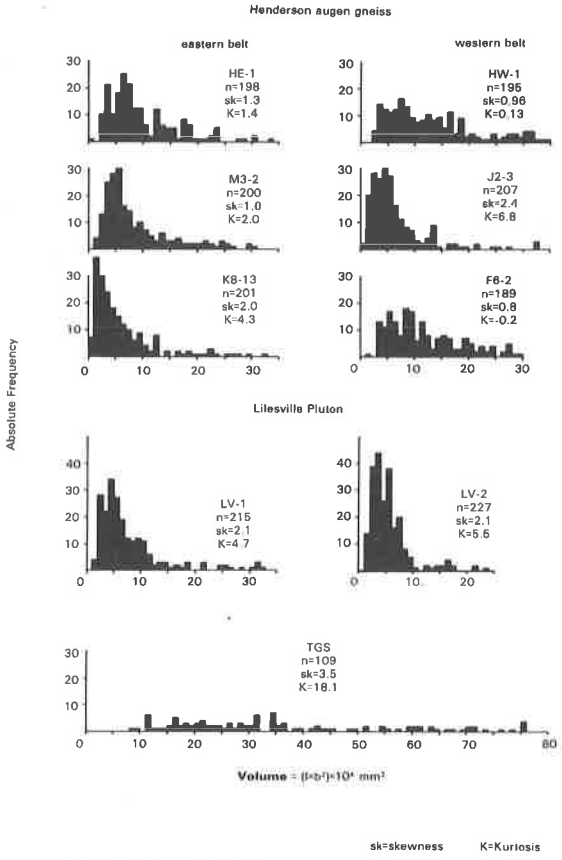


*Figure 3. Zircon volume-frequency plots.*

were measured on double terminated, unbroken crystals, or the longest dimension (which may or may not correspond to the C-axis) and the shortest normal dimension of rounded grains. All parameters that allow subjective evaluation to be imparted onto the data (such as degree of crystallinity or rounding parameters) were rejected. Digitizing equipment was not available thus precluding studies similar to Byerly and others, (1975).

Mean and standard deviation of length, breadth, length/breadth and volume for all samples are summarized in Table 1. Several statistical techniques have historically been used in presenting zircon morphology data. Figures 2 and 3 present the data in frequency plots to allow comparisons with the literature. Skewness and kurtosis are given for the length/breadth and volume plots. The mode maxima are determined from Figure 2.

Figure 4 presents length and breadth data using the reduced major axis statistical method discussed by Imbrie (1956) and used earlier by Larson and Poldervaart (1957). The plot shows the mean breadth vs mean length (represented by closed circles) and the slope of the line is the ratio of the respective standard deviation ($S_b/S_l$). The length of the lines is established by eliminating the extreme 2-1/2 percent of the largest and smallest crystals.

The data does not satisfy the assumptions of parametric techniques; therefore, the nonparametric Mann-Whitney statistical U test is used. It is a test for the significance of difference between the medians of two samples. The U test uses ordinal measurements to test whether two independent groups have been drawn from the same population. It is one of the most powerful of the nonparametric tests in that it considers the rank values of each observation rather than simply its location with respect to the combined median, thus using more of the information in the data. No

*Table 1. Summary data for zircon suites.*

| | | | |
|---|---|---|---|
| **Henderson Augen gneiss - Western Belt** | | | |
| | J2-3 | L6-2 | HW-1 |
| Mean*Length in mm | 0.153 ± 0.045 | 0.190 ± 0.048 | 0.189 ± 0.052 |
| Mean Breadth in mm | 0.060 ± 0.017 | 0.075 ± 0.016 | 0.078 ± 0.017 |
| Mean Volume x $10^4$ mm$^3$ | 6.49 ± 5.63 | 11.7 ± 6.65 | 12.8 ± 7.99 |
| Mean L/B | 2.65 ± 0.77 | 2.60 ± 0.71 | 2.46 ± 0.62 |
| (r) correlation coefficients for length-breadth plots | 0.497 | 0.387 | 0.520 |
| Slope | 2.67 | 2.94 | 3.00 |
| n | 207 | 189 | 195 |
| L/B-Mode max from frequency plots | 2.0 - 2.1 | 2.3 - 2.4 | 2.2 - 2.3 |
| **Eastern Belt** | | | |
| | M3-2 | K8-13 | HE-1 |
| Mean Length in mm | 0.162 ± 0.049 | 0.133 ± 0.044 | 0.164 ± 0.040 |
| Mean Breadth in mm | 0.067 ± 0.016 | 0.060 ± 0.019 | 0.073 ± 0.016 |
| Mean Volume x $10^4$ mm$^3$ | 8.41 ± 6.23 | 6.15 ± 6.02 | 9.81 ± 6.37 |
| Mean L/B | 2.46 ± 0.67 | 2.27 ± 0.48 | 2.29 ± 0.48 |
| (r) correlation coefficients for length-breadth plots | 0.529 | 0.799 | 0.634 |
| Slope | 2.98 | 2.36 | 2.47 |
| n | 200 | 201 | 198 |
| L/B Mode max from frequency plots | 2.1 - 2.2 | 2.0 - 2.1 | 2.0 - 2.1 |
| | **Lilesville Pluton** | | **Texasgulf, Inc.** |
| | LV-1 | LV-2 | TGS |
| Mean Length in mm | 0.182 ± 0.056 | 0.167 ± 0.050 | 0.193 ± 0.042 |
| Mean Breadth in mm | 0.061 ± 0.015 | 0.054 ± 0.012 | 0.135 ± 0.034 |
| Mean Volume x $10^4$ mm$^3$ | 7.76 ± 6.26 | 5.46 ± 3.79 | 40.5 ± 33.6 |
| Mean L/B | 3.03 ± 0.78 | 3.13 ± 1.01 | 1.46 ± 0.30 |
| (r) correlation coefficients for length-breadth plots | 0.597 | 0.391 | 0.672 |
| Slope | 3.85 | 4.26 | 1.24 |
| n | 215 | 227 | 109 |
| L/B Mode max from histogram plots | 3.0 - 3.1 | 3.0 - 3.1 | 1.3 - 1.4 |

*Mean is arithmetic mean ± one standard deviation, ($\bar{x}$ ± S)

grouping of data is required in the U test thus avoiding misleading results. A detailed development of the technique originated by Mann and Whitney, (1947) is discussed in Siegel, (1956).

The length/breadth ratios were compared for the six Henderson augen gneiss samples using all paired combinations (15) and two samples of the Lilesville Pluton. The null hypothesis ($H_0$) states that parameters used to characterize zircons within suites from two samples taken randomly from the same geologic body are equal and, therefore, the suites come from the same population. The alternate hypothesis ($H_1$) states that the zircon suites contain differing populations. The level of significance was set at $\alpha = 0.01$, thus any values of Z which are so extreme that their associated probability (p) is equal to or less than 0.01 causes $H_0$ to be rejected in favor of $H_1$.

## RESULTS AND DISCUSSIONS

The Mann-Whitney U test was used on the length/breadth ratios of all zircon suites (Table 2). U tests for the Henderson augen gneiss samples collected from the western belt indicate that the paired samples have two-tailed probability values greater than $\alpha = 0.01$. Zircon suites from the western belt of augen gneiss appear to come from the same population. Test pairs from the augen gneiss-eastern belt indicate that zircons from two suite combinations come from the same population. Sample pair (M3-2, K8-13) exhibit a statistically significant difference indicating that zircons from these suites may contain differing populations. All possible paired combinations were tested for zircon suites taken from eastern and western belts of the augen gneiss. The two-

*Table 2. Mann-Whitney U-test parameters and associated probability (p) for length/breadth ratios of paired zircon suites.*

| | | | | Mann-Whitney 2-tailed probability |
|---|---|---|---|---|
| Henderson Augen Gneiss | | | | |
| Eastern Belt | | U | Z | p |
| HE- 1 | M3- 2 | 17066.5 | -2.385 | 0.017 |
| HE- 1 | K8-13 | 19004.5 | -0.778 | 0.437 |
| M3- 2 | K8-13 | 16544.5 | -3.068 | 0.002 |
| Western Belt | | | | |
| HW- 1 | J2- 3 | 17398.0 | -2.393 | 0.017 |
| HW- 1 | F6- 2 | 16212.0 | -2.038 | 0.042 |
| J2- 3 | F6- 2 | 19082.0 | -0.422 | 0.673 |
| Mixed | | | | |
| East | West | | | |
| HE- 1 | HW-1 | 16399.0 | -2.584 | 0.010 |
| HE- 1 | J2- 3 | 14665.0 | -4.955 | 0.000 |
| HE- 1 | F6- 2 | 13630.5 | -4.622 | 0.000 |
| M3- 2 | HW-1 | 19206.5 | -0.259 | 0.796 |
| M3- 2 | J2- 3 | 17451.5 | -2.740 | 0.006 |
| M3- 2 | F6- 2 | 16263.5 | -2.380 | 0.017 |
| K8-13 | HW-1 | 15932.5 | -3.222 | 0.001 |
| K8-13 | J2- 3 | 14259.5 | -5.501 | 0.000 |
| K8-13 | F6- 2 | 13260.5 | -5.157 | 0.000 |
| Lilesville Pluton | | | | |
| LV- 1 | LV- 2 | 24077.0 | -0.243 | 0.808 |

tailed probabilities for length/breadth ratios indicate that seven out of nine pairs were significantly different.

Within the eastern and western belts of the Henderson augen gneiss (Figure 1) zircon suites appear to have come from the same populations, with the possible exception of sample pair M3-2, K8-13. The two belts merge southwestward in the Hendersonville Quadrangle and have been mapped as the same geologic unit based on mesoscropic, microscopic and geochemical data (Hadley and Nelson, 1971; Lemmon, 1973, Lemmon and Dunn, 1973a, 1973b). There does appear to be a subtle but real difference between the two belts of augen gneiss based on zircon populations.

Frequency plots of length/breadth ratios (Figure 2) indicate a positive skewness and have mode maxima of 2.0 - 2.4 for the augen gneiss, 3.0 - 3.1 for the Lilesville Pluton and 1.3 - 1.4 for the TGS sample. Caution should be used in interpreting these plots for the mode maximum is dependent on the grouping of the data. Regrouping of the data may significantly shift the maximum, thereby biasing the interpretation. four known igneous plutons indicates a reduced major axis range of 2.14 - 4.26 with a mean of 3.26 (unpublished data). Based on this information zircon suites from the Henderson augen gneiss appear igneous in origin.

Coefficients of correlation (r) for length-breadth plots have been used as one of several parameters in determining the origin of protoliths in metamorphic terrains (Eckelmann and Helenek, 1980). They suggested high r values are characteristic of zircon suites from plutonic protoliths. Larsen and Poldervaart (1957) determined r values for ten samples of known magmatic origin to average 0.680. Work by Conley and Fordham (in press) gives a mean r value of 0.579 for four samples of igneous origin. Work by this author on eight samples from four plutonic bodies has determined a mean r of 0.565 (unpublished data). Coefficient of correlation values for the Henderson augen gneiss range 0.387 - 0.799, with a mean of 0.570 (Table 1). Based on r values, the scatter in the length-breadth data for zircon suites from the augen gneiss is in the range encountered by others working with zircon suites from bodies of plutonic origin. Comparison of r values for the augen gneiss and the Lilesville pluton (mean r = 0.551) with the sedimentary TGS sample (r = 0.672) shows that in all but one suite, scatter in the length-breadth distribution plots is greater than that of the TGS sample. Based

on this study, coefficients of correlation of length-breadth plots as an indicator of protolithic origin has limited usefulness.

Ragland (1969) used volume histograms to check for multiple populations within zircon suites reasoning that greater dispersion might be expected when more than one population is present. Volume frequency diagrams are shown in Figure 3 where visual comparisons may be made. Assuming that the zircon suites for the Lilesville are a single population of igneous origin, which is documented by the U-test and all other statistical parameters; comparisons may be made to the Henderson augen gneiss samples. In four of the augen gneiss samples, volume frequency distributions resemble the Lilesville pluton samples and reflect single zircon populations. Samples HW-1 and F6-2 show some dispersion.

The dispersion in the volume frequency of samples HW-1 and F6-2 is incompatable with other data. The Mann-Whitney U test of length/breadth data indicates the zircon suites from the western belt come from the same population. Further, the reduced major axis data, elongation ration, and the length/breadth mode maxima suggest an igneous origin for these samples. The cause(s) for the dispersion in two augen gneiss samples is unexplained at this time. Causes may include; (1) mixed or multiple zircon populations within each sample; however, the Mann-Whitney U-test statistic should indicate differing populations, (2) variations in parameters during separation, (3) some reaction within the environment that may have selectively altered zircons in these samples, possibly increase $P_{H_2O}$. Eckelmann and Helenek (1980) suggest contoured length-breadth plots may give some insights into mixed populations. This feature is currently being developed.

## RADIOMETRIC DATA

Radiometric ages of rock units discussed in this paper are given in Table 3. Rb/Sr rock analysis established a 535 ± 27 m.y. old age for the Henderson augen gneiss (Odom and Fullagar, 1973). They interpret the Cambrian age to be the age of crystallization for magma derived from the lower crust or upper mantle, based on the $(Sr^{87}/Sr^{86})_o$ initial ratio of 0.7039. Seven of the eight samples used to establish the isochron are from the western belt or were collected within several kilometers of the Brevard Zone, southwest of the study area.

*Table 3. Radiometric age dates.*

| Unit | Age m.y. (Method) | $(Sr^{87}/Sr^{86})_o$ | Reference |
|---|---|---|---|
| Henderson augen gneiss (Cag) | 535±27 m.y. (Rb/Sr-whole rock) | 0.7039±0.0004 | Odom & Fullagar (1973) |
| | 530-540 m.y. (U-Pb-zircons) | | Odom & Fullagar (1973) |
| | 593 m.y. ($Pb^{207}/Pb^{206}$) | | Sinha & Glover (1978) |
| Biotite granitic gneiss (OSgg) | 438±22 m.y. (Rb/Sr-whole rock) | 0.7045 | Odom & Russell (1975) |
| Lilesville Pluton (LV) | 326±27 m.y. (Rb/Sr-whole rock) | 0.7047±0.0007 | Fullagar & Butler (1979) |

Pb-U analysis of zircons from the augen gneiss define a chord that intersects the concordia plot giving an age of 530-540 m.y. (Odom and Fullagar, 1973). All samples used to define the chord were collected from the western belt of augen gneiss.

Sinha and Glover (1978) have determined a $Pb^{207}/Pb^{206}$ age of 593 m.y. from zircon residuals after leaching with hydroflouric acid for 120 minutes. They suggest that the 593 m.y. age more closely defines the age of crystallization of the Henderson augen gneiss and that the 535 m.y. age reflects the lower temperatures required to close the Rb-Sr system. The significance of the 593 m.y. date is difficult to assess due to the severity of the leaching process and because only one sample from the augen gneiss was analyzed.

The correlative ages by differing techniques (Odom and Fullagar, 1973) suggests an igneous origin for the Henderson augen gneiss. The results from the Mann-Whitney

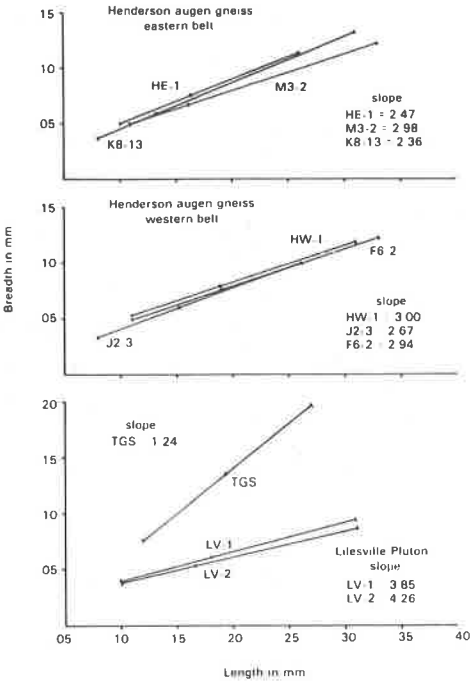


*Figure 4. Zircon reduced major axis plots.*

U test of length/breadth ratios, the mode maxima of the length/breadth ratios, elongation ratios, and the reduced major axis plots further confirm an igneous origin for zircon suites from both belts of augen gneiss. Two of the volume frequency plots for samples taken from the western belt are inconsistent with this conclusion.

The Mann-Whitney U test of zircon suites between the two belts of augen gneiss suggests that there is a significant difference in the zircon populations in seven of the nine cases. Zircon morphology data indicate that the augen gneiss of the eastern belt is igneous in origin. Only one sample (#795, Odom and Fullagar, 1973) from the eastern belt has been used in the Rb/Sr whole rock radiometric determinations and it falls close to but not on the isochron. It cannot be assumed at this time that both belts of the augen gneiss represent a single igneous event crystallizing at the same time.

The biotite granite gneiss (OSgg) intrusive into the Henderson augen gneiss has a Rb/Sr whole rock age of 438 $\pm$ 22 m.y. based on work by Odom and Russell (1975). The $(Sr^{87}/Sr^{86})_o$ initial ratio of 0.7045 further verifies that the Ordovician- Silurian age is the age of crystallization.

Age of the Lilesville Pluton is 326 $\pm$ 27 m.y. based on Rb/Sr-whole rock analysis (Fullagar and Butler, 1979).

## CONCLUSIONS

1. The non-parametric Mann-Whitney U test of length/breadth data pairs indicates that zircon suites from the western belt of the Henderson augen gneiss comprise a single population. Test results for suites collected from the eastern belt indicate that in two of the three cases, zircons make up a single population. Paired tests between the two belts indicate that in seven of the nine cases, the zircon suites form significantly different populations. There does appear to be a subtle but real difference between the two belts of augen gneiss based on the U test.

2. Mode maxima from length/breadth frequency data, elongation ratios, and the slopes from reduced major axis plots suggests an igneous origin for zircon suites from both belts of augen gneiss. Zircons from the Lilesville Pluton are more acicular when compared with suites from the augen gneiss.

3. Coefficients of correlation (r) for length-breadth plots are not conclusive as a method of determination of protolithic origin based on this study.

4. The lack of dispersion in volume histograms in all samples from the eastern belt and one sample from the western belt of augen gneiss suggests an igneous origin when compared with the Lilesville Pluton.

5. Zircon morphology studies indicate that the eastern belt is igneous in origin and that zircon suites are significantly different than those of the western belt.

6. Correlative age determinations using different radiometric methods and $(Sr^{87}/Sr^{86})_o$ initial ratios argue for an igneous origin for the Henderson augen gneiss. With one exception, samples used for all determinations were collected from the western belt or within a few kilometers of the Brevard Zone.

7. It cannot be stated that both belts of augen gneiss have the same age of crystallization based on only one radiometric analysis from the eastern belt.

8. Dispersions in volume histograms for two zircon suites from the western augen gneiss belt are inconsistent with radiometric and other morphological data. Additional statistical techniques testing for multiple or mixed zircon populatios are being developed.

9. The Henderson augen gneiss is igneous in origin based on data presented in this paper.

## ACKNOWLEDGEMENTS

Support for the geologic mapping of the Bat Cave, Fruitland and Hendersonville 7-1/2 minute guadrangles was provided by North Carolina Division of Mineral Resources and the Geologic Division of the Tennessee Valley Authority. Sample collection and preparation was funded in part by a grant from the Citadel Development Foundation. The Minerals Research Laboratory of North Carolina State University provided equipment and advice on mineral separation techniques. J. Conley and O. Fordham reviewed the manuscript and made helpful suggestions and criticisms.

## REFERENCES CITED

Alper, A.M., and Poldervaart, A., 1957, Zircon from the Animas Stock and associated rocks, New Mexico: Economic Geol. v. 52, p. 952-971.

Bond, P.A., 1974, A sequence of development for the Henderson augen gneiss and its adjacent cataclastic rocks: Unpublished M.S. thesis, Univ. of North Carolina at Chapel Hill, 53 p.

Butler, J. Robert and Ragland, P.C., 1969, A petrochemical survey of plutonic intrusions in the Piedmont, southeastern Appalachians, USA: Contr. Mineralogy Petrology, v. 24, p. 164-190.

Byerly, G.R., Mrakovich, J.V., and Malcuit, R.J., 1975, Use of Fourier Shape Analysis in Zircon Petrographic Studies: Geol. Soc. of America Bull., v. 86, p. 956-958.

Cazeau, C.J., 1967, Geology and minerals resources of Oconee County, South Carolina: South Carolina Devel. Board Div. Geology Bull., v. 34, 38 p.

Conley, J.F. and Fordham, O.M., in press, Statistical study of zircon populations from igneous and metamorphic rocks: Southeastern Geology.

Eckelmann, F.D. and Helenek, H.L., 1980, Recognition of felsic volcanic and plutonic protoliths in metamorphic terraines using the dimensional morphology signature of relic zircon populations (abs): Geol. Soc. America, Abstracts with Programs, v. 12, no. 4, p. 176.

Eckelmann, F.D. and Kulp, J.L., 1956, The sedimentary origin and stratigraphic equivalence of the so-called Cranberry and Henderson granites in western North Carolina: Amer. Jour. Sci., v. 254, p. 288-315.

Eckelmann, F.D. and Poldervaart, A., 1957, Geologic evolution of the Beartooth Mountains, Montana and Wyoming. Part I, Archean history of the Quad Creek area: Geol. Soc. of America Bull., v. 68, p. 1225-1262.

Fullagar, Paul D. and Butler, J. Robert, 1979, 325 to 265 M.Y. - Old granite plutons in the Piedmont of the Southern Appalachians: American Jour. Sci., v. 279, p. 161-185.
Gastil, R.G., Delisle, M., and Morgan, J., 1967, Some effects of progressive metamorphism on zircons: Geol. Soc. of America Bull., v. 78, p. 879-906.
Griffin, V.S., Jr., 1971, Stockwork tectonics in the Appalachian Piedmont of South Carolina and Georgia: Geol. Rundschau, v. 60, p. 868-886.
Hadley, J.B. and Nelson, A.E., 1971, Geologic Map of the Knoxville quadrangle, North Carolina, Tennessee and South Carolina: U.S. Geol. Survey, Misc. Geologic Investigation Map, I-654.
Hatcher, R.D., Jr., 1969, Stratigraphy, petrology, and structure of the low rank belt and part of the Blue Ridge of northwestern most South Carolina: Carolina Geol. Soc. Guideboook, S.C. Div. Geol., Geologic Notes, v. 13, no. 4, p. 105-141.
_____, 1970, Stratigraphy of the Brevard Zone and Poor Mountain Area, Northwestern South Carolina: Geol. Soc. of America Bull., v. 81, p. 933-940.
Imbrie, J., 1956, Biometrical methods in the study of invertebrate fossils: American Mus. Nat. Hist., Bull., v. 108, p. 215-252.
Jagannadham, G., 1972, A comparative study of potash feldspar structural states from selected granites and augen gneisses: Unpublished Ph.D. dissertation, Univ. of North Carolina at Chapel Hill, 116 p.
Justus, P.S., 1971, Structure and petrology along the Blue Ridge front and Brevard Zone, Wilkes and Caldwell Counties, North Carolina: Unpublished Ph.D. dissertation, Univ. of North Carolina at Chapel Hill, 89 p.
Kalsbeck, F., 1967, Evolution of zircons in sedimentary and metamorphic rocks; a discussion: Sedimentology, v. 8, p. 163-167.
Keith, A., 1903, Description of the Cranberry quadrangles, North Carolina-Tennessee: U.S. Geol. Survey, Geol. Atlas, Folio 90, 14 p.
_____, 1905, Description of Mt. Mitchell quadrangles, North Carolina-Tennessee: U.S. Geol. Survey, Geol. Atlas, Folio 124, 9 p.
_____, 1907, Description of the Pisgah quadrangle, North Carolina-South Carolina: U.S. Geol. Survey, Geol. Atlas, Folio 147, 8 p.
Larson, L.H. and Poldervaart, A., 1957, Measurements and distribution of zircons in some granitic rocks of magmatic origin: Mineral Mag., v. 31, p. 544-564.
Lemmon, R.E., 1973, Geology of the Bat Cave and Fruitland Quadrangles and the origin of the Henderson Gneiss, western North Carolina: Unpublished Ph.D. thesis, Univ. of North Carolina at Chapel Hill, 145 p.
Lemmon, R.E. and Dunn, D.E., 1973a, Geologic Map and mineral resources summary of the Bat Cave Quadrangle, North Carolina: N.C. Dept. of Nat. and Econ. Resc., Office of Earth Resources, GM 202-NE.
_____, 1973b, Geologic Map and mineral resources summary of the Fruitland Quadrangle, North Carolina: N.C. Dept. of Nat. and Econ. Resc., Office of Earth Resources, GM 202-NW.
Mann, H.D. and Whitney, P.R., 1947, On a test of whether one or two random variables is stochastically larger than the other: Ann. Math. Statist., v. 18, p. 50-60.
Odom, A.L. and Fullagar, P.D., 1973, Geochronologic and tectonic relationships between the Inner Piedmont, Brevard Zone and Blue Ridge Belts, North Carolina: American Jour. Sci., v. 273-A, p. 133-149.
Odom, A.L. and Russell, G.S., 1975, The time of regional metamorphism of the Inner Piedmont, N.C. and Smith River Allochthon: Inferences from whole-rock ages: Geol. Soc. America, Abs., v. 7, no. 4, p. 522.
Poldervaart, A., 1955, Zircons in rocks, I. Sedimentary rocks: American Jour. Sci., 253, p. 433-461.
_____, 1956, Zircon in rocks, II. Igneous rocks: American Jour. Sci., v. 254, p. 521-554.
Ragland, P.C., 1969, Alpha-autoradiography and morphology of accessary zircon suites: Southeastern Geol., v. 11, p. 1-20.
Reed, J.C., Jr., 1964, Geology of the Lenoir quadrangle, North Carolina: U.S. Geol. Survey Bull., 1161-B, p. B1-B53.

Roper, P.J. and Dunn, D.E., 1973, Superposed deformation and polymetamorphism, Brevard Zone, South Carolina: Geol. Soc. of America Bull., v. 84, p. 3373-3386.

Schidlowski, M.O.G., 1963, Recrystallization of zircons as an indication of metamorphism: Nature, v. 197, p. 68-69.

Siegel, S., 1956, Non parametric statistics for the Behavioral Sciences: McGraw-Hill Book Co., 312 p.

Sinha, A.K. and Glover, Lynn, III, 1978, U-Pb systematics of zircons during dynamic metamorphism: Contrib. Mineral. and Petrol., v. 66, p. 305-310.

Waskom, J.D. and Butler, J. Robert, 1971, Geology and Gravity of the Lilesville Granite Batholith: Geol. Soc. America Bull., v. 82, p. 2827-2844.

# PETROLOGY AND PALEOENVIRONMENTS OF THE ST. LOUIS LIMESTONE (MIDDLE MISSISSIPPIAN), SOUTH CENTRAL TENNESSEE

by

Joseph L. Cooper

and

David N. Lumsden
Department of Geology
Memphis State University
Memphis, Tennessee 38152

## ABSTRACT

The St. Louis Limestone was investigated at five complete and two partial exposures in and near the Sequatchie Valley of Tennessee. Lime mudstone, wackestone, packstone, grainstone, dolostone, silicastone and minor shale lithologies are present. Although corals are common (*Lithostrotion*) no reef buildups were found. Chert is common, but shows no pattern of distribution either vertically or geographically. All localities have dolostone units varying from 15 to 50% of the exposure thickness. Dolomite nonstoichiometry shows no vertical or geographic pattern. There is an overall change from low energy micrite dominated fabrics in the lower St. Louis to a relatively larger proportion of spar dominated lithologies in the upper St. Louis. We interpret this to be the result of an overall increase in environmental energy consequent upon gradual deepening of the shallow marine waters to the point where wave and current agitation was sufficient to remove fines from the study area. The western Andros Island area of the Bahamas is an excellent modern analogue.

## INTRODUCTION

Our objective is to provide a detailed study of the petrology and a paleoenvironmental interpretation of the St. Louis Limestone in southeast Tennessee. Specifically we will: (1) identify St. Louis lithologies, sedimentary structures, and biological components; (2) identify the dominate sedimentary processes operative during the deposition of the lithofacies; (3) interpret the depositional environments represented in the St. Louis Limestone and (4) discuss dolomitization and chertification.

Except for the broad stratigraphic studies of Vail (1959), Peterson (1962), Thomas (1967, 1972, 1979); McLemore (1972), and Milici et al. (1979), and the more detailed studies of Handford (1978) and Bergenback (1972, 1978) little has been written on the Mississippian of southeast Tennessee. This report is a detailed look at the St. Louis; it is part of a planned overall study of Mississippian rocks in Tennessee. We ultimately hope to be able to explain the tectonic-sedimentary processes that controlled deposition during Mississippian time over the State of Tennessee.

Seven outcrops were examined in the southern Cumberland Plateau of Tennessee (Fig. 1). Explicit direction to exposures are in Cooper (1979). Except for the Monteagle and South Pittsburg locations both top and bottom contacts were present. The outcrops are primarily along two trends, one northeast trend along the Sequatchie Valley and a second roughly perpendicular to the first near the Tennessee-Alabama boundary.

The St. Louis Limestone of the study area is a Middle Mississippian unit deposited

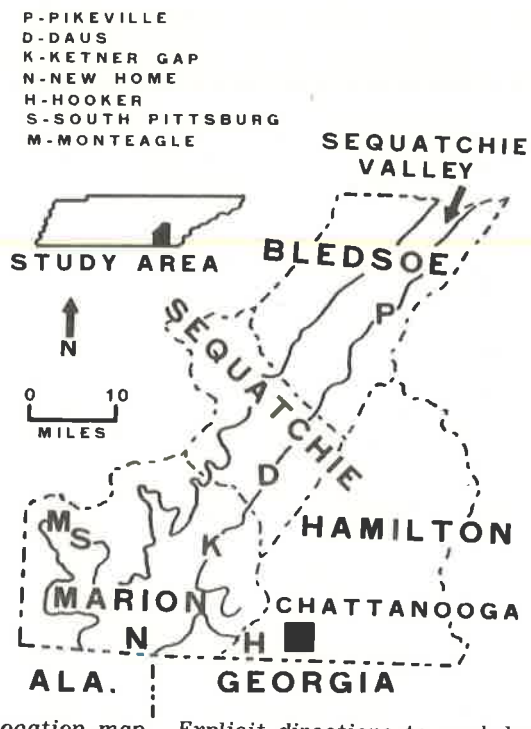


*Figure 1. Outcrop location map. Explicit directions to each location can be found in Cooper (1979).*

| SYSTEM | FORMATION | THICK. | LITHOLOGY |
|---|---|---|---|
| MISSISSIPPIAN | PENNINGTON FM. | 150 To 450 Ft. | SHALE AND SILTSTONE (RED AND GREEN), SANDSTONE, DOLOSTONE AND LIMESTONE. |
| | BANGOR LS. | 150 To 300 Ft. | LIMESTONE, FOSSILIFEROUS, OOLITIC IN PART. |
| | HARTSELLE FM. | 0 To 60 Ft. | SANDSTONE, SANDY LIMESTONE, FOSSILIFEROUS SHALE, DOMINANT LITHOLOGY IS VARIABLE. |
| | MONTEAGLE LS. | 150 To 275 Ft. | LIMESTONE, FOSSILIFEROUS, OOLITIC & CROSS-BEDDED IN PART. |
| | ST. LOUIS LS. | MAX. 110 Ft. | LIMESTONE & DOLOSTONE, CHARACTERIZED BY LITHOSTROTION CORAL. |
| | WARSAW LS. | MAX. 80 Ft. | LIMESTONE, ARENACEOUS, CROSS-BEDDED IN PART. |
| | FT. PAYNE FM. | MAX. 115 Ft. | LIMESTONE AND DOLOSTONE, VERY SILICEOUS. |
| DEVO. | CHATTANOOGA SH. | MAX. 30 Ft. | SHALE, DARK GRAY TO BLACK, BITUMINOUS, FISSILE. |

*Figure 2. Mississippian terminology and general stratigraphy in the study area. After Stearns (1963).*

as a portion of a dominantly carbonate sequence on a stable craton. The name St. Louis was extended into Tennessee by Stearns (1963) and this usage is adapted here (Fig. 2).

## METHODS

Three-hundred samples were chosen representing all lithologic, textural, and sedimentary structure variations observed in outcrop. Routinely prepared thin sections were stained with a mixture of Alizarin-Red and Potassium Ferricyanide (Lindholm and

Finkelman, 1972). Samples were classified following Dunham (1962). Point count and visual estimates were used to determine the proportions of calcite, dolomite, chert, detrital quartz and clay, and the proportion of grains, micrite, spar, and non-carbonate components and the proportion of grain types. Grain and crystal sizes were measured directly. Raw data are tabulated in Cooper (1979). X-ray diffraction was used to evaluate the mineralogy of selected samples and to determine the degree of dolmite nonstoichiometry in the manner of Lumsden and Chimahusky (1980).

## STRATIGRAPHIC RELATIONSHIPS

The contact between the St. Louis and the underlying Warsaw Limestone is set between the first thick bedded dolostone or micrite above a greenish-gray, cross bedded, fossiliferous, grainstone. This usage is consistent with previous workers. The upper contact was defined at the base of the first appearance of a crossbedded, oolitic, grainstone; a lithology typical of the overlying Monteagle Limestone. Thomas (1972) and McLemore (1972) use this criteria and the uppermost cherty unit of the St. Louis. Tennessee stratigraphers commonly use the "Lost River" chert as an upper contact marker but this bryozoan bearing unit is not always present and opinions as to where the contact should be placed relative to the chert are inconsistant (Milici et al., 1979). We believe our choice of a distinct mappable lithologic change has merit and is consistant with stratigraphic practice. Upper and lower contacts appear conformable.

The St. Louis is fairly uniform in thickness at the complete measured sections; 102 ft at Pikeville, 133 ft at Daus, 128 ft at Ketner, 126 ft at Newhome, and 138 ft at Hooker. The partial exposures at South Pittsburg (129 ft probable) and at Monteagle (94 ft probable) are comparable in thickness to the St. Louis elsewhere in the study area.

To the south and east the St. Louis merges into the upper Tuscumbia Limestone (Thomas, 1972, 1979). To the north and west the St. Louis thickens somewhat (250 ft in north central Tennessee (Marcher, 1962)) and is more variable in lithology. Gypsum and anhydrite beds occur in Kentucky (McGrain and Helton, 1964; Rice et al., 1979). Overall the St. Louis of the study area appears to be somewhat thinner and more dolomitic than in adjacent areas.

## RESULTS

### Components

Calcite and dolomite are present as micrite, cement and in grains. Chert, though much less abundant, is a common component. Detrital quartz is a minor accessory. Clay minerals are present not only as thin beds but disseminated in the carbonate in quantities ranging up to a maximum of 8%. Gypsum and calcite and chert pseudomorphs after gypsum were observed.

### Lithofacies

Seven lithofacies were defined, lime mudstone, wackestone, packstone, grainstone, dolostone, silicastone and shale. These are interpreted in the light of modern analogues.

*Lime Mudstone.* Burrows, birdseye and fenestral structures, laminations, and mudcracks are variably abundant. The fine (0.5-5.0 mm) cryptalgal laminations (Aitken, 1967) have low relief and are smooth. Chert and detrital quartz are common and many samples are partially dolomitzed. Scattered normal marine fossil fragments are present and pellets are common in laminated lithologies. Lime mudstone forms one-quarter of the total section at Pikeville, one-tenth at Hooker, is less abundant at Ketner and South Pittsburg and is virtually absent elsewhere (probably replaced by dolomite). The sum of these structures and textures, not all present everywhere, suggests high

*Table 1. Comparison of St. Louis Micrites with Features Associated with Holocene and Ancient Carbonate Tidal Flat Deposits.*

| Holocene and Ancient Analogues | St. Louis Micrites |
|---|---|
| Dolomite | Common |
| Lime Mud Pelleted Mud | Both Common |
| Algal or Cryptalgal Laminations | Cryptalgal Present |
| Mudcracks | Common |
| Birdseye Structure | Common |
| Evaporites | Rare |
| Burrowing | Abundant |
| Root Tubules | Absent |
| Intraclasts | Common |
| Pebble Conglomerates | Absent |
| Storm Layers | Absent |

intertidal to low supratidal environments of deposition (Table 1).

*Wackestone.* Wackestone units have more burrows, fewer mudcracks and fewer fenestral structures than lime mudstones. Chert is more common than in lime mudstones. Some units show fine laminations and many beds are dolomitized. The 10 to 30% allochems present are dominated by pellets with subordinate quantities of fragments of normal marine organisms. The allochems occasionally form laminations that alternate with micrite laminae. Wackestones nowhere comprise more than 5% of a section. They are interpreted as intertidal to shallow subtidal deposits and are included with lime mudstones in interpretations to follow.

*Packstones.* More resistant to weathering than lime mudstone or wackestone units, packstone units tend to form ledges in otherwise slope topography. Primary sedimentary structures are uncommon, but include rare cross-bedding and cut and fill. Three subdivisions are; 1) *Lithostrotion* (coral) bearing, 2) medium grained, 3) fine graied. *Lithostrotion* bearing packstones were found everywhere except at New Home and are most common at Ketner and Daus. They are found only in the lower two-thirds of the St. Louis. No biohermal buildups were observed, rather *Lithostrotion* is found as scattered heads, sometimes in growth position, but more often on their sides. *Lithostrotion* heads are found in laterally persistant units composed of sand and silt size material. Apparently the genus does not need a solid substrate for growth. In the medium grained subdivision megascopic echinodern, brachiopod, and bryozoan fragments are abundant. Pellets and fine fossil fragments are visible only with the microscope in the fine grained facies. Many units are partially dolmitized with the dolomite confined to the fine matrix. Some samples are partially winnowed and have subequal spar and micrite in the grain intersticies. Chert is more abundant in the fine grained group.

This is the dominant lithology at most outcrops; 50% Monteagle, and South Pittsburg; 33% Hooker; 25% Ketner, Daus, and Pikeville; but only 12% at New Home.

Packstones were probably deposited on a subtidal sea floor which was occasionally swept by storms.

*Grainstones.* Units of this lithology tend to be thicker bedded than other lithologies (1 to 7 ft, average 3 ft) and form ledges. Cross-beds and cut and fill structures are common and the Monteagle section has a grainstone mound visible from Interstate 24.

Dolomite crystals and chert patches are not common in grainstones. Dolomite rhombs are larger than in other lithologies (40-60 microns) and replace both cement and grains. Microscopically grainstones exhibit abundant crinoid columnals with bryozoan, brachiopod, foram, ostracode, pelecypod, and intraclast grains in approximate order of abundance. There are scattered voids. Cement is commonly fine to medium crystalline spar with lesser but common syntaxial overgrowths on crinoid grains.

Grainstone units are not abundant forming 10% of the section at Daus; 16% at Ketner and Hooker; 20% at Pikeville and South Pittsburg; and 25% at New Home. At Monteagle the mound is 40% grainstone. Although more common toward the top of the section this lithology is found throughout the St. Louis.


*Figure 3. Photomicrograph of gypsum crystals (A) growing centripitally from the margin of a dolomite lined void that later completely filled in with ferroan calcite (B). Daus section (D-2-2), alizarin red stain, uncrossed nicols.*

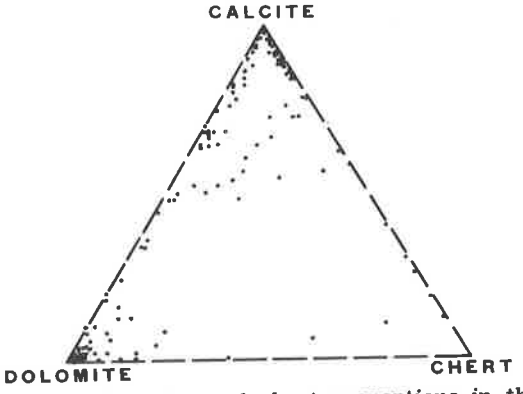


*Figure 4. Plot of calcite, dolomite and chert proportions in the St. Louis. For this plot clay and detrital quartz are ignored and the calcite, dolomite, and chert sum to 100%.*

Grainstones represent high energy marine environments. We interpret them here as related to subtidal conditions where tidal currents or waves kept fines suspended.

*Dolostones.* These units are thin to massive bedded. Chert is variably abundant and *Lithostrotion* was found in dolostone at Ketner and Daus. Sedimentary structures include birdseye structure, burrows, slightly undulant fine laminations, and mudcracks, these latter are less common than in the micrites. One to three inch shale beds are interlayed with the dolostones.

Texturally dolostones are composed of 10 to 40 micron euhedral to anhedral dolomite crystals. Some iron bearing dolomite was identified by its light blue stain. Unreplaced gypsum and chert and calcite pseudomorphs after gypsum were observed but are rare (Fig. 3).

Dolostones form the basal bed at all locations except Pikeville (micrite). Dolostone forms 50% of the Daus and New Home sections, is 33% of Ketner, 25% of Hooker, and is 15% or less elsewhere.

Most of the criteria for supratidal dolomite origin are met by the St. Louis (Table 2).

*Silicastone and Chert.* The term silicastone is employed here for rocks with over 50% chert and otherwise calcite or dolomite. Chert is used in its classic sense. The microscopic texture of the chert varies widely with equant crystals of 0.01 to 0.10 mm size dominating minor fibrous chalcedony.

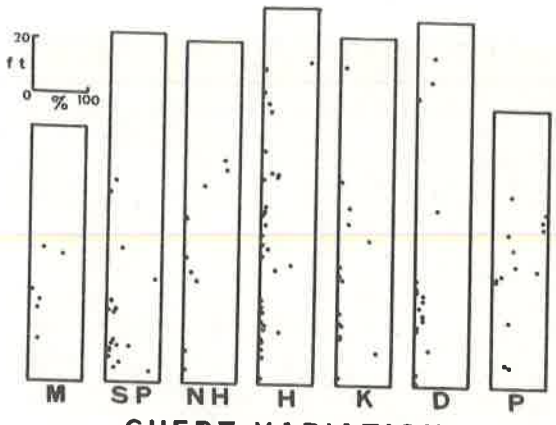


*Figure 5. Plots of the vertical variation in the proportion of chert at the study locations.*

Chert is found in all carbonate rock types but is more abundant in dolostone and less abundant in grainstone lithologies. There does not appear to be any pattern relating the abundance of dolomite and the abundance of chert (Fig. 4). There does not appear to be any pattern in chert abundance geographically or stratigraphically (Fig. 5).

Field observation suggests that most silicastone and chert formed by alteration of pre-exhisting limestones or dolostones (e.g. chert mudcracks, partial to complete chert replacement of fossils including *Lithostrotion* heads, patches of host rock enclosed in chert nodules). No chert nodules were found with bedding draped around them. In some dolostones allochems are preserved in chert patches and destroyed in the surrounding dolomite. Elsewhere dolomite crystals are isolated in the chert. Pseudomophs of chert after dolomite were observed in insoluble residues. These observations suggest chertification after neomorphic recrystallization of the dolomite.

*Shales.* Small amount of green, gray, and black illitic shales form 2% of the St. Louis. Beacuse of their low resistance to weathering they are poorly exposed and were not studied in detail. There is no apparant pattern to their stratagraphic or geographic distribution.

### Dolomite Nonstoichiometry

The mineral dolomite rarely achieves its stoichiometric formula of $Ca_{0.50}$ $Mg_{0.50}$ $CO_3$. Typically there is an excess of calcium and formulas of $Ca_{0.52}$ $Mg_{0.48}$ to $Ca_{0.57}$ $Mg_{0.43}$ are the norm. Lumsden and Chimahusky (1980) sought a relation between dolomite nonstoichiometry and a variety of textural and stratigraphic variables. We have attempted to correlate dolomite nonstoichiometry with 1) lithology, 2) dolomite percentages in the whole rock, 3) dolomite crystal size, and 4) stratigraphic position. No pattern of relationship was observed.

## ENVIRONMENTAL INTERPRETATION

### Modern Model

A comparison of the St. Louis with possible modern analogues suggests that the Great Bahama Bank is the most suitable, particularly the area west of Andros Island, i.e. the area interior to the bank in which shallow subtidal, intertidal, and supratidal environments cover subequal areas (Purdy 1963). The scale of the study area is appropriate and the various modern facies in the Bahamas can be matched to the observed St. Louis lithologies on a one for one basis (Tables 1 and 2).

*Table 2. Composite List of Ten Criteria for Penecontemporaneous Supratidal Dolomite.*

| Ancient Penecontemporaneous Supratidal Dolomite Deposits | St. Louis Dolostones |
|---|---|
| Desiccation Cracks | Common |
| Birdseye Structure | Common |
| Evaporite Minerals, Molds or Pseudomorphs | Anhydrite and Clacite Pseudomorphs After Gypsum |
| Burrows, Especially Vertical | Vertical Dominate Over Horizontal Burrows |
| Algal Stromatolites or Cryptalgal Laminites | Cryptalgal Laminites |
| Thin Extensive Dolostone Beds | Medium to Thick Bedded Dolostones |
| Bituminous Stringers | Anastamosing Bituminous Stringers |
| Dolomite Intraclasts | Common in Packstone Beds |
| Sparsity of Marine Fossils | Very Sparse in Very Finely Crystalline Dolostones |
| Dolomite in Two Size Classes | 5 to 25 Microns<br>40 to 90 Microns |

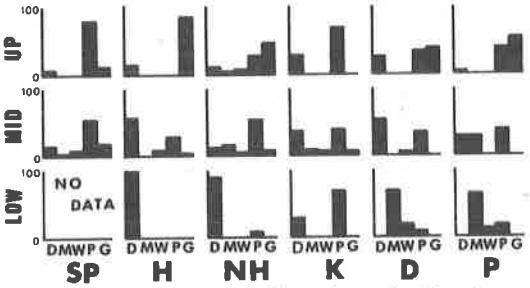


*Figure 6. Histograms of the proportion of various facies in the lower (20 ft.), upper (30 ft.) and middle (the balance) St. Louis. D-dolomite, M-lime mudstone, W-wackestone, P-packstone, G-grainstone. SP-South Pittsburg, NH-Newhome, H-Hooker, K-Ketner, D-Daus, P-Pikeville location.*

Data for the physical conditions on the Great Bahama Bank have been summarized by Bathurst (1975, p. 96-141). Figures 6, 7, and 8 summarize the lithologic variation in the St. Louis. Of particular importance is the observation that higher energy (coarser grained, less micrite) facies are found in deeper water whereas micrite and micrite charged facies are found in shoreline related environments. The analogy to the St. Louis is as follows.

Dolostones formed as a response to supratidal conditions similar to those along the western margin of Andros Island. Lime muds and wackestones were deposited in the thin intertidal belts that flank the supratidal areas. The present tide ranges on west Andros are very low, mostly less than a foot, and the lime mudstone-wackestone area consequently is small. Lime mudstones and wackestones were also deposited in very shallow water flanking the intertidal area and swept by weak tidal currents. Packstones were deposited in somewhat deeper water ( $\pm$ 20 ft (6 m) ) and grainstones were formed where tidal currents, channel currents, waves or storms kept the water waves or storms kept the water agitated enough to keep micrite in suspension.

## Lower St. Louis

The lower portion of the St. Louis is dominated by dolostone and micrite lithologies (Figs. 6, 7, and 8). This suggests that broad areas of supratidal environments, with flanking intertidal areas, covered most of the study area (Fig. 9).

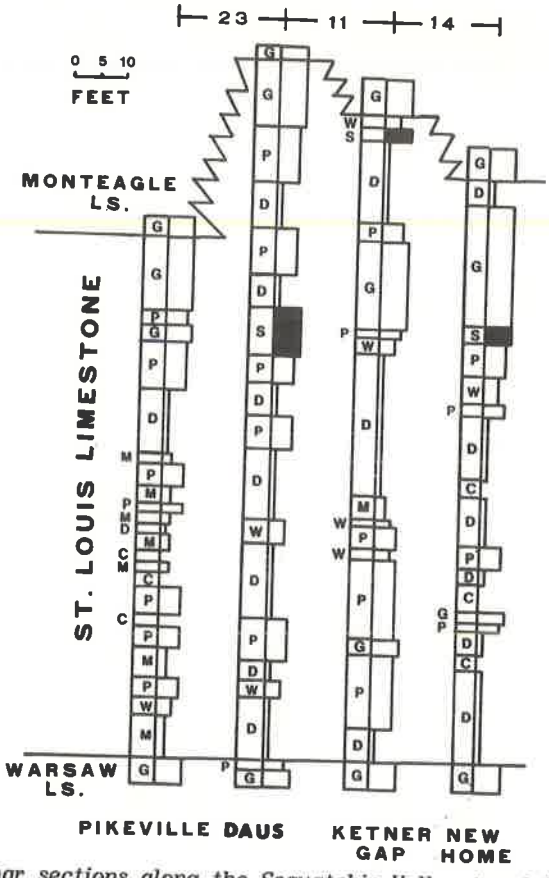


*Figure 7. Columnar sections along the Sequatchie Valley trend (NE-SW). Lithologies are coded as; D-dolomite, W-wackestone, P-packstone, G-grainstone, S-silicastone (and colored black), C-covered. The relative energy of the environment of deposition of the various carbonate litholgies is implied by the width of the column, the more energy the wider.*

Packstones form 70% of the lower St. Louis at Ketner suggesting that this may have been the site of tidal current agitation that brought nutrients to a flourishing biota. Relatively uniform conditions prevailed during deposition of the lower 20 ft of the St. Louis as indicated both by the limited variety of lithologies (Fig. 6) and by the relatively limited vertical variation (Figs. 7 and 8).

## Middle St. Louis

This is the balance of the St. Louis between the lower 20 ft and upper 30 ft. Typically there is more vertical variation and a greater spread of lithologic types in this interval (Figs. 6, 7, and 8). This suggests that the environment changed to more varied conditions in which a large number of small, low relief, islands were scattered on a very shallow shelf (Fig. 9). The increased abundance of normal marine organisms present in the increased proportion of packstone suggests normal marine, clear water, environments were more widespread than in the lower St. Louis. The pattern of vertical variation was tested using Markov Chain analysis (see Lumsden, 1971, for technique) and was found to be random. We hypothesize that supratidal, intertidal, and shallow subtidal environments migrated irregularly creating a mosaic of environments that resulted in a random variation in lithologies both in space and time.

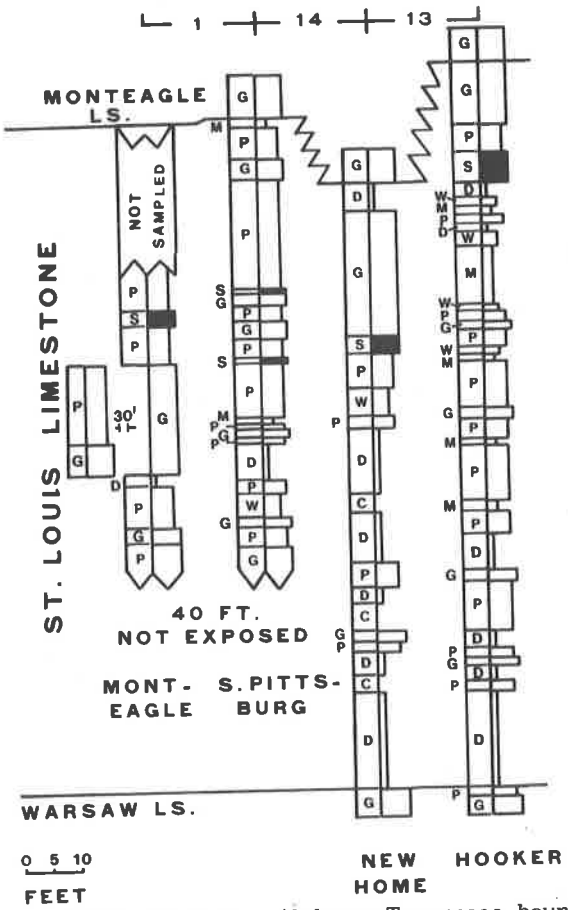


*Figure 8. Columnar sections along the Alabama-Tennessee boundary (E-W). Key in Figure 7.*

## Upper St. Louis

The upper 30 ft of the St. Louis is transitional to the high energy oolitic grainstones of the overlying Monteagle Limestone. At all locations packstones and grainstones dominate the lithology (Figs. 6, 7, and 8). This indicates a generally high environmental energy; probably the result of an overall increase in water depth sufficient to reduce the frictional drag between the sea water and the bottom, thus permitting larger waves to form and keep fines suspended. We hypothesize an open shelf set of conditions, swept by currents and waves, with relatively fewer low relief islands (Fig. 9C).

## Vertical Facies Pattern

A generalized representation of the overall pattern of vertical facies changes in the St. Louis is presented in figure 10. The curve was created by assigning each carbonate rock type a number representing its relative energy, assembling all the data into a single combined section, and then using an eleven term smoothing equation to smooth the data. The resultant curve is somewhat more quantitative than a simple subjective interpretation. There are 3 cycles of lime mudstone (or dolostone) to packstone and back to lime mudstone (or dolostone) surmounted by a fourth cycle of lime mudstone (or dolostone) to grainstone, representing the transition to the overlying Monteagle.

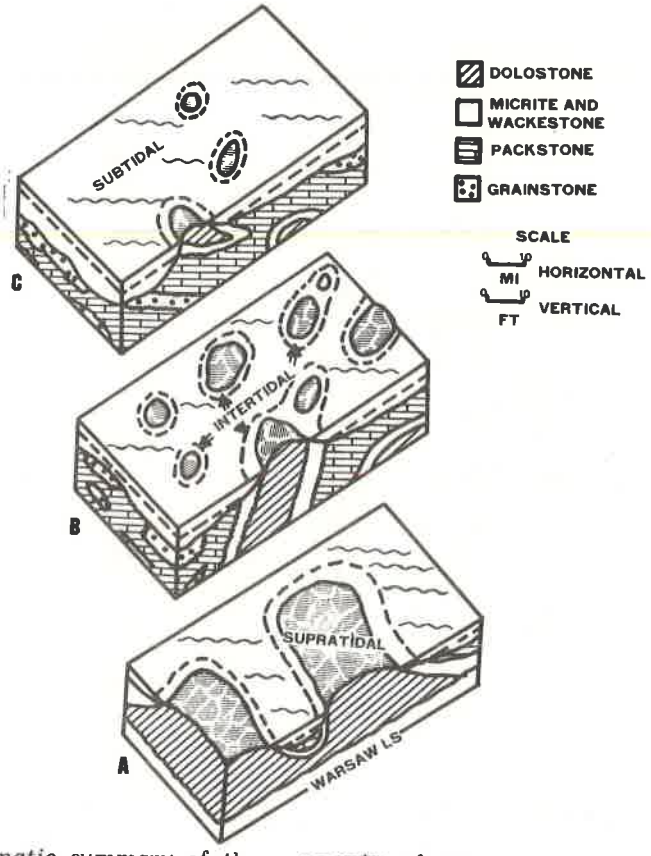


*Figure 9. Schematic summary of the geography of the study area during the time of St Louis deposition. A-lower St. Louis, B-Middle St. Louis, C-Upper St. Louis.*

The Monteagle is a cross-bedded, oolitic grainstone, a very high energy deposit. The great lateral extent of the Monteagle implies high energy wave and tidal conditions across a shallow shelf during deposition (Handford, 1978). The Monteagle - St. Louis contact is sharp but apparently conformable.

## SUMMARY AND CONCLUSIONS

The St. Louis of the study area is somewhat thinner and contains more carbonate than its clastic equivalents to the southeast and its evaporite rich facies to the northwest. The proportion of dolomite is higher here than elsewhere.

The pattern of environments of deposition in the St. Louis is analogous to those west of Andros Island in the modern Bahamas where low carbonate mud islands are scattered in very shallow normal marine waters.

The lower St. Louis is dominated by low energy micrite rich lithologies. The middle St. Louis contains varied lithologies composed of dolostone, lime mudstone, wackestone, packstone, and grainstone. The upper St. Louis is dominated by spar rich fabrics. This change in lithology from lower to upper St. Louis suggests a gradual increase in overall environmental energy possibly due to a gradual deepening of the waters from two to three feet to over 10 feet. The variable pattern of lithologies vertically and laterally suggests a shifting mosaic of environments in which ephemeral supratidal islands expanded, contracted, and migrated in response to local variations in weather, currents and tectonics.

Dolostones of the St. Louis fulfill most of the criteria for supratidal origin. They are invariably nonstoichiometric and commonly ankeritic. Chert formed after the

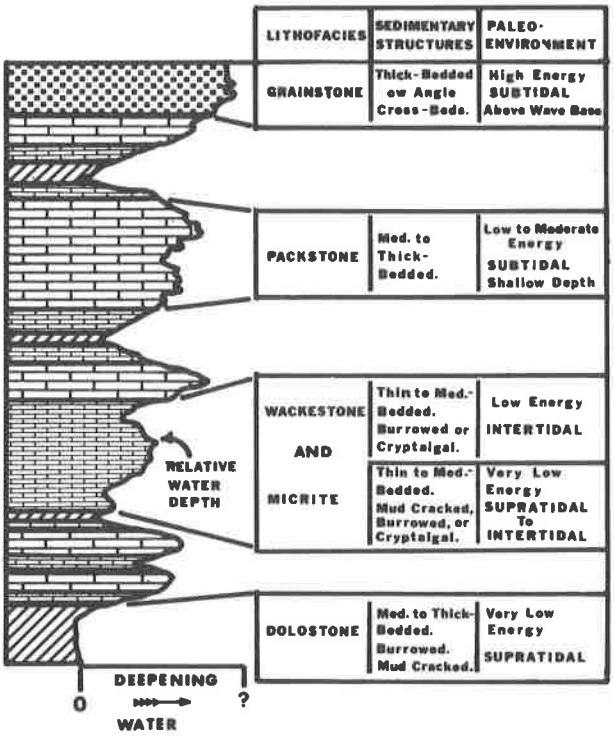


*Figure 10. Subjective summary of the ideal coarsening (increasing energy, increasing water depth) upwards lithologic sequence of the St. Louis Limestone in the study area.*

dolomite underwent neomorphic recrystallization and preferentially replaces calcite leaving dolomite relatively unaffected.

## ACKNOWLEDGEMENTS

Robert Milici guided early field work. An Amoco Foundation Fellowship provided financial support for one of us (Cooper). A Union Oil Company grant for faculty travel is also acknowledged. Richard Stearns and Leonard Alberstadt reviewed an early version of the manuscript.

## REFERENCES CITED

Aitken, J.D., 1967, Classification and environmental significance of cryptalgal limestones and dolomites, with illustrations from the Cambrian and Ordovician of southwestern Alberta: Jour. Sed. Petrology, v. 37, p. 1163-1178.

Bathurst, R.G.C., 1975, Carbonate Sediments and Their Diagenesis, 2nd Ed., Elsevier Sci. Pub., Oxford, 658 p.

Bergenback, R.E., Horne, J.C., and Inden, R.F., 1972, Depositional environments in Mississippian carbonate rocks at Monteagle, Tennessee, *in*, Carboniferous Depositional Environments in the Cumberland Plateau of Southern Tennessee and Northern Alabama: Tennessee Div. Geology Rept. Inv. 33, p. 14-18.

Bergenback, R.E., 1978, Carboniferous depositional environments in the Southern Cumberland Plateau, *in*, Field Trips in the Southern Appalachians: Tennessee Div. Geology Rept. Inv. 37, p. 63-85.

Cooper, Joseph L., 1979, The Petrology of the St. Louis Limestone (Middle Mississippian), Southeast Tennessee: Unpub. MS Thesis, Memphis State Univ., Memphis, TN, 165 p.

Dunham, R.J., 1962, Classification of carbonate rocks according to depositional texture, *in*, Ham, W.E., ed., Classification of Carbonate Rocks, a Symposium: Am. Assoc. Petroleum Geologists Mem. I.

Handford, C.R., 1978, Monteagle Limestone (Upper Mississippian)--oolitic tidal-bar sedimentation in Southern Cumberland Plateau: Am. Assoc. Petroleum Geologists Bull., v. 62, p. 644-656.

Lindholm, R.C., and Finkelman, R.B., 1972, Calcite staining: semiquantitative determination of ferrous iron: Jour. Sed. Petrology, v. 42, p. 239-242.

Lumsden, D.N., 1971, Markov Chain analysis of carbonate rocks: applications, limitations, and implications as exemplified by the Pennsylvanian System in Southern Nevada: Geol. Soc. America Bull., v. 82, p. 476-462.

Lumsden, D.N., and Chimahusky, J.S., 1980, Relationship between dolomite nonstoichiometry and carbonate facies parameters, *in*, Zenger, D.H., and Dunham, J.B., eds., Concepts and Models of Dolomitization: Soc. Econ. Paleontologists and Mineralogists Spec. Pub. 27.

Marcher, M.V., 1962, Geology of the Dover Area, Stewart County, Tennessee: Tennessee Div. Geology, Rept. Inv. 16, 46 p.

McGrain, P., and Helton, W.L., 1964, Gypsum and anhydrite in the St. Louis Limestone in Northwestern Kentucky: Kentucky Geologic Survey Inf. Cir. 13, 26 p.

McLemore, W.H., 1972, Depositional environments of the Tuscumbia-Monteagle-Ford interval in Northwest Georgia and Southeast Tennessee, *in*, Sedimentary Environments in the Paleozoic rocks of northwest Georgia: Georgia Geologic Soc. Guidebook II, p. 69-73.

Milici, R.C., Briggs, G., Knox, L.M., Sitterly, D., and Statler, A.T., 1979, The Mississippian and Pennsylvanian (Carboniferous) Systems in the United States-Tennessee: USGS Prof. Paper 1110-G, 36 p.

Peterson, M.N.A., 1962, The mineralogy and petrology of the Upper Mississippian carbonate rocks of the Cumberland Plateau in Tennessee: Jour. Geology, v. 70, p. 1-31.

Purdy, E.G., 1963, Recent calcium carbonate facies of the Great Bahama Bank: I. Petrography and reaction groups: Jour. Geology, v. 71, p. 334-355.

Rice, C.L., Sable, E.G., Denver, G.R., and Kehn, T.M., 1979, The Mississippian and Pennsylvanian (Carboniferous) Systems in the United States-Kentucky: USGS Prof. Paper 1110-F, 28 p.

Stearns, R.G., 1963, Monteagle Limestone, Hartselle Formation, and Bangor Limestone--A New Mississippian Nomenclature for use in middle Tennesse, with a history of its development: Tennessee Div. Geology Information Cir. 11, 18 p.

Thomas, W.A., 1967, Mississippian Stratigraphy of the Tennessee Valley, Alabama, *In* A Field Guide to Mississippian Sediments in Northern Alabama and South-central Tennessee: Alabama Geologic So. 5th Annual Field Trip, p. 4-9.

Thomas, W.A., 1972, Mississippian Stratigraphy of Alabama: Alabama Geologic Survey Mon. 12, 121 p.

Thomas, W.A., 1979, The Mississippian and Pennsylvanian (Carboniferous) Systems in the United States--Alabama: USGS Prof. Paper 1110-I, 45 p.

Vail, P.R., 1959, Stratigraphy and Lithofacies of Upper Mississippian Rocks in the Cumberland Plateau: Ph.D. Thesis, Northwestern Univ., 143 p.

# ORIGIN OF SPESSARTINE-RICH GARNET IN META-RHYOLITE, CAROLINA SLATE BELT

By

R. V. Fodor
and
E. F. Stoddard
Department of Geosciences
North Carolina State University
Raleigh, North Carolina 27650

and

E. R. Burt
Geological Survey Section
North Carolina Department of Natural Resources
and Community Development
Raleigh, North Carolina 27611

## ABSTRACT

Meta-rhyolites ($SiO_2$ > 74 wt.%) in the Carolina slate belt, Montgomery County, North Carolina, contain clusters (< 1 cm in size) of chlorite + epidote ± garnet (+ quartz + muscovite). Textural relationships show that epidote growth preceded chlorite and garnet crystallization, and electron-microprobe analyses reveal that the garnet is spessartine-rich ($Sp_{55}Al_{20}Gr_{20}An_5$), a variety commonly observed in both silicic plutonic and low-grade metamorphic rocks, though not in silicic volcanic rocks. The garnet demonstrates weak compositional zoning where MnO increases from rim to core, accompanied by decreases in FeO and CaO. Textures and garnet composition and zoning support a metamorphic origin for the spessartine-rich garnet where growth occurred during greenschist-facies (chlorite-grade) metamorphism from Mn-chlorite + epidote.

## INTRODUCTION

Garnet in silicic volcanic and plutonic rocks has a special interest to petrologists because of its potential to help estimate pressures and temperatures associated with origins of host rocks. Green and Ringwood (1972), for example, pointed out that almandine garnet in a rhyodacite suggests a depth of origin of at least lower crust, and Green (1977) related Mn content in igneous garnet to compatibility with an upper crustal regime. However, because much garnet is metamorphic in origin, the history and significance of this mineral in volcanic rocks that have experienced metamorphism is not immediately clear. Yet the distinction is important to make because each origin of garnet--whether igneous or metamorphic--leads to widely different interpretations for the petrogenesis of the host rocks.

The Carolina slate belt, a region of late Precambrian to early Paleozoic sedimentary and volcanic rocks associated with a proto-Atlantic volcanic arc and which has suffered regional metamorphism (Butler and Ragland, 1969; Hatcher, 1972), is one such dual environment where the significance of garnet is equivocal: the garnet occurs in meta-rhyolites. Previous investigations in this geologic province (Burt, 1965; Seiders, 1978) showed that these meta-volcanic garnets are spessartine-rich, a variety compatible with both igneous and metamorphic origins. There have been no studies, however, directed at the origin of the spessartine-rich garnets, and at what that origin implies about slate belt history. This report, then, is a study of the significance of spessartine-rich garnet in meta-rhyolite of the Carolina slate belt.

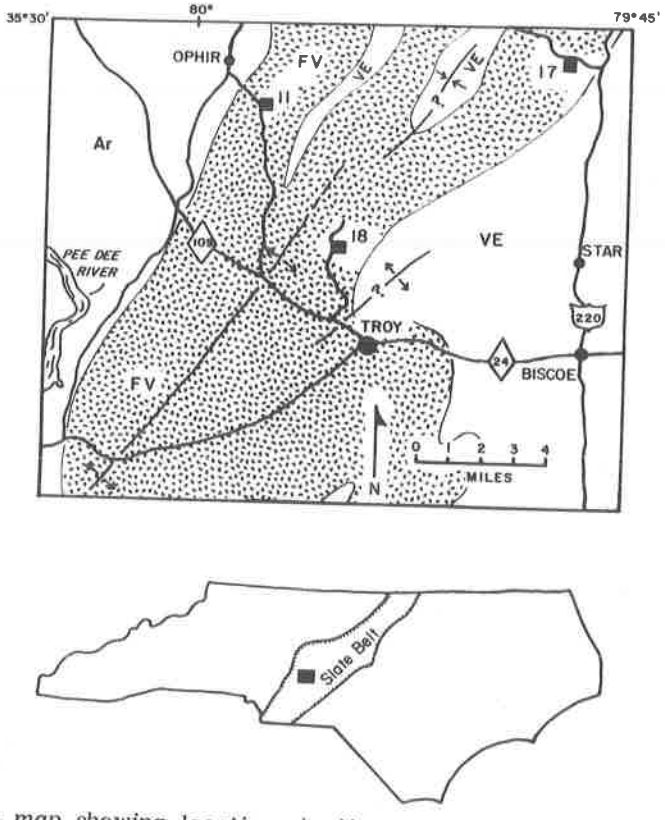


*Figure 1. Index map showing locations in Montgomery County, North Carolina, for garnet-bearing chlorite + epidote assemblages (11 and 17) and garnet-free chlorite + epidote assemblages (18). FV = felsic volcanic rocks; VE = mixed volcanic and epiclastic rocks; and Ar = argillites. The Troy anticlinorium of Conley (1962) trends northeast-southwest.*

## GENERAL GEOLOGY AND PETROGRAPHY

Samples collected from three outcrops of meta-volcanic rock in Montgomery County, North Carolina, were analyzed for this study (Fig. 1a). Each locality has clusters up to 1 cm in size of epidote and chlorite, and at two localities, garnet crystals 1 to 2 mm in size are present in these green-colored assemblages.

Conley (1962) included these meta-volcanic rocks in the Uwharrie Formation, a sequence of felsic volcaniclastic rocks and lava flows more than one thousand meters thick and mainly subaerial in origin. Structurally, the garnet-bearing rocks are exposed within the Troy anticlinorium (Fig. 1). Each of the meta-volcanic units is dense, almost glassy in texture, gray-black in color, and flow banded. Distinguishing features of the units include weakly developed slaty cleavage in one of the garnet-bearing units, and a relict quartz- and feldspar-phyric texture in the unit lacking garnet.

The assemblages of epidote + chlorite $\pm$ garnet occur as rare (< 1 volume % of outcrop) clusters, sometimes nodular, but more commonly irregular in form. The chlorite is deep green in color and occurs in book-like form, closely resembling biotite in habit. Epidote is olive green in color, and the garnet occurs as cinnamon-red crystals sparsely mixed among the epidote and chlorite. Flow bands in the two garnet-bearing units wrap above and below the epidote and chlorite clusters, indicating the presence of phenocrysts or glomerocrysts (or some other obstacle to flow) at the time of lava-flow emplacement (Fig. 2a, b).

Thin-section examination reveals the felted quartz-feldspar texture of the rhyolite groundmass, and local stringers of small magnetite grains and/or interlocking (recrystallized) quartz grains. Where phenocrysts are present, they are mainly Na-rich

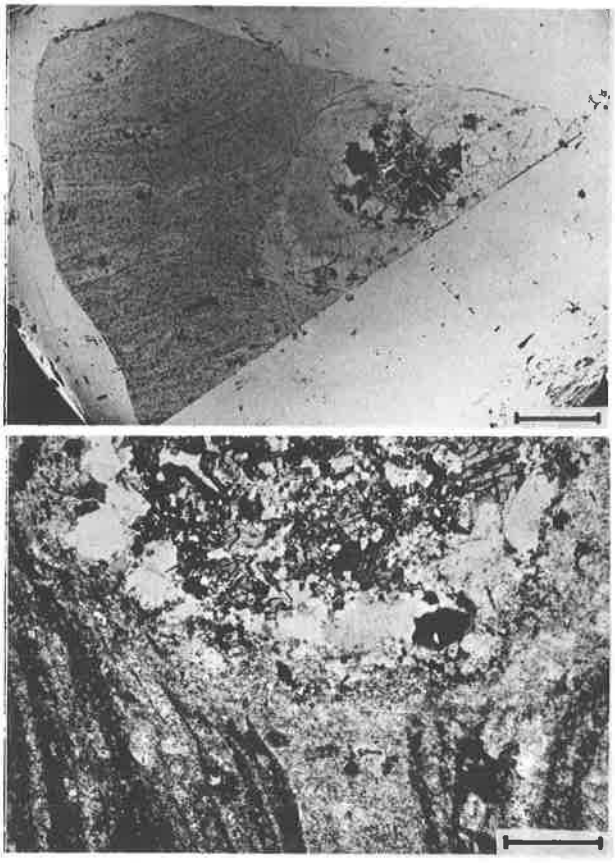

*Figure 2.(a) An overview of a chlorite-epidote assemblage (surrounded by a quartz rim) from locality 11. Flow bands in the host meta-rhyolite bend around the assemblage. Plane polarized light; scale bar equals 2 mm. (b) Close-up of flow bands that bend around a chlorite + epidote + quartz + garnet assemblage (garnet not visible) from locality 11. Partially crossed nicols; scale bar equals 1 mm.*

*Figure 3. An assemblage of chlorite (dark gray, center) + epidote (moderate gray) + garnet (two high-relief grains near center) + quartz (white) + magnetite in a meta-rhyolite host (gray, lower lift) from locality 17. Plane polarized light; scale bar equals 1 mm.*

plagioclase, some containing epidote grains (produced by saussuritization); quartz occurs as rare phenocrysts.

The chlorite and epidote have subhedral to anhedral forms, and the clusters of

*Table 1. Whole-rock compositions (in wt.%) of three meta-rhyolites, 11, 17 (both garnet-bearing) and 18 (no garnet) from the Carolina slate belt, Montgomery County, North Carolina.*

| | 11 | 17 | 18 |
|---|---|---|---|
| $SiO_2$ | 74.40 | 76.75 | 76.59 |
| $TiO_2$ | 0.29 | 0.17 | 0.23 |
| $Al_2O_3$ | 13.48 | 11.95 | 11.94 |
| $Fe_2O_3$ | 0.87 | 1.01 | 1.17 |
| FeO | 0.97 | 0.42 | 0.78 |
| MnO | 0.08 | 0.04 | 0.06 |
| MgO | 0.23 | 0.25 | 0.24 |
| CaO | 0.53 | 0.75 | 0.70 |
| $Na_2O$ | 6.10 | 4.05 | 5.90 |
| $K_2O$ | 2.17 | 3.55 | 2.34 |
| $H_2O^-$ | < 0.01 | < 0.01 | < 0.01 |
| $H_2O^+$ | 0.43 | 0.48 | 0.49 |
| $P_2O_5$ | 0.03 | 0.01 | 0.03 |
| TOTAL | 99.58 | 99.37 | 99.47 |
| $Na_2O/K_2O$ | 2.81 | 1.14 | 2.10 |

analyst: J.W. Husler, Univ. New Mexico

these two minerals are also associated with abundant (20 to 40 vol.%) anhedral and interlocking quartz grains (Fig. 3). Most of the quartz surrounds the epidote + chlorite clusters and serves as a transition zone between the clusters and the host rocks. Pleochroism of the chlorite ($2V_x \sim 10^o$) is green to pale green; epidote ($2V_x \sim 80^o$ is almost colorless, only slightly yellow in plane-polarized light.

The garnet crystals examined microscopically are subhedral to anhedral in outline. None of the garnet crystals are perfectly isotropic, but show weak birefringence. White mica is a sparse phase associated with the chlorite + epidote assemblages, and subhedral to euhedral magnetite is present and usually restricted to the outer portions of the clusters. Calcite was observed as a rare interstitial phase in the clusters.

Textural relationships provide information on the relative order of crystallization. Most relevant is that epidote occurs as subhedral inclusions in both chlorite and garnet (Fig. 4a, b), and therefore probably preceded garnet growth.

## ANALYTICAL DATA

### Analytical Techniques

Whole-rock analyses were done at the University of New Mexico by the following techniques: Silica was determined gravimetrically. Total Fe, $Al_2O_3$, MgO, CaO, $Na_2O$, $K_2O$, $TiO_2$, and MnO were determined by atomic absorption using calibration curves prepared from U.S. Geological Survey standards. For determination of $P_2O_5$, an adaptation of the Molybdenum Blue spectrophotometric method was employed. Water was determined by ignition loss, but the amount of $Fe_2O_3$ oxidation was taken into account by $K_2Cr_2O_7$ titration of ferrous iron in both the ignited and unignited samples.

Mineral compositions were determined with an ARL-EMX-SM electron microprobe operated at 15 keV accelerating voltage and 0.015 to 0.20 μA sample current. The standards used were Mn-garnet and clinopyroxene for garnet; biotite and clinopyroxene for white mica, chlorite, and epidote; albite, orthoclase, and labradorite for albite; and magnetite for magnetite.

### Whole-rock Compositions

The bulk compositions of the rocks are rhyolitic ($SiO_2$ > 74 wt.%) and have high $Na_2O/K_2O$ ratios (1 to 3) (Table 1). Similar compositions were previously reported for Carolina slate belt rhyolites (Butler and Ragland, 1969; Sieders, 1978) and for rhyolites in the geographic extension of this meta-volcanic belt in Georgia (Whitney et al., 1978). Although bulk-rock compositions display no obvious effects of metamorphism (the relatively high $Na_2O$, however, may be a product of Na-metasomatism; Sieders, 1978)

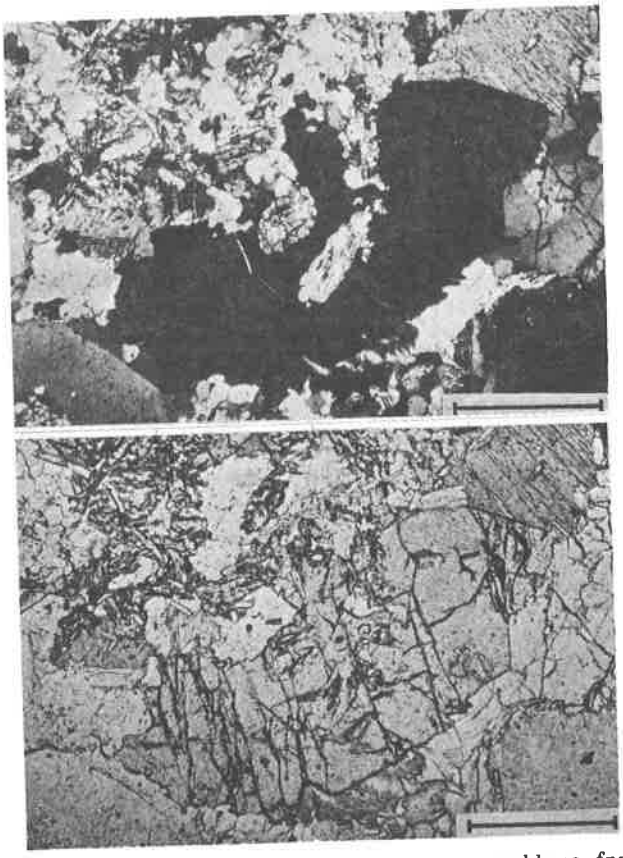

*Figure 4.(a) Large garnet grain (~ 1.5 mm) in an assemblage from locality 11. It contains inclusions of epidote. Crossed nicols; scale bar equals 0.5 mm. (b) Same view as 4a, but plane polarized light.*

and are virtually free of weathering (essentially no $H_2O^-$ present), the assemblages of chlorite and epidote in these rocks are clear manifestations of the low grade metamorphism (greenschist facies) these rocks experienced. Previous investigations have noted similar low-grade metamorphism in the Carolina slate belt (e.g., Butler and Ragland, 1969; Tobisch and Glover, 1969).

## Mineral Compositions

Compositionally, the chlorite is moderately rich in FeO (29 wt.%) and has substantial amounts of MnO, about 2 wt.% (Table 2). Except for the MnO, however, these chlorites are similar in composition to those in other greenschist rocks (e.g., Brown, 1967; Atherton, 1968). Similarly, the co-existing epidote contains moderate amounts of FeO and is locally enriched in the piedmontite molecule, having MnO up to 1.5 wt.% (Table 2). White mica, too, contains MnO and rather high FeO contents (Table 2).

The MnO content of the garnet averages about 24 wt.%, but moderate compositional zoning shows slightly increased MnO away from crystal margins and near crystal centers, reaching ~27 wt.% (Fig. 5). The increasing MnO from rim to core is attended by a subtle decrease in FeO and CaO (Fig. 5). In molecular percent endmembers, spessartine increases inward from 50 to 60%, and almandine and grossular decrease from 22 to 17%, and from 22 to 15%, respectively.

Magnetite associated with the chlorite + epidote is nearly pure $Fe_3O_4$ in composition (MnO 0.2 wt.%). Plagioclase, which is not directly associated with the chlorite + epidote assemblages, but present as phenocrysts in the rocks, is nearly pure

*Table 2. Average compositions (in wt.%; by electron microprobe) of chlorite, epidote, and white mica in meta-rhyolites 11, 17 (both garnet bearing), and 18 (no garnet), Carolina slate belt, Montgomery County, North Carolina.*

| | Chlorite | | | Epidote | | | White Mica | | |
|---|---|---|---|---|---|---|---|---|---|
| | 11 | 17 | 18 | 11 | 17 | 18 | 11 | 17 | 18 |
| $SiO_2$ | 25.3 | 25.3 | 25.0 | 38.6 | 38.6 | 38.5 | 47.8 | 47.0 | 48.1 |
| $TiO_2$ | 0.04 | 0.03 | 0.01 | 0.11 | 0.08 | 0.15 | 0.06 | <0.01 | 0.03 |
| $Al_2O_3$ | 19.3 | 19.0 | 19.7 | 25.9 | 25.7 | 24.6 | 31.5 | 29.7 | 29.5 |
| FeO | 32.0 | 29.5 | 29.9 | 10.7 | 10.2 | 11.0 | 6.1 | 6.2 | 6.9 |
| MnO | 2.5 | 2.3 | 2.1 | 1.1+ | 0.26 | 0.28++ | 0.08 | 0.12 | 0.16 |
| MgO | 10.2 | 11.7 | 11.2 | 0.1 | <0.01 | 0.01 | 1.3 | 1.8 | 1.7 |
| CaO | 0.02 | 0.01 | 0.01 | 22.6 | 23.3 | 23.2 | <0.01 | 0.02 | <0.01 |
| $Na_2O$ | 0.05 | 0.03 | 0.04 | 0.01 | <0.01 | 0.01 | 0.18 | 0.19 | 0.15 |
| $K_2O$ | 0.03 | 0.01 | 0.02 | 0.02 | 0.01 | 0.02 | 7.6 | 7.8 | 7.9 |
| TOTAL* | 89.44 | 87.88 | 87.98 | 99.14 | 98.15 | 97.77 | 94.62 | 92.83 | 94.44 |
| Number of ions on the basis of 0 = 28 for chlorite; 0 = 12.5 for epidote; and 0 = 22 for white mica | | | | | | | | | |
| Si | 5.500 | 5.521 | 5.455 | 3.066 | 3.083 | 3.107 | 6.434 | 6.479 | 6.533 |
| $Al^{IV}$ | 2.500 | 2.479 | 2.545 | – | – | – | 1.566 | 1.521 | 1.467 |
| $Al^{VI}$ | 2.437 | 2.405 | 2.516 | 2.422 | 2.418 | 2.338 | 3.426 | 3.300 | 3.251 |
| Ti | 0.007 | 0.005 | 0.002 | 0.006 | 0.005 | 0.009 | 0.007 | 0.714 | 0.004 |
| Fe | 5.817 | 5.382 | 5.453 | 0.710 | 0.681 | 0.733 | 0.686 | 0.014 | 0.783 |
| Mn | 0.461 | 0.425 | 0.388 | 0.074 | 0.018 | 0.019 | 0.009 | 0.014 | 0.019 |
| Mg | 3.302 | 3.805 | 3.642 | 0.012 | – | 0.001 | 0.261 | 0.370 | 0.344 |
| Ca | 0.004 | 0.003 | 0.003 | 1.925 | 1.996 | 2.008 | – | 0.003 | – |
| Na | 0.020 | 0.014 | 0.016 | 0.002 | – | 0.002 | 0.046 | 0.054 | 0.040 |
| K | 0.008 | 0.002 | 0.006 | 0.002 | – | 0.002 | 1.304 | 1.370 | 1.368 |
| Z | 8.000 | 8.000 | 8.000 | 3.066 | 3.083 | 3.107 | 8.000 | 8.000 | 8.000 |
| X | 12.056 | 12.041 | 12.026 | 5.150 | 5.118 | 5.112 | 5.739 | 5.825 | 5.809 |

* Totals low due to presence of $H_2O$, which is not detectable by electron probe.

\+ Range, 0.25–2.3 wt.%

++ Range, 0.19–1.5 wt.%

albite ($Ab_{97}An_{2.4}Or_{0.6}$).

## DISCUSSION AND CONCLUSIONS

The main objective of this study is to establish the origin of the spessartine-rich garnets in the metamorphosed rhyolites. They may be (1) primary phenocrysts in rhyolite which were later enveloped by or which contributed to the chlorite + epidote metamorphic assemblage, or (2) products themselves of the low-grade metamorphism characteristic of the Carolina slate belt. That spessartine-rich garnet could possibly be a phenocryst phase in these silicic rocks is suggested by numerous occurrences of garnet-bearing silicic rocks (granites and pegmatites) where the garnet is almost invariably Mn-rich in composition (e.g., Wright, 1938; Miller and Stoddard, 1978). Presumably, the formation of these igneous spessartine-rich garnets is related to simple fractional crystallization processes where Mn is concentrated in late-stage liquids (e.g., Miller and Stoddard, 1978) and controlled somewhat by the pressures and oxygen fugacities of the silicic regime (Green, 1977; Mueller and Schneider, 1971). These Mn-rich garnets from plutonic rocks are invariably low in CaO (< 15 mole % grossular + andradite) and MgO (< 15 mole % pyrope), and thus they are essentially spessartine-

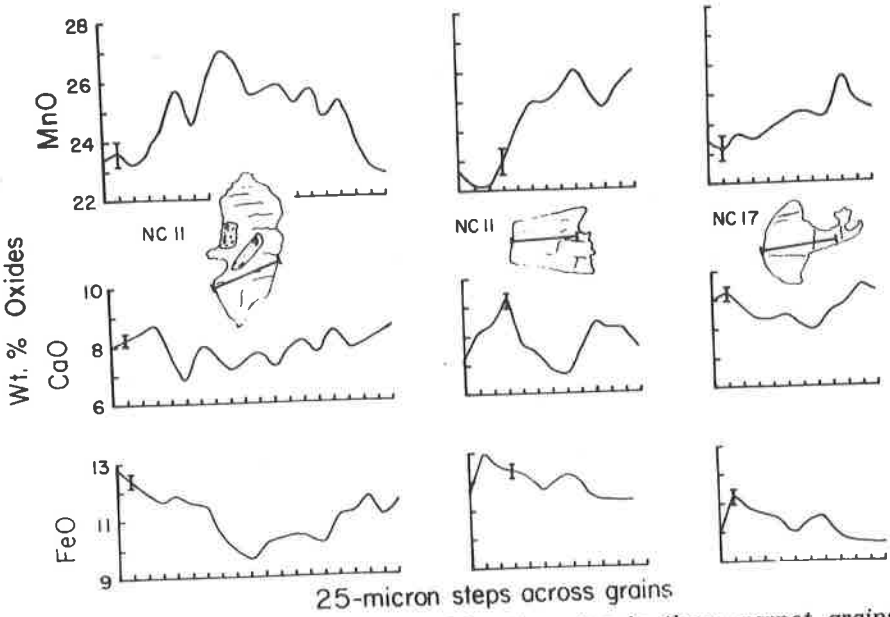


*Figure 5. Line graphs depicting compositional zoning in three garnet grains. The microprobe traverses are illustrated on the sketches of each grain. Vertical bars are standard deviations of analyses. The first traverse appears to extend from rim through core to rim; the following two grains are fragments and the traverses may not reach the true crystal core.*

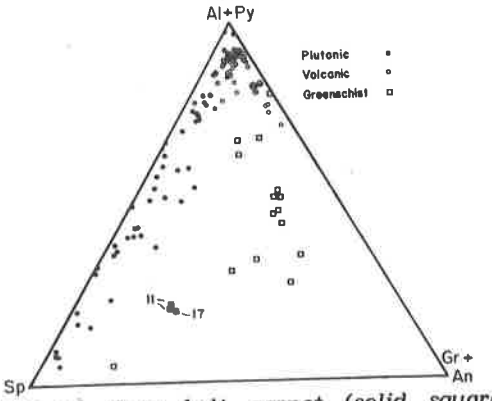


*Figure 6. Compositions of slate belt garnet (solid squares) expressed as the endmembers Al (almandine) + Py (pyrope); Sp (spessartine); and Gr (grossularite) + An (andradite), and compared to garnet compositions in plutonic (Wright, 1938; Vennum and Meyer, 1979), volcanic (Oliver, 1956; Green and Ringwood, 1968; Fitton, 1972; Wood, 1974; and Brousse et al., 1972), and greenschist (Brown, 1967, 1969) environments. Slate belt and greenschist garnets are higher in Gr + An than igneous garnets.*

almandine solid solutions (Miller and Stoddard, in press).

In silicic volcanic rocks, however, occurrences of garnet as a primary phase are relatively uncommon. The well-documented cases of Oliver (1956), Green and Ringwood (1968), Fitton (1972), and Wood (1974) show that these volcanic garnets are also almandine-rich but compositionally distinct from the plutonic garnets. Specifically, they are relatively poor in MnO (spessartine $\leq$ 13 mole %) and may contain considerable pyrope content (up to 28 mole %; e.g. Fitton, 1972). Both types of igneous garnets, plutonic and volcanic, are low in CaO ( < 16 mole % grossular + andradite), and this appears to distinguish them from most, if not all, of the greenschist-facies metamorphic garnets.

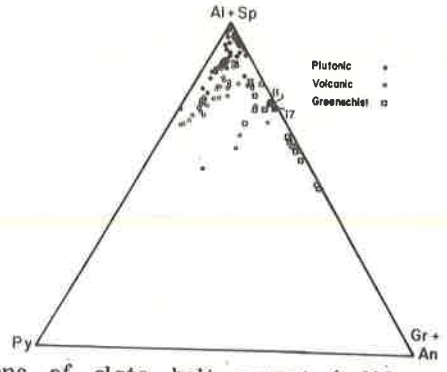


*Figure 7. Compositions of slate belt garnet (solid squares) expressed as the endmembers Al (almandine) + Sp (spessartine); Py (pyrope); and Gr (grossularite) + An (andradite), and compared to garnet compositions in plutonic, volcanic, and greenschist environments (see references listed under Fig. 6). Slate belt and greenschist garnets are poor in Py relative to most volcanic and some plutonic garnets.*

In general, garnets in greenschist-facies rocks have grossular + andradite > 20 mole % and can be separated from igneous garnets accordingly. On the other hand, garnets from greenschist facies metamorphic rocks are generally distinguishable from the more common higher-grade metamorphic garnets by their high spessartine and/or grossular contents (e.g., Brown, 1967). Amphibolite-grade garnets, for example, are commonly almandine rich (Miyashiro, 1953; Sturt, 1962).

Figures 6 and 7 portray the common compositional fields of garnets from the three environments of formation. Garnets from plutonic rocks overlap the range of volcanic garnets when plotted with almandine and pyrope combined (Fig. 6), but volcanic garnets are better distinguished in Figure 7 by their slightly higher pyrope (MgO) contents. The documented greenschist-facies garnets (as well as the Carolina slate belt garnets) are separable from plutonic garnets by their relatively high CaO (Fig. 6), and from volcanic garnets by their high MnO (Fig. 6) and low MgO contents (Fig. 7).

Although most igneous garnets are not strongly zoned, those that have compositional zoning commonly have spessartine content increasing from core to rim (Green, 1977). This may be directly related to the progressive enrichment of MnO in the crystallizing magma. In contrast, metamorphic garnets in the greenschist facies are commonly zoned with Mn-rich cores and Mn-poor rims (e.g., Brown, 1967, 1969; Atherton, 1968). This feature has been attributed to steady depletion in MnO available during garnet growth and explained by a model based on Rayleigh fractionation (Hollister, 1966). The garnet in the Carolina slate belt meta-volcanic rocks fits this pattern. That is, where compositional variation is great enough to detect, Mn is richer nearer the cores than the rims of garnet crystals (Fig. 3).

If the spessartine-rich garnet was a primary phase in these igneous rocks, its present association with epidote and chlorite would suggest that there was a breakdown of garnet during low-grade metamorphism to form these two green phases. As described by Amit (1976), retrograde metamorphism of garnet to chlorite is likely to produce garnet margins enriched in MnO and depleted in FeO and MgO. Also, pseudomorphs of chlorite after garnet may be produced by garnet breakdown (Edmunds and Atherton, 1971). In contrast, the slate belt garnets are depleted in Mn at their margins, and chlorite did not form pseudomorphs after garnet. Other features that might also suggest garnet alteration, such as chlorite rims, are also lacking (Figs. 3 and 4).

The textural features observed in the slate belt rocks argue for prograde metamorphic crystallization of garnet, in apparent equilibrium with the epidote + chlorite $\pm$ white mica $\pm$ calcite assemblage. Furthermore, the occurrence of epidote inclusions in some garnets suggests that garnet growth succeeded that of epidote during metamorphism. Epidote is also included in some chlorite.

Because neither garnet composition, compositional zoning, nor metamorphic texture support an igneous origin, the spessartine-rich garnet is interpreted as a

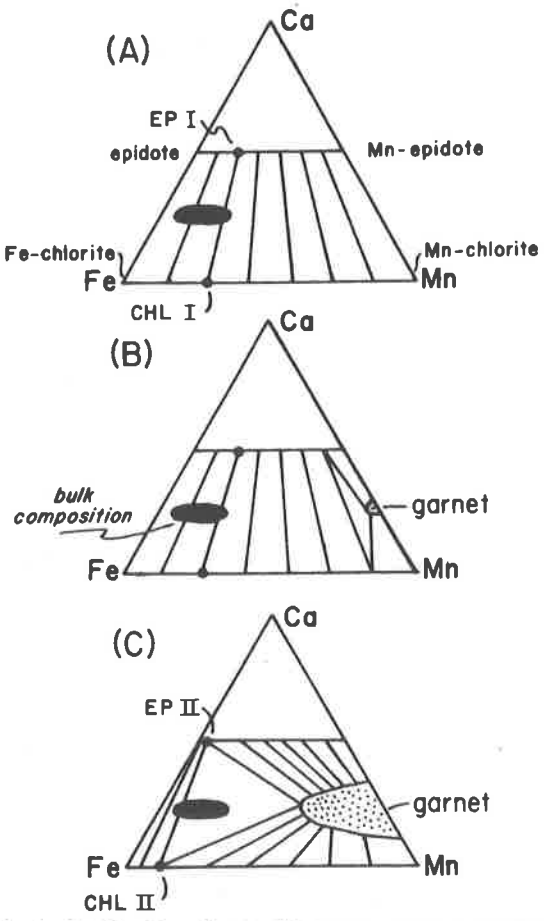


*Figure 8. Hypothetical Fe-Ca-Mn phase diagrams with (possible) bulk-compositional field for epidote-chlorite clusters. (A) Epidote I and chlorite I are possible coexisting parent phases for the spessartine-rich garnet at lowest metamorphic grade. (B) Initial metamorphic reactions produce Mn-garnet stable only with Mn-richest epidote and chlorite. (C) As temperature increases, the three-phase triangle chlorite + epidote + garnet sweeps across the diagram toward more Fe-rich, Mn-poor compositions, ultimately consuming epidote I and chlorite I to form epidote II + chlorite II + garnet (from Table 2). The assemblage lacking garnet (sample 18) is represented by the extreme left of the bulk composition oval.*

product of greenschist facies metamorphism, as it is in some metapelites and metamorphosed Mn-chert (e.g., Brown, 1967). And because the slate belt rocks have cluster assemblages of quartz + epidote + Mn-rich chlorite $\pm$ white mica $\pm$ calcite that occur without garnet (e.g., sample 18, Table 1), some of these phases may have served as the parent material for the garnet where it is present.

Two problems remain: to determine (1) the garnet-forming reaction and (2) the nature of the original volcanic material that was recrystallized to form the garnet-bearing clusters during metamorphism. Kretz (1973) suggested that spessartine-rich garnet may be formed in the greenschist facies at the expense of Mn-rich chlorite. However, in the present case, the high grossular content of the garnet necessitates the participation of a Ca-rich reactant phase in the garnet-forming reaction. Therefore, a more appropriate reaction (Brown, 1969) is:

(Fe, Mn, Al) chlorite + epidote + quartz = garnet + oxygen + water (eq. 1)

However, the relatively abundant magnetite in the metamorphic clusters argues

*Table 3. Average* compositions (in wt.%; by electron microprobe) of garnet crystals in meta-rhyolites 11 and 17, Carolina slate belt, Montgomery County, North Carolina.*

| | 11 | 11 | 17 |
|---|---|---|---|
| $SiO_2$ | 37.0 | 37.0 | 37.1 |
| $Al_2O_3$ | 19.6 | 19.5 | 19.8 |
| FeO** | 11.0 | 11.3 | 10.3 |
| MnO | 24.8 | 24.4 | 24.1 |
| MgO | 0.13 | 0.13 | 0.17 |
| CaO | 8.0 | 7.9 | 8.7 |
| Total | 100.53 | 100.73 | 100.17 |
| Number of ions on the basis of O = 12 | | | |
| Si | 3.008 | 3.016 | 3.015 |
| Al | 1.877 | 1.872 | 1.897 |
| $Fe^{+3}$*** | 0.123 | 0.128 | 1.897 |
| $Fe^{+2}$ | 0.602 | 0.628 | 0.586 |
| Mn | 1.708 | 1.684 | 1.659 |
| Mg | 0.015 | 0.016 | 0.020 |
| Ca | 0.698 | 0.691 | 0.758 |
| $R^{VI}$ | 5.023 | 5.019 | 5.023 |
| Molecular endmembers | | | |
| Sp | 56.5 | 55.8 | 54.9 |
| Gr | 19.0 | 18.7 | 21.7 |
| Al | 19.9 | 20.8 | 19.4 |
| An | 4.1 | 4.2 | 3.4 |
| Py | 0.5 | 0.5 | 0.7 |

* Averages of 10 to 20 point analyses
** Total Fe as FeO
*** $Fe^{3+}$ calculated assuming Al + $Fe^{3+}$ = 2.000 cations

for oxidation of primary ferrous iron, and the abundance of quartz (up to 65 modal percent of the clusters) suggests that quartz was produced, not consumed, during the garnet-forming reaction. Moreover, the occurrences of epidote inclusions in both garnet and chlorite show that garnet (all?) and at least some chlorite formed later than epidote.

We favor garnet formation by a continuous reaction involving the breakdown of Mn-rich chlorite + epidote analogous to equation 1, but giving rise to a second pair of (less Mn-rich) chlorite and epidote. The reaction also involved partial oxidation of iron to form magnetite, and producted quartz. Such a reaction, compatible with the phase compositions of Tables 2 and 3, might be:

hypothetical Mn-rich chlorite I

$$3.0\ Fe_{8.6}Mn_{2.0}Mg_{0.4}Al_{1.0}(Si_{7.0}Al_{1.0})O_{20}(OH)_{16} \quad + \qquad \text{(eq. 2)}$$

hypothetical Mn-rich epidote I

$$2.5\ Ca_2Fe^{3+}_{0.55}Mn^{3+}_{0.08}Al_{2.37}Si_3O_{12}(OH) \quad + \ 3.4\ O_2 \ =$$

garnet (Table 3)

$$4\ Mn_{1.5}Fe_{0.75}Ca_{0.75}Al_2Si_3O_{12} \quad +$$

chlorite II (Table 2)

$$0.33\ Fe_{5.5}Mg_{3.6}Mn_{0.4}Al_{2.5}(Si_{5.5}Al_{2.5})O_{20}(OH)_{16} \quad +$$

epidote II (Table 2)

$$1.0\ Ca_2Fe^{3+}_{0.67}Mn^{3+}_{0.06}Al_{2.27}Si_3O_{12}(OH) \quad +$$

magnetite quartz fluid

$$7.23\ Fe^{3+}_{2}Fe^{2+}O_4 \quad + \quad 11.69SiO_2 \quad + \quad 22.11H_2O.$$

The above reaction and the phase compatibilities that should result after the appearance of garnet are portrayed on the hypothetical Ca-Fe-Mn phase diagrams of Figure 8. Other similar reactions are also possible, some of which might involve the production of calcite.

Where garnet is not associated with the chlorite and epidote, as in sample 18, either a critical temperature was not reached for garnet crystallization, or more likely, the bulk compositions of the non-garnetiferous clusters were not high enough in MnO to produce Mn-garnet at the temperatures reached during metamorphism. The Ca-Fe-Mn diagrams in Figure 8 illustrate the importance of both temperature and bulk composition (of the clusters). The bulk compositions of the clusters in samples 11 and 17 were rich enough in Mn to fall within the epidote-chlorite-garnet three-phase triangle in Fig. 8c; had the peak temperature of metamorphism been higher, the three-phase triangle may have extended to include the bulk composition of sample 18 (represented by the extreme left of the bulk composition oval in Fig. 8c).

The metamorphism of all original volcanic phenocrysts in these rocks precludes determination of exactly what igneous phases were present but are now represented as metamorphic assemblages. No relict phenocrysts were observed except plagioclase and perhaps quartz. But the flow bands around some of the metamorphic clusters provide strong evidence that accumulations of phases were in fact present at the time of lava emplacement

Three possible candidates for precursor material come to mind: (i) amygdules filled with secondary minerals; (ii) spherulites; and (iii) phenocrysts or glomerocrysts of mafic minerals. The first two can probably be ruled out because amygdules are generally restricted to much more mafic, volatile-rich lavas. And spherulites, though common in rhyolites, are composed of radial aggregates of albite, sanidine, and silica minerals (Carmichael et al., 1974), material chemically unsuitable in the present case. Ferromagnesian phenocrysts in rhyolitic lavas are rarely abundant, but when present are commonly biotite, orthopyroxene, clinopyroxene, and amphibole. These, mixed with small amounts of plagioclase, are all good igneous candidates for the formation of greenschist facies chlorite and epidote in the meta-rhyolite.

## ACKNOWLEDGEMENTS

We thank the North Carolina State University Faculty Research and Development Fund for financial assistance, and we are grateful to K. Keil for permission to use the electron microprobe at the University of New Mexico, supported by National Aeronautics and Space Administration Grants NGL 32-004-063 and NGL 32-004-064 (K. Keil, Principal Investigator).

## REFERENCES CITED

Amit, O., 1976, Retrograde zoning in garnets of Elat-Wadi Magrish metamorphic rocks: Lithos, v. 9, p. 259-262.

Atherton, M.P., 1968, The variation in garnet, biotite, and chlorite composition in medium grade pelitic rocks from the Dalradian, Scotland, with particular reference to the zonation of garnet: Contrib. Mineral. Petrol., v. 18, p. 347-371.

Brown, E.H., 1967, The greenschist facies in part of eastern Otago, New Zealand: Contrib. Mineral. Petrol., v. 14, p. 259-292.

Brown, E.H., 1969, Some zoned garnets from the greenschist facies: Amer. Mineral., v. 54, p. 1662-1677.

Brousse, R., Bizouard, H., and Solat, J., 1972, Grenats des andesites et des rhyolites de Slovaquie, origine des grenats dans le series andesitiques: Contrib. Mineral. Petrol., v. 35, p. 201-213.

Burt, E.R., 1967, Geology of the northwest eighth of the Troy, North Carolina quadrangle: Master's Thesis, Univ. of North Carolina, Chapel Hill, N. C., 34 p.

Butler, J.R., and Ragland, P.C., 1969, Petrology and chemistry of metaigneous rocks in the Albemarle area, North Carolina slate belt: Amer. Jour. Science, v. 267, p. 700-726.
Carmichael, I.S.E., Turner, F.J., and Verhoogen, J., 1974, Igneous Petrology. McGraw-Hill, Inc., New York, N. Y., 739 p.
Conley, J.F., 1962, Geology of the Albemarle quadrangle, North Carolina: North Carolina Dept. Conserv. and Devel., Div. Mineral Resources Bull. 75, 26 p.
Edmunds, W.M., and Atherton, M.P., 1971, Polymetamorphic evolution of garnet in the Fanad aureole, Donegal, Eire: Lithos, v. 4, p. 147-161.
Fitton, J.G., 1972, The genetic significance of almandine-pyrope phenocrysts in the calc-alkaline Borrowdale volcanic group, northern England: Contrib. Mineral. Petrol., v. 36, 231-248.
Green, T.H., 1977, Garnet in silicic liquids and its possible use as a P-T indicator: Contrib. Mineral. Petrol., v. 65, p. 59-67.
Green, T.H., and Ringwood, A.E., 1968, Origin of garnet phenocrysts in calc-alkaline rocks: Contrib. Mineral. Petrol., v. 18, p. 163-174.
Green, T.H., and Ringwood, A.E., 1972, Crystallization of garnet-bearing rhyodacite under high-pressure hydruns conditions: Jour. Geol. Soc. Australia, v. 19, p. 203-212.
Hatcher, R.D., Jr., 1972, Developmental model for the southern Appalachians: Geol. Soc. Amer. Bull., v. 83, p. 2735-2760.
Hollister, L.S., 1966, Garnet zoning: an interpretation based on the Rayleigh fractionation model: Science, v. 154, p. 1647-1651.
Kretz, R., 1973, Kinetics of the crystallization of garnet at two localities near Yellowknife: Canadian Mineral., v. 12, p. 1-20.
Miller, C.F., and Stoddard, E.F., 1978, Origin of garnet in granitic rocks: an example of the role of Mn from the Old Woman-Piute Range, California: Geol. Soc. Amer. Abstracts with Prog., v. 10, p. 456.
Miller, C.F., and Stoddard, E.F., in press, The role of manganese in the paragenesis of magmatic garnet: an example from the Old Woman-Piute Range, California: Jour. Geology.
Miyashiro, A., 1953, Calcium-poor garnet in relation to metamorphism: Geochim. Cosmochim. Acta., v. 4, p. 179-208.
Mueller, G., and Schneider, A., 1971, Chemistry and genesis of garnets in metamorphic rocks: Contrib. Mineral. Petrol., v. 31, p. 178-200.
Oliver, R.L., 1956, The origin of garnets in the Borrowdale volcanic series and associated rocks, English Lake District: Geol. Mag., v. 93, p. 121-139.
Rumble, D., and Finnerty, T.A., 1974, Devonian grossularite-spessartine overgrowths on Ordovician almandine from eastern Vermont: Amer. Mineral., v. 59, p. 558-562.
Seiders, V.M., 1978, A chemically bimodal, calc-alkalic suite of volcanic rocks, Carolina volcanic slate belt, central North Carolina: Southeastern Geology, v. 19, p. 241-265.
Sturt, B.A., 1962, The composition of garnets from pelitic schists in relation to the grade of regional metamorphism: Jour. Petrology, v. 3, p. 181-192.
Tobisch, O.T., and Glover, I. III, 1969, Metamorphic changes across part of the Carolina slate belt-Charlotte belt boundary, North Carolina and Virginia: U.S. Geol. Survey Prof. Paper 650-C, C1-C7.
Vennum, W.R., and Meyer, C.E., 1979, Plutonic garnets from the Werner batholith, Lassiter Coast, Antarctic peninsula: Amer. Mineral., v. 64, p. 268-273.
Whitney, J.A., Paris, T.A., Carpenter, R.H., and Hartley, M.E., 1978, Volcanic evolution of the southern slate belt of Georgia and South Carolina: a primitive oceanic island arc: Jour. Geology, v. 86, p. 173-192.
Wood, C.P., 1974, Petrogenesis of garnet-bearing rhyolites from Canterbury, New Zealand: New Zealand Jour. Geol. Geophys., v. 17, p. 759-787.
Wright, W.I., 1938, The composition and occurence of garnets: Amer. Mineral., v. 23, p. 436-449.